Otto-von-Guericke Universität Magdeburg
Fakultät für Elektro- und Informationstechnik
Institut für Automatisierungstechnik

Nonlinear Output Feedback Control of a Pneumatic Muscle Actuator System

Diploma Thesis

Submitted in March 2005

by

Sabine Haumann

(* 12.05.1979 in Iserlohn)

Supervisor:	Prof. Dr. Fabio Previdi[1]
First Examiner:	Prof. Dr.-Ing. habil. Jörg Raisch[2]
Second Examiner:	Dipl.-Ing. Thomas Schauer[2]

[1]Department of Management and Computer Science, University of Bergamo, Italy
[2]Lehrstuhl für Systemtheorie technischer Prozesse, Otto-von-Guericke Universität Magdeburg

Abstract

Humanoid robots and protheses for humans are demanded to be lightweight and controllable precisely. One promising approach is the use of pneumatic actuation technologies. In this thesis a Pneumatic Muscle Actuator (PMA) is investigated and used for actuating a joint. The main drawback of these actuators is their highly nonlinear behavior.

Chapter 1 gives a summary about this thesis. Chapter 2 introduces further into the technology of the PMA and the approaches of modeling and nonlinear control. In Chapter 3 an overview about existent research work about modeling and control is given. One of these models is modified, extended to the model of a joint and implemented in MATLAB/ Simulink in Chapter 4. The model is validated. In Chapter 5 a flatness based controller of the PMA and the joint actuated by a PMA is designed and implemented in MATLAB/ Simulink. The performance of the controller is tested by adequate simulations. Chapter 6 resumes the results of this thesis and gives a short outlook to some further research topics.

Kurzfassung

Humanoide Roboter und Prothesen sollen leicht und präzise kontrollierbar sein. Ein vielversprechender Ansatz ist die Anwendung von pneumatischen Technologien. Diese Diplomarbeit untersucht den Einsatz von pneumatischen Muskeln bei der Steuerung von Gelenken. Ein wesentlicher Nachteil dieser pneumatischen Muskeln ist ihr stark nichtlineares Verhalten.

Kapitel 1 faßt die wesentlichen Inhalte dieser Diplomarbeit zusammen. In Kapitel 2 wird die Technologie der pneumatischen Muskeln dargestellt. Bestehende Modelle und Regler werden in Kapitel 3 vorgestellt. Eines dieser Modelle wird in Kapitel 4 abgeändert, auf das Modell eines Gelenkes erweitert und in MATLAB/ Simulink implementiert und validiert. In Kapitel 5 wird ein flachheitsbasierter Regler für den pneumatischen Muskel und das Gelenk entworfen und ebenfalls in MATLAB/ Simulink implementiert. Durch geeignete Experimente wird das Verhalten des Reglers simulativ getestet. Kapitel 6 faßt die Ergebnisse dieser Diplomarbeit zusammen und gibt einen kurzen Ausblick auf weitere Fragestellungen.

Ich versichere, daß ich diese Diplomarbeit selbständig verfaßt und keine anderen als die angegebenen Hilfsmittel verwendet habe.

Magdeburg, 31.03.2005

Contents

1 Preface **7**

2 Introduction **11**

2.1 Pneumatic Muscle Actuators (PMA) 11

2.2 Modeling objects and processes 14

2.3 Control of nonlinear systems 16

2.3.1 Robust controller design 16

2.3.2 Linearization methods 16

2.3.3 Adaptive controller design 17

3 State of the art concerning modeling and control of a Pneumatic Muscle Actuator **20**

3.1 Existent models of the PMA 20

3.1.1 Physical based models 21

3.1.2 Mixed models 31

3.1.3 Black box models 35

3.1.4 Applications 36

3.2 Performed control strategies 37

3.2.1 Linearization technologies 37

3.2.2 Robust control technologies 40

3.2.3 Adaptive control technologies 40

3.2.4 Robust adaptive control 42

4 Model of the Pneumatic Muscle Actuator (PMA) **44**

4.1 Physical model 44

4.1.1 General Structure of the Model 44

4.1.2 Assumptions and properties 45

4.1.3 Expected behavior 46

4.1.4 Valve 46
4.1.5 PMA 47
4.1.6 Load 48
4.2 State space model 52
4.3 Extension of the model to a joint driven by PMAs 54
4.4 Implementation of the model in MATLAB/ Simulink 59
4.4.1 Actual values of the model parameters 59
4.4.2 Simulation results of the model 59

5 Closed-loop control 65
5.1 Flatness based control 65
5.1.1 Basic idea of the controller 66
5.1.2 Prerequisites and necessary tools 66
5.2 Length control of the single PMA 68
5.2.1 Fulfilment of the prerequisites 68
5.2.2 Controller equations 71
5.2.3 Application of the Karnopp friction 73
5.3 Extension to the control of the joint 74
5.4 Implementation of the controller in MATLAB/ Simulink 74
5.4.1 Performed experiments with the closed loop control system 75
5.4.2 Actual parameters for the closed-loop control experiments 80
5.4.3 Results of the experiments 80

6 Conclusions and outlook 89

A Mathematical derivations 99
A.1 Derivation of the volume of the PMA 99
A.2 Development of the state space form 101
A.2.1 Assembling and simplification of the modeled properties: 101
A.2.2 Overall system 103
A.2.3 State space form 103

B Programs 105
B.1 Initialization 105
B.2 Simulink model of the closed loop PMA control system 107

B.2.1 Control of the driven load with proportional friction law 107
B.2.2 Control of the driven load with Karnopp friction law 117
B.2.3 Control of the driven joint with Karnopp friction law 127

List of Symbols

$(\bar{\cdot})$ ..... equilibrium value

$(\dot{\cdot})$ ..... time derivative

$(\underline{\cdot})$ ..... vector

a_i for i = 1,...,10 ..... abbreviations of the model parameters

C ..... proportional friction constant

c ..... constant of proportionality of the valve

e ..... error of the actual trajectory

f ..... diametric distance parameter of the PMA

$F_{(\cdot)}$ ..... force

g ..... gravitational constant

h ..... helical fiber length of the PMA

K ..... elastic force constant

K_i for i = 0,1,2 ..... controller parameter

L ..... length of the link

m_s ..... solid mass driven by the PMA

$\dot{m}_g$ ..... gaseous mass flow into the PMA

n ..... order of the system

p ..... pressure inside the PMA

p_0 ..... environment pressure

P_i for i = 1,2,3 ..... desired poles of the closed loop control system

p_s ..... supply pressure

R ..... specific gas constant of air

r ..... relative nonlinear degree

$\mathbb{R}$ ..... set of real numbers

T ..... temperature

t ..... time

$T_{(\cdot)}$ ..... torque

U ..... command voltage to the valve

u ..... input into the system

V ..... volume of the PMA

x ..... state of the system

y ..... output of the system

y_d ..... desired output of the system

z ..... length of the PMA

α ..... angle of the joint

χ ..... polytrophic exponent

η ..... specific heat ratio of air

ν ..... input into the inverse system

ψ_i for i = 1,...,6 ..... abbreviations of the model equations

Chapter 1

Preface

The aim of this thesis is to develop a closed loop control of an artificial joint actuated by Pneumatic Muscle Actuators (PMA). This chapter gives an overview about the progress of the thesis.

A PMA consists of a closed rubber tube with a valve. When the PMA is inflated with compressed air, it widens in radial direction and contracts in longitudinal direction. Therewith a force in longitudinal direction is induced which can be used for actuation. The PMA is only a pulling actuator, which means that it has to be extended by an antagonistic action like a spring, a driven mass or a second PMA. This property is similar to the physiological muscles, because also they can only contract and have to be extended passively by antagonistic actions. The main drawback of the PMAs is their strongly nonlinear behavior.

The use of a model for the PMA is helpful, because not all of the properties of the PMA have to be regarded and so the model can be simplified. This is important, because a general requirement for the treatment of systems is that they have to be as complex as necessary, but as simple as possible for a better handling. Also, with a model the behavior of the PMA can be simulated. The derived model is physical based. One important advance of physical based models it that parameters can be varied easily. Black box models have to be identified again experimentally if a parameter is changed. Also, in this thesis no identification experiments are performed.

In this thesis the PMA is extended by the weight of a driven mass. In the basic form the PMA is modeled to drive a load vertically. For deriving the model the system is split into the valve, the intrinsic PMA and the mass driven by the PMA. The control variable is the command voltage

to the valve and the desired controlled variable is the PMA length.

This system is extended to a joint. The joint is actuated by one PMA which connects the middle points of the links. This setup is adequate to the physiological setup where the muscles which actuate a joint affect at the bones which are connected by the joint. The contraction occurs actively by the PMA and the extension occurs passively by the weight of the driven link. The controlled variable is the angle of the joint. It depends geometrically on the PMA length. The intern calculations take place with the PMA length. The desired angle trajectory is transformed into the PMA length and the simulated output length is re-transformed into the angle. The system shall track a given trajectory and it behaves very unstable, so a closed loop control is necessary.

Due to the strong nonlinearities of the model the controller has to be designed by advanced methods. The main adequate approaches are a linearization of the system model or the feedback combined with a linear controller and the design of a nonlinear controller. The controller should be designed as complex as necessary, but as simple as possible, so if the performance of a linearization method is sufficient it should be preferred to a nonlinear controller design. The chosen method is a flatness based controller. A flatness based controller works with exact feedback linearization. The linearization uses the differential flatness of the model. A differential flat system is invertible, and the nonlinearities of the system can be canceled exactly. In the working range the PMA system is differential flat, so this control method can be applied. The linear controller which is combined with the linearization method is a pole placement controller. The results of the simulated experiments show that the controller performance is very good.

This thesis is organized as follows:

In Chapter 2 the technology of the PMA is presented and outlined against other actuation technologies. Also some important requirements and properties of the PMA are discussed. This chapter also presents some basic principles of mathematical modeling, the black box models and the physical based models. In the black box approaches the model is identified with experimental data whereas in the physical based approach the model is derived from physical quantities. Also the complexity of the model and the determination of the input and the output variables are discussed. Third the basic approaches of nonlinear control are outlined. For weak

nonlinearities a robust controller design can be applied. The approach of feedback linearization is discussed. Classification criteria are exact and approximated linearization and input-output and input-state linearization. One main approach for nonlinear controller design is an adaptive controller which can be designed direct and indirect.

Chapter 3 gives an overview about existent models and controllers for PMAs and their applications. All of the models are nonlinear, but time-invariant. There are two physical based models presented. Some other models which are mainly physical based regard important properties in the way of black box. One pure black box model is given. In some models the complete PMA system is described, which means that there is a PMA which drives a mass. In some models and the applications the PMA actuates a joint. Some of the articles give models of single parts or investigate the influence of the regard or neglect of properties like valve characteristics, the thickness of the PMA wall and the area of the end caps. There is also one extra model of the friction force presented. Many of the models are given incomplete, and only one of them is validated. Second some implemented controller strategies for tracking control of PMAs are reviewed. The performed controller strategies are linearization methods, adaptive controllers, one robust controller and some robust adaptive approaches. Some of the controllers are designed as switching controllers which differentiate between the PMA contraction and extension. The requirements to a tracking controller are exactness and speed of the tracking and a smooth control signal. Most of the articles do not validate the controller performance sufficient, but the best results are achieved with linearization methods.

One important step in this thesis is to find an adequate model of the PMA in the literature and implement it in MATLAB/ Simulink. The model has to be physical based, because no experiments for model identification are performed in this thesis. In the literature there is no adequate model given, so the best one is modified by replacing some parts with more adequate models. The resulting model is described in Chapter 4. At first a PMA which drives vertically a mass is modeled. Mainly there are models for the valve which generated the mass flow into the PMA and for the intrinsic PMA with the PMA length as output. The model is brought into state space form with the command voltage to the valve as input, the inner pressure, PMA length and the first time derivative of the PMA length as states and the PMA length as output. There are two different models of friction compared, one simple proportional law and one friction model which switches between slipping and sticking mode. The third main part of the model is

the extension to a joint driven by a PMA. The model is validated by some MATLAB/ Simulink simulations.

The aim of this thesis is to design a joint which is driven on a desired trajectory. Therefore a closed loop control is necessary. As controller strategy a flatness based controller is chosen. After the linearization a linear third order pole placement controller is designed. The principle and the design of the controller are presented in detail in Chapter 5. First the controller is designed for the simple proportional friction law and second the friction model is exchanged. In a third step the controller is extended to the control of the joint. The controller is implemented in MATLAB/ Simulink and the performance of the closed loop control system is proved in different simulated experiments. The controller requires a three times differentiable desired trajectory, but it can deal with abruptly changed moved masses. Fluctuations of the supply pressure do not affect the states and the output, only the control signal. The controller is also robust against fluctuations in the temperature. Also, the performances for different friction parameters are investigated. The exactness of the tracking and the smoothness of the control signal are reduced slightly. Summarizing, the controller yields a good tracking behavior concerning speed and exactness with a smooth control signal.

Chapter 6 resumes the results of this thesis and gives a short outlook to some further research topics.

Chapter 2

Introduction

Pneumatic Muscle Actuators (PMA) are a promising technology used for prostheses and humanoid robotics. This chapter introduces further into the principles applied in this thesis. Section 2.1 gives an overview about the technology of PMAs and its main properties. Section 2.2 introduces into the basic principles of mathematical modeling. In Section 2.3 the main approaches of controller design for nonlinear systems are presented.

2.1 Pneumatic Muscle Actuators (PMA)

During the last decades many research groups are working on humanoid robots and robotic prostheses. One main subject in the development of robotics is the transfer of energy into the form of mechanical movements. For this transfer actuators are used. There are several different technologies existent. According to the concrete application different requirements have to be fulfilled and the best suitable technology has to be chosen. Important parameters of the technologies are the power/weight and power/volume ratios, strength, response rate, physical size, speed of motion, reliability, controllability, compliance and cost [2].

Humanoid robots and protheses for humans are demanded to be lightweight and controllable precisely. The lightweight is important to reduce inertia and motion power, and the precise control is necessary because mainly little movements are performed. A small physical size is demanded, because the needed equipment has to be carried along. The energy transfer is desired to occur effectively, because the more effective the technology works, the smaller and more lightweight the equipment can be dimensioned. Another important property is the safety. If the technology fails, it is demanded that the human is not injured. Especially the prostheses

are desired to have low cost, so that also private persons can buy them.

There are several actuation technologies existent, but many of them are not useful for humanoid movements. Combustion systems e.g. which use thermal cycles to convert chemical energy into motion are used for transport, but they are overdimensioned for the described applications. Hydraulic power is mainly used outside, for indoor applications it is too noisy and too unclean due to oil leaks. Also it is less reliable [2]. Electric motor technology is more suitable, because it is clean, quiet and precisely controllable. A disadvantage of this technology is the limited operation range in outdoor applications, because batteries are heavy compared to their power. Also for humanoid robots which shall perform movements like hopping and running the provided motor torque is too small [29]. One problem of electric and hydraulic actuators is that failures can lead to bad injuries of the human.

Pneumatic actuators have got a high power/weight ratio (1 kW/kg [2]) and power/volume ratio (1000 kW/m^2 [24]). They work clean and can easily be miniaturized, and they are very safe. Also they have got a low cost. One advantage is that they act very similar to a human skeletal muscle. The main disadvantage is the difficulty in accurate control due to the the compressibility of the air which causes high nonlinearities. Also, the elasticity of the solid material causes problems.

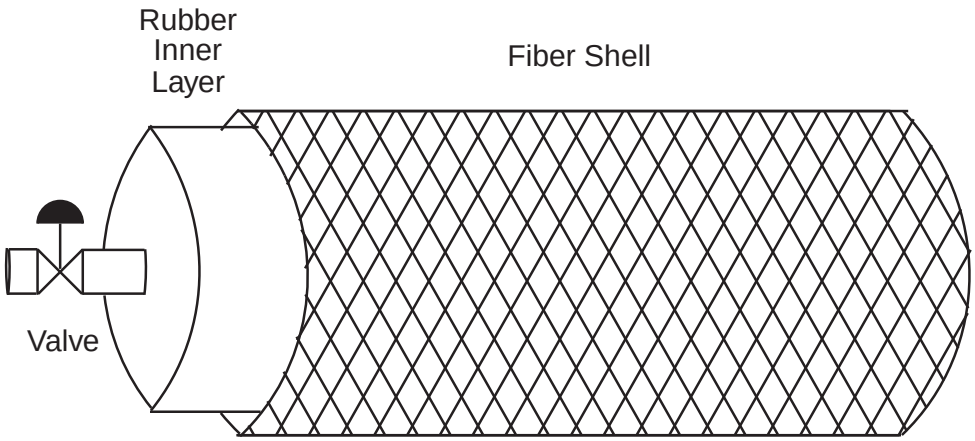

Figure 2.1: Braided Pneumatic Muscle Actuator (PMA)

There are different possible structures of the Pneumatic Muscle Actuator (PMA). The most common structure is a braided shell PMA, also called McKibben Muscle or Rubbertuator. It is

principally drawn in Figure 2.1. It consists mainly of a rubber inner layer which is braided with a fiber shell. The material of the fibers is non-elastic, e.g. nylon. On one end of the PMA there is a valve which lets pressurized air into resp. out of the PMA. On the other end the PMA is closed.

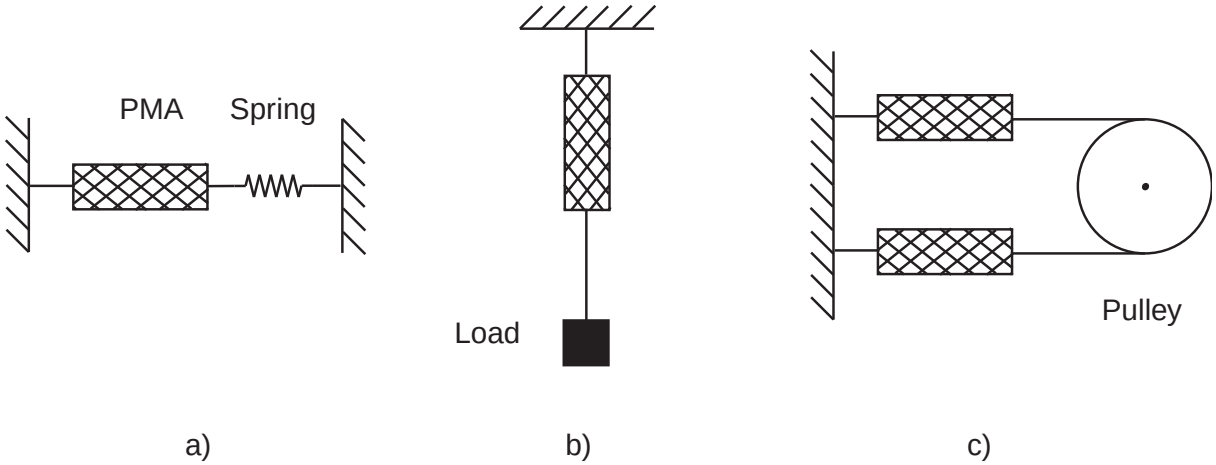

Figure 2.2: Possible antagonistic designs of a PMA: a) PMA coupled with a spring, b) PMA coupled with a mass, c) two coupled PMAs

As soon as there is air pressed into the PMA, the inner pressure rises and the PMA extends in radial direction and contracts in longitudinal direction. This contraction generates a strong force which is used in the application. One important property of the PMA is the fact that it is only a pulling actuator. The PMA can contract, but not extend actively. Following, a PMA must always be coupled with an element which extends it. There are mainly three possibilities, pictured in Figure 2.2. The PMA can be extended by a spring (Figure 2.2.a), by a mass which is driven vertically by the PMA (Figure 2.2.b) or by a second PMA which is designed antagonistically (Figure 2.2.c). This property is very similar to human muscles which also induce forces and movements by contractions of an agonist and its antagonist.

Two problems caused by the combination of the rubber inner layer and the braided shell are a threshold pressure which has to be overcome before the PMA expands in radial direction and the dry friction between the inner layer and the shell.

With PMAs a joint can be driven. There are some different possible designs. One design consists of one PMA driving a joint. This approach is illustrated in Figure 2.3.a). The PMA is extended by the weight of the moved link. With an antagonistic design also two PMAs can

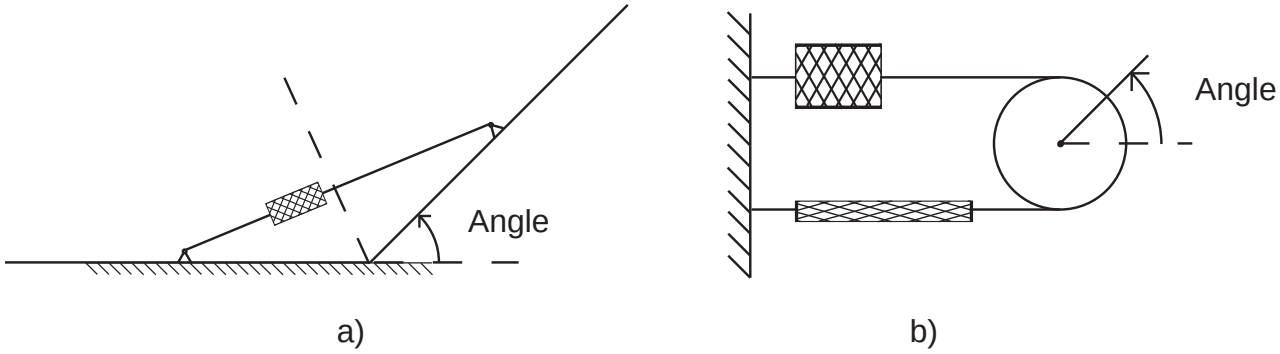

Figure 2.3: Angle formed by PMAs: a) one PMA, b) two antagonistic PMAs

drive a joint. This joint has got the two properties compliance and angle which can be controlled independently. This computation of the angle is illustrated in Figure 2.3.b). The compliance depends on the weighted sum of the pressures inside the PMA, and the angle depends on the weighted difference of the lengths of the PMAs.

2.2 Modeling objects and processes

Most objects or processes respectively their behavior are very complex, but often it is not necessary to regard all of their properties. In other processes it is important to predict their behavior before testing it in reality, for example a nuclear power plant should not be dimensioned by 'trial and error'. With a mathematical model which represents the important properties the object or the process can be simulated and its behavior can be tested.

The main approaches for modeling are physical based and black box models. The physical models are derived theoretically from physical basic principles. In the black box approach the model is derived by experiments. In these experiments some determined input signals are fed into the object or process, and the output is measured. From this data the model is identified. This kind of model is also called input-output model, because it contains no information about the inner processes. Physical based models have got state variables which describe inner processes.

Physical based models are valid for a larger range of different objects or processes of the same category, because their parameters are related directly to the physical quantities. Following, the

new values can be inserted easily. In a black box model the identification procedure must be repeated with the new values. On the other hand, black box models are normally less complex than physical based models. In some cases it is useful to develop a physical based model and generate with this model some input-output data. From the obtained data a black box model can be identified and used for simulations.

One important subject of modeling is the definition of the input and the output of the model. The output is the desired control variable, and with the input variable the object or process is manipulated. Following, the input variable should be adjustable easily.

Another important subject is the decision about the complexity of the model. For black box models this means the choice of the order. In physical based models the complexity means the regard and neglect of properties of the modeled object or process. The model should be as detailed as necessary to represent the object or process adequate, but also as simple as possible for a better and faster handling. Between both requirements a compromise must be found.

Section 3.1 gives a review about existing models. There are some pure physical based models, several mixed models whose main structure is physical based but some of their properties are described by a black box model and one pure black box model. Also, there are some incomplete models described.

In this thesis an existing model is chosen from the literature and implemented in MATLAB/ Simulink. This model is described detailed in Chapter 4.

2.3 Control of nonlinear systems

In typical control problems a closed loop control system is developed. As described in Section 2.2, many of the objects or processes, in the following called plants, are very complex and often also nonlinear. It is possible to neglect some of their properties and nonlinearities, but then the controller has to be designed so that it can deal with uncertainties. For weak nonlinearities a robust control technology can be applied. For dealing with stronger nonlinearities there are mainly two approaches, linearization technologies combined with a linear controller and adaptive control technologies. In the following, only time-invariant systems are regarded.

2.3.1 Robust controller design

In robust control technologies the controller is constant, but designed for a class of plants. A class means that there is the nominal plant model with ideal behavior and a modeled error which describes determined bounded variations. There are parametric uncertainties e.g. in parameters of the plant or nonparametric uncertainties e.g. due to non modeled dynamics. Weak nonlinearities are considered as uncertainties. This way of control is useful for arbitrary fast time variations of the uncertainties which are bounded. The robust control design is described in [22].

2.3.2 Linearization methods

One method for a dynamical linearization is the feedback linearization, described in [17]. The main idea is to compute a new input into the plant which cancels its nonlinearities. There are mainly two variants, input-state linearization and input-output linearization. The linearization can be exact or approximated.

For input-state linearization only the state equation of the state space form is used. The pair (A,B) has to be controllable. The system has to be brought into the following form, if necessary by a transformation:

$$\dot{x(t)} = Ax(t) + B\omega(x(t))[u(t) - \phi(x(t))] \tag{2.1}$$

This is possible if the pair (A,B) is controllable. The corresponding control law is

$$u(t) = \phi(x(t)) + \omega^{-1}(x(t))\nu(t) \tag{2.2}$$

and the resulting state equation is

$$\dot{x}(t) = Ax(t) + Bv(t) \tag{2.3}$$

with $v(t)$ being the new input into the system. This system is linear time-invariant and also controllable.

In tracking control problems, the output of the system is more interesting than the state. Therefore, a second way of feedback linearization is the input-output linearization. The output equation of the state space form

$$y(t) = h(x(t)) \tag{2.4}$$

is derived until the input $u(t)$ appears. The necessary number of derivations r is called the *relative degree* of the system. If r is identical to the order n of the plant model the pair (A,C) of the state space form is observable and the linearization is exact. In that case the input-output linearization leads to the input-state linearization [17].

If r is smaller than n, the plant is not fully observable, and the internal dynamics, also called zero dynamics, which describe the unobservable part of the plant have to be considered. Here the linearization is approximated, and the effectiveness of the input-output linearization depends on the stability of the internal dynamics.

The feedback linearization does not consider desired properties of the system like stability. For this a second controller has to be designed, but therefore linear methods can be used.

One drawback of the method is that it cancels all nonlinearities, but this is not always desired. For example a term x^i with odd i provides additional damping for large values of x. Also the canceled nonlinearities of the system appear in the control law. For large values of x this may be not be feasible in practical use due to limits e.g. of the actuator.

2.3.3 Adaptive controller design

In adaptive control technologies the controller is adapted during the process to variations of the plant. Following, adaptive controllers are always nonlinear. This design is useful for slowly varying parameters which are not necessary bounded. An adaptive controller guarantees the

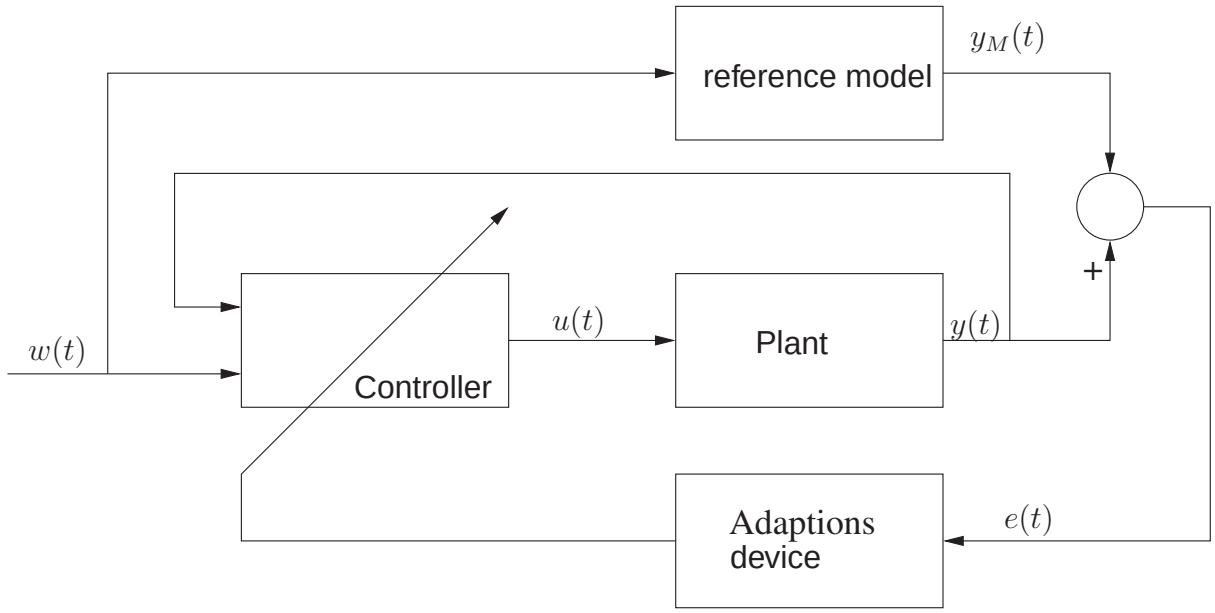

Figure 2.4: Control system of a model reference adaptive controller (MRAC), adapted from [31]

convergence of the tracking error to zero also with a small gain [10]. There are parameter adaptive technologies which deal with parameter variations and structure adaptive technologies which deal with uncertainties in the structure like order and number of states.

The main classification criterion is whether the adaptive control occurs directly or indirectly.

Direct adaptive control means that at each sample the controller parameters are estimated directly. This method is called Model Reference Adaptive Control (MRAC), and the description is taken from [31]. The structure of the MRAC is shown in Figure 2.4. In this method a reference model of the plant is required. A known time-dependent reference signal $w(t)$ is put into the controller and with this indirectly into the plant, and into the reference model. The output $y_M(t)$ of the reference model is compared to the output $y(t)$ of the plant, and an adaption device tunes the parameter of the controller.

The second approach is an indirect adaptive control. At each sample the model parameters are estimated, then used for computing the controller polynomial/parameters. This method is called Self-Tuning Control (STC), also described in [31]. A STC-design, shown in Figure 2.5, contains an identification device for the plant and an adaption device for the controller. The identification device detects variations of the plant parameters by using the plant input $u(t)$,

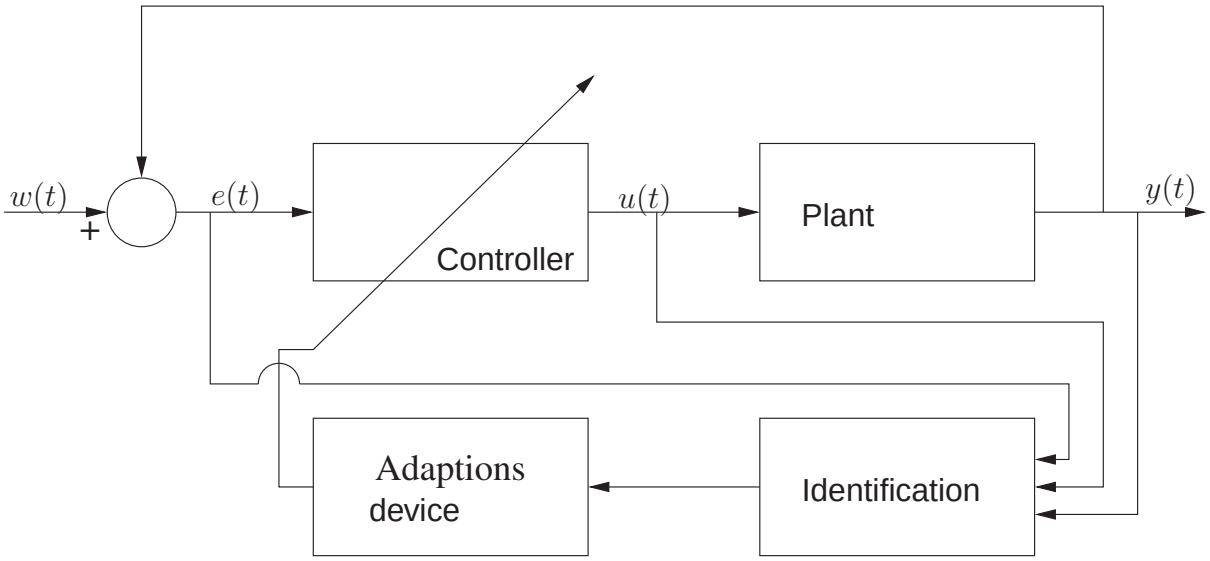

Figure 2.5: Control system of a self-tuning controller (STC), adapted from [31]

the plant output $y(t)$ and the error $e(t)$ from the reference signal $w(t)$. The adaption device computes the according controller polynomial resp. the controller parameters and adapts the controller.

In practical use, there are often fast switching variations with slowly varying boundaries. Because of this robust and adaptive control technologies are often combined with each other.

In Section 3.2 existent controllers for a Pneumatic Muscle Actuator are presented. One of the presented methods for controller design is implemented in this thesis. It is presented in Chapter 5.

Chapter 3

State of the art concerning modeling and control of a Pneumatic Muscle Actuator

In this thesis a Pneumatic Muscle Actuator (PMA) is discussed. As described in Section 2.2 the use of a model is helpful. This chapter gives a review about the existent work of some other research groups. In Section 3.1 their models are discussed. Section 3.2 reviews their implementations of advanced model-based controller strategies.

3.1 Existent models of the PMA

There are many different approaches and variants for developing an adequate model. Some of the properties like the desired control variable are determined by the application. Finally the angle formed by PMA's shall be controlled. This angle depends geometrically on the length change of the PMA's, so the desired control variable is the length change of the actuator (see Section 2.1). The input variable is not determined, the request to it is that it has to be adjustable easily. Possible inputs are for example the pressure inside the PMA or the gas flow into the PMA.

This section gives a review about different existing models. Subsection 3.1.1 deals with physical based models of the intrinsic actuator. A classification profile within these models is wether the given model is complete and how detailed it is described. Subsection 3.1.2 reviews two mixed models. Their main model structure is physical based, but important parts are described by black box models. In Subsection 3.1.3 one pure black box model is presented. Subsection 3.1.4 presents some applications of the PMA.

3.1.1 Physical based models

At first the complete models of the actuator are given. They are classified on the chosen input and output variables. Two of these models use the length change of the actuator as output, one uses the gas flow and one the pressure as input. The last model uses the pressure and the actuator length change as input and the PMA force as output.

Gas flow as input, actuator length change as output

First the model which uses the gas flow as input and the actuator length as output is discussed. It was developed by Hildebrandt et al. [13]. Their experimental setup consists of one PMA which drives vertically a trolley which can carry a variable load mass. It is very similar to Figure 2.2.b). The weight force extends the PMA, and the induced PMA force contracts it again. So the load acts antagonistically to the PMA. The measured output is the z-coordinate of the trolley with respect to the maximum extension, which is the same absolute value as the length change of the PMA but with opposite direction. The model is derived for the PMA and the trolley, where the trolley can move nearly frictionless. The used parameters of the model are assembled in Table 3.1.

One main model equation is the balance of forces:

$$m_s \ddot{z}(t) = F_m(t) - F_f(t) - m_s g \tag{3.1}$$

m_s - total mass, assumed to be concentrated in the driven mass

$z(t)$ - z-coordinate of the driven mass, corresponds negative to the length change of the PMA

$F_m(t)$ - longitudinal PMA force

$F_f(t)$ - friction force of bearing

g - gravitation constant

The PMA force of the PMA F_m is modeled to depend on the inner pressure of the PMA and on the volume change due to the length change. Experimental results with this model result in large failures, so the model of the PMA force is improved by using the PMA area instead of the volume change due to the length change. In this model the PMA is regarded as a piston with variable piston area which depends on the PMA length. This is modeled as fifth order polynomial with experimental identified parameters.

The second main model equation is a differential equation for the pressure:

$$\dot{p}(t) = \frac{\chi}{V(t)} \left(RT\dot{m}_g(t) - p(t)\dot{V(t)} \right) \tag{3.2}$$

$p(t)$	-	pressure inside the PMA
$V(t)$	-	Volume of the PMA
R	-	specific gas constant of air
T	-	temperature, assumed to be constant
$\dot{m}_g(t)$	-	gas mass flow into the PMA

Due to the compressibility of the gas the pressure is no linear function of the mass flow. Their relationship is derived by the ideal gas equation. The state change is described polytrophic. The polytrophic exponent χ is identified experimentally.

The volume of the PMA is assumed to depend only on the length of the PMA. It is modeled as a third order polynomial with experimentally identified parameters. With the PMA getting shorter, the volume increases.

The friction force of the bearing is supposed to be a combination of coulomb friction and viscous friction, both dependent proportional on the velocity of the PMA length change. The constants of proportionality are not explained.

Additionally the valve function is modeled. There a relationship between the gas flow and the set point voltage is developed analytical and additionally identified experimentally. The result of the identification is presented in an imprecise plot. All parameters of the analytical equation except the specific ratio of the valve type c are described.

The derived model of the PMA is given in nonlinear state space form with gas flow as input, length change of the PMA as output and inner pressure, length change and length change velocity as states.

The model is very detailed. It gives a relationship for the valve (gas flow dependent on the set point voltage). To model the length change of the PMA dependent on the gas flow, there are relationships for the force depending on pressure and area, for the inner volume depending on the length change, for the pressure depending on the volume and the gas flow and for the

Table 3.1: Parameters and variables of Hildebrandt et al. [13]

symbol	meaning	validity	obtained	values given?	experiment described?
M	mass	specific	measured	-	-
χ	polytrophic exponent	general	experimentally	yes	-
T	temperature	general	literature	standard cond.	-
p_0	environment pressure	general	literature	standard cond.	-
R	gas constant	general	literature	-	-
$\dot{m}_g$	gas flow	specific	experimentally	(no)	yes
c	valve ratio	specific	?	no	no
η	specific heat ratio	general	literature	standard cond.	-
b_i	volume coefficients	specific	experimentally	no	no
c_i	area coefficients	specific	experimentally	no	no
f_c, f_v	friction coefficients	specific	?	no	no

friction force depending on the velocity of the contraction resp. extension of the PMA.

On the other hand, there are several properties which are not regarded, as static friction between the PMA rubber tube and the braided shell and dynamical effects of the underlying position controller for the valve-slide stroke. This means that there is a cascade control strategy and the inner loop seems not to be fast enough, because there is an overlap of the two frequency bands. Also there is no threshold pressure regarded which has to be overcome before any action in radial direction can take place, and the thickness of the PMA wall is also neglected (discussed by Chou et al. [6], see Page 25). For the developed controller the pressure is measured instead of estimated by the given model, because the model of the PMA force which uses the pressure is not exact enough, e.g. due to the used model of the volume which is too simple. The friction force is questionable, because there is no static friction of the trolley regarded. Also for the modeled properties and relationships there are several parameters not given respectively not described detailed enough. The model itself is not validated.

Summarizing, several parts of this model can be used in this thesis, but the model of the PMA volume and the model of the friction force will be replaced by other models. Those parts of the model which are used in this thesis are presented deeper in Chapter 4.

Pressure and actuator length as input, actuator force as output

The second discussed model uses the pressure and the actuator length as input and the actuator force as output. It was published by Chou et al. [6]. This article contains many different parts and experiments. At first a physical based static model for the force depending on the inner pressure and the surface area of the PMA is derived. The used PMA is a braided shell PMA, that means it consists of a rubber tube sheathed with a braided shell. The angle of the braid fibers with respect to the longitudinal axis is called interweave angle. Figure 3.1 illustrates the surface of the PMA. The interweave angle changes during the contraction of the PMA. Depending on this interweave angle the surface area and the inner volume of the PMA are modeled.

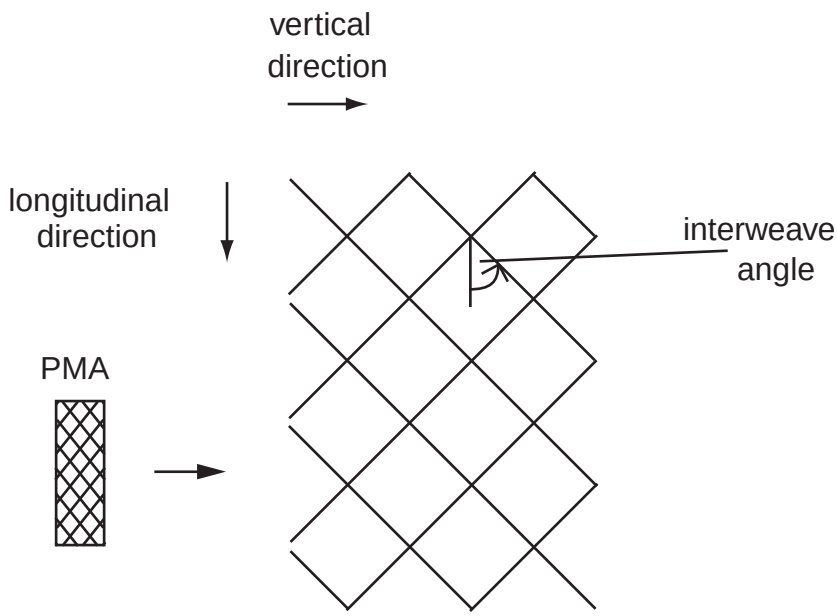

Figure 3.1: Illustration of the interweave angle

This interweave angle cannot be measured online. It has to be substituted with other described parameters. Because of the input-output constellation the given model cannot be used in this thesis.

Next, performed quasi-static and dynamic experiments are described in detail. The measured pressure and force are graphically shown as response to displacements with illustration of the

hysteresis. With these experiments the hysteresis is investigated deeper. It is caused by dry friction between the rubber tube and the braided shell. The result of the study is that the hysteresis is nearly independent from the velocity. That means the existent friction consists mainly of Coulomb-friction which is independent from velocity, and the viscous friction is so small that it can be neglected.

The article gives also a correction term for the influence of the thickness of the PMA wall. The simulation results of the static model with and without the correction are given. In the estimated diameter there is a difference of around 20 % and in the estimated volume a difference of around 30 %.

The described model is simplified by considering the force as function of the pressure and the volume change due to the length change, that means the PMA is regarded as a gas spring modeled with experimentally identified coefficients. In this model a pressure threshold to overcome the radial elasticity of the PMA bladder is regarded. Also a nonlinear term for the non-perfect cylinder form of the PMA at extreme length is mentioned, but this is out of the usual operating range, so this term is neglected.

At last a general friction value due to the history dependence of the friction is introduced and added. It can be used if a simple friction model is sufficient.

Also the simplified model is not useful for this thesis, because it depends on experimentally identified spring and damping parameters. Although the article does not give a useful model, there are several hints and discussions about properties which can be regarded.

Partial models and hints to keep in mind

Next there are several partial models of the PMA force. They are divided into models of the PMA force depending on the interweave angle respectively on the PMA length which are presented first and a model of the PMA force depending on the contraction.

First the model of Caldwell et al. [2] is discussed. In the article there is no description of the experimental setup which was used to develop the model. The used parameters are assembled in Table 3.2. According to this article the PMA has got one point of minimal energy. At this point its internal pressure is minimal and its volume is maximal. Due to elastic effects of the material this point differs slightly from the relaxed state. The volume can be calculated from the surface, and the surface area is modeled to depend on the angle of the braid fibers with respect to the longitudinal axis which is called interweave angle (see Figure 3.1). Any change from the point of minimal energy will cause a higher pressure and induce a force to return to the minimum energy state.

The volume of the PMA is modeled to depend nonlinear on the PMA length:

$$V(t) = \frac{\pi f^2}{4h^2}\Big(h^2 - z^2(t)\Big)z(t) \tag{3.3}$$

$V(t)$	-	PMA volume
f	-	diametric distance parameter
h	-	helical fiber length
$z(t)$	-	PMA length

The PMA force is modeled as

$$F = P_{new}(S_a + 2E_a) \tag{3.4}$$

F	-	PMA force
P_{new}	-	new internal pressure after extension or contraction
S_a	-	surface area of the PMA, depending on the interweave angle
E_a	-	endplate area of the PMA

It is maximal at maximal extension, minimal in relaxed state and raises again until maximal contraction, but with opposite direction. The pressure change with interweave angle is the reciprocal of the volume change. That means that the state change is assumed to be isothermal. The gas mass inside the PMA is an important quantity, but it is not described in the article.

This article investigates the force, the surface area and the volume dependent on the interweave angle. The derived models are physical based. The model is incomplete, and there is no context given in which the PMA is driven. The interweave angle is no feasible input into the actuator,

Table 3.2: Parameters and variables of Caldwell et al. [2]

symbol	meaning	validity	obtained	values given?	experiment described?
h, f	geometric braid parameters	specific	calculated	yes	yes
E_{Eff}	efficiency factor	general	literature	yes	-

but it can be substituted by the geometric braid parameters h and f combined with the actual length of the PMA. The model of the volume thus dependent on the length of the PMA is used in this thesis to replace the correspondent model of Hildebrandt et al. [13]. The resulting model equations are introduced in Chapter 4.

For the design of the controller a black box model is used (see Subsection 3.1.3) with duty cycle which represents the gas input as model input and length of the PMA as output.

In a later article Caldwell et al. [3] discuss Polymeric Pseudo Actuators and Pneumatic Muscle Actuators (PMA). For the PMA they give again a model of the PMA force depending on the interweave angle, but the pressure is held constant during the transitions. Depending on the interweave angle the surface area of the PMA is estimated, and depending of the surface area the force is modeled. This article discusses whether the end caps of the PMA should be included into the calculation or not. The resulting plot shows that there is only a difference in nearly maximal extended state, so this property can be neglected in practical use. Also in this article there is no context given, and the model is not feasible in practical use, because the interweave angle cannot be measured online. For substituting this angle there are not enough parameters given. In this later article the geometric braid parameters are reduced to one parameter which is not described well enough for use. Also there is no relationship given between the PMA force and the length change.

Hannaford et al. [12] use a system of two PMAs in parallel with a hydraulic damper, and both in series with a bi-linear, two spring implementation of an artificial tendon. They give a parabolic

length-force equation and a hyperbolic length-velocity-force equation, both without describing the obtainment of the parameters, and they perform work loop experiments with concentric activation profiles. They develop a new sensor which acts like a robotic PMA spindle and compare it to a natural PMA spindle. Because of the input-output constellation with PMA length as input and the force as output the given model is not useful for this thesis.

Van Ham et al. [11] discuss several properties like the used valves for the PMAs in detail. Their experimental setup consists of two pneumatic PMAs and one joint. In the text description the pressure is used as input into the PMAs, and as output the angle and the compliance of the joint are chosen. According to this, the input of the single PMAs is the pressure and the output the length change. The angle of the joint depends on a weighted difference of both inner PMA pressures, and the compliance is determined by a weighted sum of pressures. These different dependencies allow an independent adjustment of the angle and the compliance. The mathematical model describes the force dependent on the PMA contraction:

$$F_t = p \cdot l^2 \cdot f_t \left(\epsilon, \frac{l}{R} \right) \tag{3.5}$$

F_t	-	generated force
p	-	supplied gauge pressure
l	-	maximum PMA length
R	-	unloaded radius
ϵ	-	contraction
f_t	-	dimensionless function, given for different $\frac{R}{l}$ as graph $\rightarrow$ too imprecise for use

One problem described earlier in this section is the threshold pressure due to the elasticity of the rubber tube and the braid of the PMA which has to be overtaken before any action in radial direction can occur. Also there is some hysteresis caused by friction between the rubber tube and the braid. Van Ham et al. avoid both problems by using a pleated instead of a braided pneumatic PMA, pictured in Figure 3.2. The pleated PMA consists mainly of a membrane which is arranged into radially laid out folds that can fold and unfold without a pressure threshold or friction.

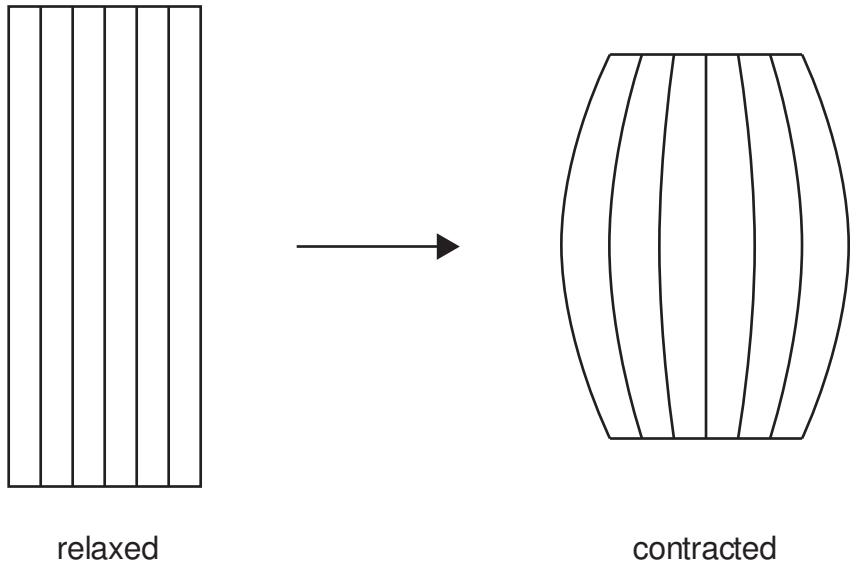

Figure 3.2: Pleated Pneumatic Muscle Actuator (PMA)

The main focus of the article is a detailed investigation of the valves which control the pressure inside the PMA. The discussion mainly regards the opening and closing time of the valves and also postulates the use of light-weighted valves. There are two different kinds of valves: valves which work continuously and valves which work with an on-off control. Continuous working valves are too heavy and too slow, but one valve with on-off control cannot work precisely enough. As a solution, the article presents an array of fast switching and light on-off-valves. One of these valves weights 25 g and switches in around 1 ms. The inner volume of the PMA is set constant. The increasing of the pressure occurs twice as fast as the decreasing, so the double number of outlet valves with respect to the inlet valves should be used. In experiments the best number of valves is identified to two inlet and four outlet valves. The inlet mass flow will although be larger than outlet mass flow due to different supported pressure differences of the valves.

Summarizing, this article gives no useful model, but some ideas about the valves. Also the article describes some advantages of pleated pneumatic PMAs instead of braided PMAs. Because of the missing model this idea cannot be used in this thesis.

Chou et al. [6] investigate a pneumatic circuit in order to separate properties of pneumatics and actuator mechanics. They model the pneumatic circuit with elements of an electrical circuit.

The parameters of the model are regarded as lumped. The most important state variables in a pneumatic circuit are pressure and mass flow. So the mass flow ω is represented by the current. The pressure is measured at the beginning (P_1) and at the end of the PMA (P_2) and their difference ($P_1 - P_2$) is regarded as voltage. The gas viscosity caused by tubing and the connections is modeled as resistance R, and the gas accumulator is regarded as linear capacitor C. The volume of the tube is neglected, only the volume of the accumulator is regarded. The state change is assumed to be isothermal.

The article gives three different successive models with P_1 as input and P_2 as output. In the first model, the whole system is modeled as a linear low pass filter. In the second model, the model of the resistance is improved, and the third model contains additionally a term for the gas inertia. The parameters of the models are given and their obtainment is described. The results are very satisfying. In this thesis there is no model of the pneumatic circuit needed, because the pressure is supplied and therefore the behavior of the gas can be regarded as ideal.

Model of the Friction Force

In the models described above the friction force of the load is not regarded satisfying. Chou et al. [6] propose to add a typical constant value, Hildebrandt et al. [13] regard only dynamic friction and the partly models do not regard a load.

Dry friction force behaves very nonlinear. It consists of several components. If the velocity of the regarded object is different from zero, the object is slipping. During slipping the friction component which depends on the velocity has got more influence than the static component. For this dynamic dependency a simple model can be chosen. If the velocity is zero, the object sticks on the ground or wall, and a friction component which is independent from velocity is more important. This sticking friction behaves very nonlinear, because a threshold has to be overcome before the object can move. Models with continuous friction force are very complex and numerically difficult to handle, so Karnopp [16] presents another way of modeling the dry friction. He deals with dry slip-stick friction. His approach is to divide the movement of the regarded object into two states, slipping and sticking. Karnopp defines a region around zero

velocity. Inside this region the velocity is assumed to be zero, and the object sticks. There the friction is modeled to depend on the other forces. Outside this region, the object slips, and there is an arbitrary friction force law used which depends on the velocity. The principle is illustrated in Figure 3.3.

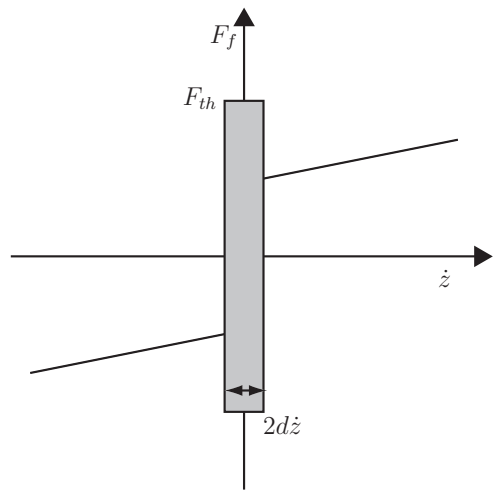

Figure 3.3: Characteristics of the Karnopp friction force model, adapted from [16]

3.1.2 Mixed models

In this group of models two different models are discussed. The first one was developed by Repperger et al. [23, 24]. Their experimental setup is not described exactly, but also consists of one PMA and a driven mass. The PMA is modeled as a mechanical system with passive parallel elements, one viscous element and one spring element, and a pressure source as contractile element. Its parameters are assembled in Table 3.3. The main model equation is the balance of forces:

$$M\ddot{x} + B(\dot{x})\dot{x} + K(x)x = u \tag{3.6}$$

M	-	mass
x	-	length change of the actuator
K	-	spring variable
B	-	damping variable
u	-	input, contains pressure and area, unit of force

The spring and the damping variables are both linear second-order polynomials depending on the length change resp. velocity of the length change of the PMA. Their coefficients are different

Table 3.3: Parameters and variables of Repperger et al. [23, 24]

symbol	meaning	validity	obtained	values given?	experiment described?
M	mass	specific	unit mass	-	-
$K(x)$	spring variable	specific	experimentally	yes	(yes)
$B(\dot{x})$	damping variable	specific	experimentally	yes	(yes)

for PMA contraction and extension, because it is easier to release the pressure inside the PMA against the environment pressure than to build it up against its own rising pressure. These coefficients are identified experimentally. The step responses of the PMA to pressure with different, constant loads are recorded. From the steady state data the spring coefficients are identified, additionally the steady state force is determined. This determination of the steady state force is not described clearly. The total force is measured, and the transient force is determined as the difference of total and steady state force. With knowing the transient force the coefficients of the damping variables are obtained by regression over velocity.

The input u is not described detailed enough. It is split into the affine control $\tilde{u}$ with unit of pressure and γ, which is an effective area variable. Together they have got the unit of force ($u = \tilde{u}\gamma$). In the descriptions the articles mix force and pressure. Force as input into the PMA is not feasible, but it is not described how the surface area is obtained which is necessary if the pressure is used as input. For calculating the force/weigth-ratio of the PMA the relationship: net force = pressure $*$ Δ surface area of PMA balloon is given and values for Δ surface area are used, but there is no further explanation about it. In the article the input u is generated directly by the controller.

The given model is very simple. It is given as nonlinear differential equation with relative degree of r = 2 with pressure / force as input and length change of the PMA as output. The different coefficients for PMA contraction and expansion represent some hysteresis of the PMA. The velocity-dependent friction is included in the damping variable, and the velocity-independent friction is included in the spring variable.

There are several properties which are not regarded. There is no term concerning the weight force, non-modeled nonlinearities or other disturbances. Also, there is no threshold pressure or

the wall thickness of the PMAs regarded. The input itself is not described clearly. An other disadvantage is that all nonlinearities are identified experimentally instead of modeled physically. The model is not validated. In this form it is not feasible for practical use.

A second model which uses pressure as input and length change as output is presented by Reynolds et al. [26]. The experimental setup consists of two PMAs connected by a pulley transmission. The pulley carries a load stack. The setup is designed antagonistically, but only one of the PMAs is used at a time and the other one is fixed, so the setup acts like one PMA and a vertically driven mass. For calculations with concrete values the 2:1 transmission of the pulley has to be regarded. Also in this model the PMA is modeled as mechanical system with passive parallel elements, a viscous element, a spring element and a contractile element. Its parameters are assembled in Table 3.4. The main model equation is the balance of forces:

$$M\ddot{x} + B(p)\dot{x} + K(p)x = F_{ce}(p) - Mg \tag{3.7}$$

M	-	total mass, assumed to be concentrated in the vertically driven mass
x	-	length change of the actuator
K	-	spring variable
p	-	inner pressure of the PMA
B	-	damping variable
F_{ce}	-	effective contraction force
g	-	gravitation constant

One main difference to the model of Repperger et al. [23, 24] is that the damping and the spring variable are assumed to depend on the inner PMA pressure instead of the PMA length change resp. its velocity. Also the effective contraction force F_{ce} is modeled to depend on the inner pressure. All three variables are modeled as linear first order polynomials. Their parameters are identified in similar experiments. For identifying the spring and the damping variables a so-called 'bell-ringer study' is performed. That means that there are different levels of pressure which are constant during the single experiments, and the step responses to load are recorded as length change against time. The spring variable is obtained via regression of the spring constant against pressure from the steady state data, and the damping variable is obtained via regression

Table 3.4: Parameters and variables of Reynolds et al. [26]

symbol	meaning	validity	obtained	values given?	experiment described?
F_{ce}	contractile force	specific	experimentally	yes	(yes)
M	mass	specific	measured	yes	-
K	spring variable	specific	experimentally	yes	(yes)
B	damping variable	specific	experimentally	yes	(yes)

of the damping constant against pressure from the dynamical data. The contractile force is constant, because it is assumed to depend only on pressure which is held constant.

To obtain the model for the contractile force, a contraction study is performed. Here the loads are different, but constant during the single tests, and the step responses to pressure are recorded. The spring and the damping variables are used from the bell-ringer study. Via regression the coefficients of the force model are obtained. The estimated contractile force is compared to a theoretical estimate from an equation given in [6]. This implementation is not described further.

A relaxation study is performed to obtain the damping variable during PMA extension. One constant load is used, and the step response to pressure is recorded. The damping variable is obtained per regression in the diagram of length change against time. The spring variable is also estimated, but identical to the spring variable for contraction.

The obtained spring and damping variables at constant pressure are assumed to be the same functions than in the dynamical case.

The described model is very simple. It is given as a second order differential equation with pressure as input and length change of the actuator as output. With the different damping variables there is also a hysteresis regarded. The differentiation whether the PMA is longer or shorter than in relaxed state is regarded in the spring and damping parameters.

There are some properties which are not regarded, e.g. a threshold pressure and the influence of the thickness of the PMA wall. Also, there is no term for non-modeled nonlinearities and disturbances. All nonlinearities in the model are identified experimentally instead of modeled

physically.

This model is the only described model which is validated, but the results are not very exact. The error comes up to 30 %. For the validation a triangular pressure wave input is used. The model seems to be feasible in the given form, but it is too simple to be useful.

3.1.3 Black box models

In this subsection a black box model is presented. It was developed by Caldwell et al. [2]. The experimental setup is the design of an arm. The shoulder and the wrist have both got three degrees of freedom, which is realized by the use of respectively three different joints. The elbow has got one degree of freedom. The system has got an air flow and a pressure regulation. The piping length from the valves to the PMAs is as short as possible to reduce transport losses, and the joints move nearly free of static friction. The input into the model is the duty cycle which is the time the PMA is connected to the pressurized air supply related to the valve pulse period (25 ms). The output of the model is the length of the PMA.

With experimental tests some input-output data records are obtained. The order of the model and with this the needed number of parameters is analyzed offline by the help of MATLAB. According to this result the model equation is

$$\left(1 + a_1 q^{-1} + a_2 q^{-2} + a_3 q^{-3}\right) y(k) = \left(b_0 q^{-3} + b_1 q^{-4} + b_2 q^{-5}\right) u(k) + d + n(k) \tag{3.8}$$

y	-	position sensor reading
u	-	duty cycle
d	-	constant which represents the effects of non-zero means in the input-output data
$n(k)$	-	noise

The parameters itself are identified online with recursive least square. For all parameters the average estimated values are given.

3.1.4 Applications

Last, some applications of the PMA are presented. Van der Linde [32] investigates the gait of a biped robot. For an energy efficient gait, he models two PMAs and a joint as pendulum, and uses the natural frequency of the robot instead of conventional servo mechanisms which obey a calculated trajectory. The activation of the PMAs occurs phasic. The results seem to be satisfying.

Takuma et al. [29] also investigate the gait of a biped robot which walks with PMAs. The robot consists of three joints actuated by respectively two antagonistic PMAs. The article gives no mathematical model of a PMA. The focal point is an investigation about the influence of dynamic and control parameters during locomotion. The main dynamic parameter the position of the center of the gravity, and the main control parameter is the waiting period to swing the leg.

Park et al. [20] also use two PMAs and a joint, but they investigate non-cyclic movements of a robot arm. For a better and softer control of the end point, a flexible link is added. This link is difficult to control because of the high frequency vibrations. The whole system is divided into a slow subsystem which represents the rigid body motions and a fast subsystem which represents the dynamics of the flexible links and the servo valves. The input into the PMAs is the pressure. The setup and the according physically based model are described in detail, also the experiments and their results, and the performance seems to be very good.

3.2 Performed control strategies

Normally a Pneumatic Muscle Actuator (PMA) shall be driven along a reference trajectory. Therefore a closed loop control is necessary. The behavior of Pneumatic Muscle Actuators is very complex and nonlinear, so the controller cannot be designed only by linear standard methods. Also there are not all properties regarded in the models, because then the model would be too complex to deal with. There are mainly the approaches to linearize the models dynamically and apply a linear standard control method respectively a robust control method afterwards, and to design a nonlinear controller.

In Section 2.3 some existent applications of these approaches are introduced. Here some of the designs and implementations are presented. Subsection 3.2.1 deals with some linearization methods. Subsection 3.2.2 introduces an application of a robust controller, and Subsection 3.2.3 presents some existing performances of adaptive controllers. Some approaches of robust adaptive control are described in Subsection 3.2.4.

3.2.1 Linearization technologies

A nonlinear plant can be dealt with e.g. by linearization. Afterwards, a linear controller can be designed. In this subsection some possible basic designs and existent implementations are discussed.

Sliding mode

One of the possible designs of feedback linearization is the sliding mode, which was applied by Carbonell et al. [4] and Repperger et al. [23]. The general idea is described in [1]. The control law drives the states of the system to a surface, and after reaching the surface the states slide along. On this surface the feedback is linear.

Carbonell et al. perform a sliding mode controller. The derived equations are given in the article, but the implementation is described very short. The exponential stability is proved.

The tracking of the controller works perfectly, but the control signal chatters, which is a general drawback of sliding mode controllers. According to Åström et al. [1] this chattering could be

reduced/ avoided by smoothing the relay characteristics.

Repperger et al. [23] also use the sliding mode, coupled with a Variable Structure Controller (VSC). They construct a time-varying sliding surface $S(t)$. The control law includes the surface variable $s(t)$ and forces the state space trajectories onto the surface by computing the model input $u(t)$. On the surface which is reached at $\dot{s}(t) = 0$ the error dynamics are simple exponential, no more nonlinear.

There are additionally switching conditions, because the controller switches between PMA contraction and extension. This switching law is modified to ensure that the composite controller provides asymptotic tracking stability. The derived equations are given, but the performance of the controller is not described.

Flatness based controller

Hildebrandt et al. [13] apply a flatness based controller which is model based and works feedforward.

This approach bases on differential flatness of the model. Differential flatness means that the model has got a (vectorial) output which is a function of the (vectorial) input and the (vectorial) state. Also, it has to be possible to express all inputs and states by the output(s) and its derivatives. So the model equation must be invertible. This property can be used for the controller. There the nonlinearities of the model are canceled by the 'inverse system'. After linearizing a simple linear control technology, here a third pole placement controller can be applied.

In the article the mathematical derivations are given complete. The experimental results are described and plotted and look very good.

Switching controller

Depending on the character of the non-linearity, it is also possible to design different controllers for different dynamics of the controlled plant, here PMA contraction and extension.

Ham et al. [11] apply two different controllers which are modified to work as switching controllers. One of them is a modified Pulse Width Modulation (PWM) controller. A positive error (pressure too low) requests an action of the two inlet valves and a negative error requests an action of the four outlet valves. Normally in a PWM controller design there is only one output. Following, the magnitude of the error is used to generate the PWM signal and the sign determines the used valve. In the article there are more valves used. An improvement of the control was reached by controlling the different valves separately. The duty cycle which is the percentage time the valve is connected to the pressure supply is calculated as if there were only one valve, and if the computed cycle is higher than 100 %, more valves are used and the duty cycle is distributed equally to the valves.

The second controller is a bang-bang controller. Normally it regards only the sign of the error. Here the output signal is split into control for inlet and outlet valves and a dead zone to avoid oscillations in the requested pressure. Also here the valves are controlled separately, but respectively two outlet valves are merged.

Both controllers are performed for constant volume of the PMA. The bang-bang controller needs fewer processor time, so in the following the bang-bang controller is used.

The complete joint controller consist of two bang-bang pressure controllers with two different action zones and a dead zone, one for each PMA, and a higher-level position controller.
The higher level position controller is an adaptive PID-controller. In the experiments it was tested to switch off temporarily parts of the PID controller, but especially after including the varying volume of the PMA it was decided to use the full PID controller.

Finally one high level adaptive PID controller combined with two bang-bang-controllers for the pressure inside the PMAs are used.

There is no result concerning the performance of the high level controller given. For the performance of the low level pressure control there are two plots given, but not described sufficient.

3.2.2 Robust control technologies

With uncertainties in the model the controller can be designed as a robust controller. A robust controller is a constant controller which regards bounded variations. The principle of this approach is described in Subsection 2.3.2. There are many different designs which are possible, one very important design is the H^∞ control, e.g. applied by Osuka et al. [19]. H^∞ control bases on a cost function which considers the desired properties. This cost function contains weighting matrices representing the importance of the properties. The controller minimizes this cost function.

Osuka et al. control the angle computed by two PMAs with servo-valves. Whether the controlled variable is the pressure or the mass flow is not clear, but also not interesting here. They give a nominal plant model which is a black box model identified from the experimentally obtained Bode diagram. Also a multiplicative uncertainty factor δ is estimated from the Bode diagram.

The article is very short. All functions and parameters are given, also a plot of a result, but not described well.

3.2.3 Adaptive control technologies

A second way of controlling nonlinear systems is to use an adaptive technology. There, the controller itself is nonlinear. There are the two different approaches direct and indirect adaptive control which are described in Subsection 2.3.3. In the direct adaption, the parameters of the controller are adapted directly, in the indirect adaption the parameters of the model are adapted and according to this the controller parameters are changed. First some applications of direct adaptive control are presented, second some applications of indirect adaptive control.

Direct adaptive control

One important direct adaptive control method is the gain scheduling, described in [28]. For applying this method it has to be known how the dynamics of a process change with the operating conditions [1]. So the operating conditions are monitored during the process and the parameters of the controller are adapted according.

Repperger et al. [24] use the gain scheduling method, but they give only two look-up tables about the changes of the process dynamics which are described as black box, but no explanation or equation.

Carbonell et al. [4] also apply a gain scheduling controller. They describe their implementation better. The performance of the controller is shown. The controller works very slowly, and the exponential stability is proved only for slowly-varying reference signals.

Indirect adaptive control

One important method of indirect adaptive control is the Backstepping control, described in [1, 30]. This is an effective method for the control of nonlinear systems, but can also be applied for linear systems. The control objective is to design a state feedback controller which guarantees that all closed loop signals are bounded and that the system output tracks a given output asymptotically. For this, an error equation is derived. Then a control law and a parameter adjustment law are constructed such that the state of the error equation goes to zero.

The backstepping approach is applied by Carbonell et al. [4]. They give the used equations and prove the ultimate boundedness of all signals.

In the article the performance of three different controllers is compared. The used controllers are a sliding mode, a gain scheduling and a backstepping controller. The backstepping controller yields the best result with a good tracking also for fast changing reference signals and the computed control signal is relatively smooth.

A second method is an adaptive pole placement controller. The poles of a system are crucial for the stability, and a pole placement controller cancels instable poles of a plant and gives it new desired poles.

This method is applied by Caldwell et al. [2]. In the article two controllers with different orders are compared. The controller with the higher order gives a significant improvement of the performance. In the text it is said that accuracies of 1° are possible, but the plotted graphs look worse.

Medrano-Cerda et al. [18] perform angle and compliance control of two antagonistically coupled PMA, also by using an adaptive pole placement controller. The plotted steady state response to a sinusoidal input does not look very good, the controller seems to react relatively slowly.

3.2.4 Robust adaptive control

Often adaptive and robust control are combined to a robust adaptive controller [28].

Park et al. [20] split their system in a slow and a fast subsystem (see Section 3.1). For the slow subsystem a robust adaptive controller was developed by using a pole placement approach which bases on μ-synthesis. The fast subsystem is controlled by sliding mode control scheme with sliding surface designed using H^∞ control.

Also Freeman et al. [10] design a robust adaptive controller. This article does not deal with PMAs. For the adaptive controller a tuning function and modular design are used, and both are made robust.

Jiang et al. [15] use a modified adaptive backstepping design for a class of nonlinear systems. Also this article does not deal with PMAs. The controller is designed for three types of uncertainties: unknown parameters, uncertain nonlinearities and unmodeled dynamics. In the article a robustification methodology is described.

In this chapter several existing models of a PMA and several performed controller strategies are discussed. In most of the models important parts are identified experimental, so it is not possible to apply them in this thesis. Many models are not described complete, and only one model is validated by comparing the simulated output to the real output. The model of Hildebrandt et al. [13] is the most detailed physical based model. Therefore, with replacing the models of the volume by the model of Caldwell et al. [2] and with replacing the model of the friction force by the model of Karnopp [16] the model can be adapted for using in this thesis.

There are also many different controller strategies implemented. Not all of the controllers are validated. Because of the different described test methods of the validated controllers a direct comparison is difficult. Also in most articles the control signal which is also important for the quality of a controller is not given. The best tracking results are achieved by the feedback linearization controllers. The control signal of the sliding mode controller implemented by Carbonell et al. [4] chatters very bad. The control signal of the flatness based controller implemented by Hildebrandt et al. [13] is not described or plotted. Nevertheless, because of the good tracking results a flatness based controller is implemented in this thesis.

Chapter 4

Model of the Pneumatic Muscle Actuator (PMA)

In this chapter the performed model of the PMA is presented. In Section 4.1 the physical model is described. The according state space form is introduced in Section 4.2. The extension of the model of a PMA to a joint driven by a PMA occurs in Section 4.3. Last, the implementation of the model in MATLAB/ Simulink is described and validated in Section 4.4.

4.1 Physical model

4.1.1 General Structure of the Model

In Section 2.2 the two possible main structures of a model are described. In this thesis there is no real PMA used, so only a physical based model can be performed, because no real input-output data can be obtained. From the models described in Section 3.1 the models of Hildebrandt et al. [13] and Caldwell et al. [2] are merged. The general structure of the model is illustrated in Figure 4.1.
The complete model consists of an intrinsic PMA, a Valve, a pressure supply and a carried load. The input into the system is the command voltage $U(t)$, and the output is the PMA length $z(t)$.

The pressure supply with the pressure p_s is separated from the PMA by a valve. The command voltage determines proportionally the orifice area $a(t)$ of this valve. The mass flow of gas $\dot{m}_g(t)$ from the pressure supply into the PMA is controlled by the valve. Due to this mass flow the inner pressure $p(t)$ and the inner volume $V(t)$ of the PMA are changing. Therefore a PMA

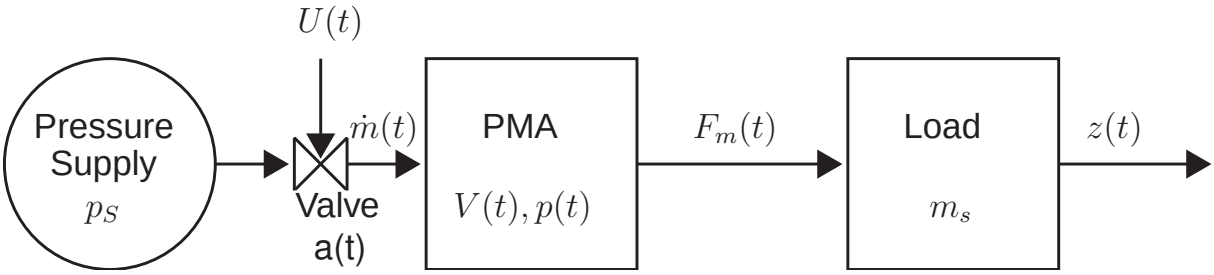

Figure 4.1: Main structure of the model

force $F_m(t)$ is generated which can be used to carry a load with the solid mass m_s. The length $z(t)$ of the PMA can be expressed by the position of the carried load.

4.1.2 Assumptions and properties

In the model of the single PMA the experimental setup consists of a PMA which drives vertically a load. This setup is pictured in Figure 2.2.b. The used gas for driving the PMA is air.

The pressure source is supplied and therewith the supply pressure is assumed to be constant. Also the temperature, the specific heat ratio of air η and the polytrophic exponent χ are assumed to be constant. The valve is assumed to behave ideal. All mass is assumed to be concentrated in the center of gravity of the driven load. The PMA is regarded as piston.

The elasticity effects of the material, the dry friction between the rubber and the shell and effects of the wall thickness cannot be regarded in this model, because therefore measurements with a concrete PMA had to be performed.

The threshold pressure which has to be overcome before any action can take place is regarded as threshold force which depends on the pressure in the Karnopp friction model, described in Subsection 4.1.6.

The complete model is highly nonlinear, but time-invariant.

4.1.3 Expected behavior

The basic principle of a PMA is that with rising pressure the PMA induces a force. So the force is expected to be at its maximum at maximum inner pressure. With raising pressure the area of the PMA raises and following the PMA shortens. This means that the pressure inside the PMA is expected to behave inverse to the PMA length.

A heavier driven mass is expected to require a higher pressure, because there a greater force is needed to drive the mass.

4.1.4 Valve

At first the valve function is modeled. The valve is a 5/3-way-function valve which means that it can work in both directions. The mass flow $\dot{m}_g$ depends on the orifice area which depends on the command voltage, on the pressure inside the PMA, on the supply pressure and on the properties of air. The relationship between the mass flow and the command voltage on the valve is developed analytical.

$$a(t) = c \cdot U(t) \tag{4.1}$$

$a(t)$	[m^2]	-	orifice area of the valve
c	$\left[\frac{\text{m}^2}{\text{s}}\right]$	-	constant of proportionality on the valve
$U(t)$	[V]	-	command voltage

$$\dot{m}_g(t) = c \cdot U(t) \cdot p_s \cdot \psi(t) \tag{4.2}$$

$$\psi(t) = \sqrt{\frac{2\eta}{RT_s(\eta-1)}\left[\left(\frac{p(t)}{p_s}\right)^{\frac{2}{\eta}} - \left(\frac{p(t)}{p_s}\right)^{\frac{\eta+2}{\eta}}\right]} \tag{4.3}$$

$\dot{m}_g(t)$	$\left[\frac{\text{kg}}{\text{s}}\right]$	-	supplied mass flow into the PMA
p_s	$\left[\frac{\text{N}}{\text{m}^2}\right]$	-	supply pressure, assumed to be constant
T_s	[K]	-	supply temperature, assumed to be identical to the environment temperature
η	[-]	-	specific heat ratio of air, assumed to be constant
$p(t)$	$\left[\frac{\text{N}}{\text{m}^2}\right]$	-	pressure at the valve output, identical to the pressure inside the PMA

For a negative mass flow the command voltage has to be negative.

4.1.5 PMA

Pressure

Next, the intrinsic PMA is modeled. The main properties of the PMA are the inner pressure and the volume. The pressure derived from the ideal gas equation:

$$m_g(t) = \frac{p(t)V(t)}{RT} \tag{4.4}$$

$m_g(t)$	[kg]	-	gas mass inside the PMA
$p(t)$	$\left[\frac{\mathrm{N}}{\mathrm{m}^2}\right]$	-	pressure inside the PMA
$V(t)$	[m^3]	-	inner volume of the PMA
R	$\left[\frac{\mathrm{J}}{\mathrm{kgK}}\right]$	-	specific gas constant for air
T	[K]	-	gas temperature, assumed to be constant and identical to the environment temperature

The state change is assumed to occur polytrophic, which means that the system can partly exchange heat energy with the environment. The polytrophic gas law is described by

$$pV^{\chi} = \text{constant} \tag{4.5}$$

χ	[-]	-	polytrophic exponent, constant

From Equation 4.4 and Equation 4.5 the following differential equation can be derived, which is taken from Hildebrandt et al. [13].

$$\dot{p}(t) = \frac{\chi}{V(t)}\left(RT\dot{m}_g(t) - p(t)\dot{V}(t)\right) \tag{4.6}$$

with

$$\dot{V}(t) = \frac{dV(t)}{dt} = \frac{dV(t)}{dz} \cdot \dot{z}(t) \tag{4.7}$$

Volume

For the volume of the PMA the model of Caldwell et al. [2] is used. There the volume is modeled to depend nonlinear on the length of the PMA. The model equation is derived in Appendix A.1. This model is based on the assumption that there is one point where the PMA is nearly relaxed.

At this point the pressure inside the PMA is minimal and the volume maximal. As soon as the PMA contracts or is elongated the inner pressure rises and the volume is reduced.

$$V(t) = \frac{\pi f^2}{4h^2} \cdot (h^2 - z^2(t)) \cdot z(t) \tag{4.8}$$

h	[m]	-	helical fiber length of the PMA
f	[m]	-	diametric distance parameter of the PMA

4.1.6 Load

The second necessary differential equation is the balance of forces which is based on Newton's second law. The affecting forces are shown in Figure 4.2.

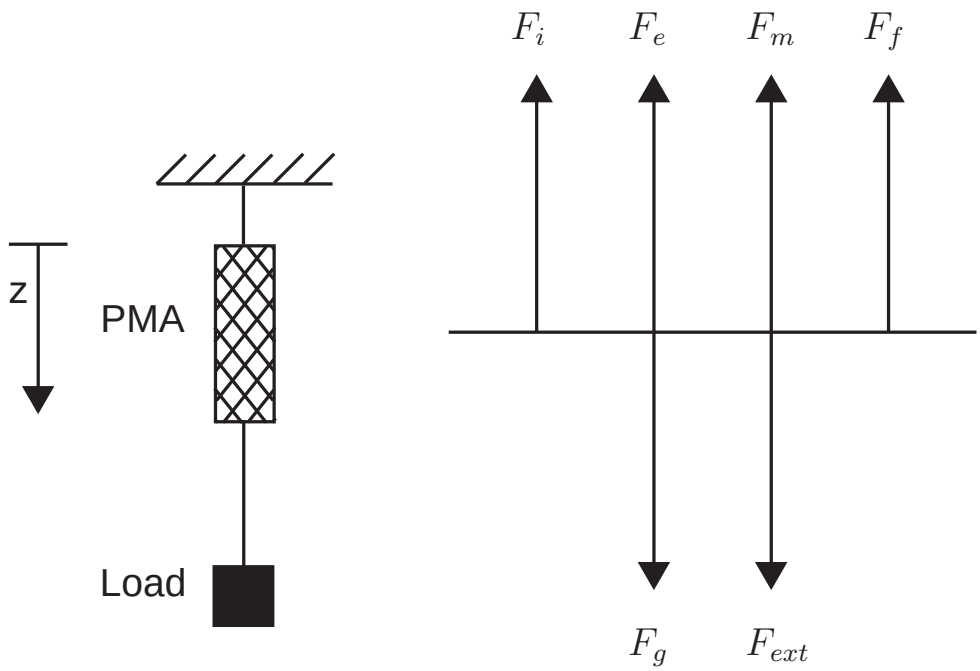

Figure 4.2: Scheme of the affecting forces on the PMA

The z-direction is defined like drawn in the figure, z rises with the elongation of the PMA. The PMA drives a mass vertically.

$$F_i(t) = F_g + F_{ext}(t) - F_m(t) - F_e(t) - F_f(t) \tag{4.9}$$

$z(t)$	[m]	-	z-coordinate of the driven mass, corresponds to the length change of the PMA
F_i	[N]	-	inertial force

F_g	[N]	-	gravitational force
$F_{ext}(t)$	[N]	-	external force
$F_m(t)$	[N]	-	longitudinal PMA force
$F_e(t)$	[N]	-	elastic force
$F_f(t)$	[N]	-	friction force of the driven load

Inertial force

The balance of forces assumes that if all forces are balanced the regarded object does not accelerate [25]. This assumption is only valid if the system is regarded from an inertial reference frame. This PMA system shall be regarded from a non-inertial frame, which means that the observer moves and accelerates with the system. The observer experiences an acceleration which does not exist for an observer outside the system. Following for the transformation to a non-inertial frame a so-called pseudoforce, also called inertial force, must be introduced. It affects the PMA in opposite direction of the movement.

$$F_i(t) = m_s \ddot{z}(t) \tag{4.10}$$

m_s	[kg]	-	total solid mass, assumed to be concentrated in the driven mass

Gravitational and external force

As written in Section 2.1 the PMA is a pulling actuator. It can only contract, so for elongation an antagonistic action must occur. Therefore a weight or an external force, e.g. computed by a second PMA can be used. These forces act in positive z-direction. In contrast to the external force $F_{ext}(t)$ the gravitational force F_g does not depend on the time.

$$F_g = m_s g \tag{4.11}$$

g	$[\frac{\mathrm{m}}{\mathrm{s}^2}]$	-	gravitation constant

PMA force

The PMA force is generated by the contracting of the PMA, which means that at maximal contraction the PMA force is maximal and at maximal elongation the PMA force is minimal. It

depends on the inner pressure and the volume change due to the length change. It helps carrying the load, so it is defined against the z-direction.

$$F_m(t) = (p(t) - p_0) \cdot \frac{dV(t)}{dz} \tag{4.12}$$

F_m	[N]	-	longitudinal PMA force
p_0	$\left[\frac{\mathrm{N}}{\mathrm{m}^2}\right]$	-	environment pressure

with

$$\frac{dV(t)}{dz} = \frac{\pi f^2}{4h^2}\left(h^2 - 3z^2(t)\right) \tag{4.13}$$

which is derived in Appendix A.1.

The static characteristics of the PMA force in contracted and relaxed state are plotted for different loads in Figure 4.3.

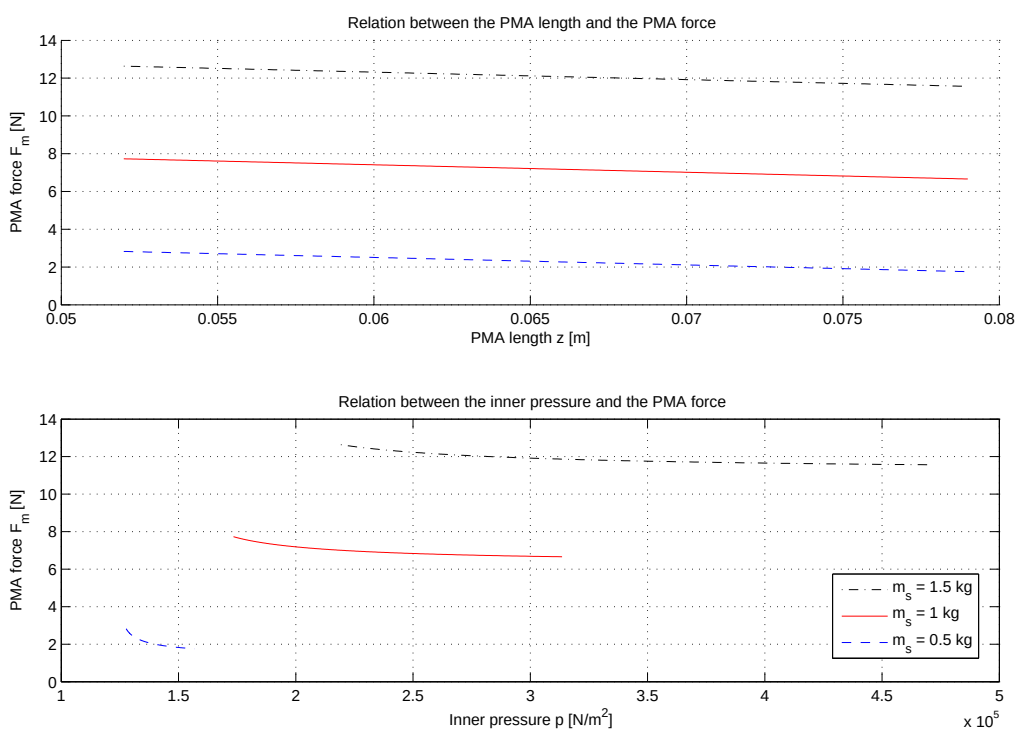

Figure 4.3: Static relation between the PMA length respectively the inner pressure and the PMA force

Elastic force

The elastic force is modeled as spring force. Therefore, it depends linearly on the length of the PMA. It causes contraction of the PMA, so its direction is also against the z-direction.

$$F_e(t) = Kz(t) \tag{4.14}$$

K	$\left[\frac{\text{kg}}{\text{s}^2}\right]$	-	proportional spring constant

Friction force

The direction of the friction force is in general defined against the z-direction. For the friction the model of Karnopp is used which is described in Subsection 3.1.1. There two different modi of the system are regarded, one describes the system during slipping and one during sticking. Both modi have got a different friction law.

For the slipping mode a proportional friction law is used:

$$F_{f,slip}(t) = C\dot{z}(t) \tag{4.15}$$

$F_{f,slip}$	[N]	-	friction force during slipping
C	$\left[\frac{\text{kg}}{\text{s}}\right]$	-	proportional friction constant

In the sticking mode the friction depends on the other affecting forces.

$$F_{f,stick}(t) = F_{ext}(t) + F_g - F_m(t) \tag{4.16}$$

$F_{f,stick}$	[N]	-	friction force during sticking

The balance of forces (Equation 4.9) has got the force of the PMA as input and the length of the PMA as output. During the movement, which means during the slipping mode, all other forces and constants are known or modeled independently. As soon as the velocity of the load is inside the zero region, the friction law is switched to the sticking law. The PMA length is known from the last value before the law was switched respectively from the initial condition, and instead the friction force can be calculated with the balance of forces. Due to pressure or load changes also the friction force changes. As soon as it overcomes a threshold force, the load begins to move again and the friction law is switched to the slipping law.

4.2 State space model

In Figure 4.4 the general view of a system is shown. The view contains the intrinsic system, inputs and outputs. The intrinsic system is described by a (vectorial) state variable $\underline{x}(t)$. The input $\underline{u}(t)$ and the output $\underline{y}(t)$ can also be vectorial.

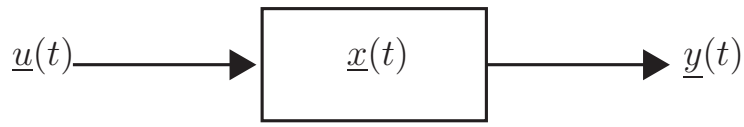

Figure 4.4: General view of a system

One method of describing this system mathematical is the state space form. The general state space form for nonlinear models is:

$$\dot{\underline{x}}(t) = f(\underline{x}(t), \underline{u}(t), t) \tag{4.17}$$

$$\underline{y}(t) = h(\underline{x}(t), \underline{u}(t), t) \tag{4.18}$$

with $\underline{x}(t) \in \mathbb{R}^n$ being the state vector, $\dot{\underline{x}}(t) \in \mathbb{R}^n$ being the first time derivative of the state vector, $\underline{u}(t) \in \mathbb{R}^m$ being the input vector, $\underline{y}(t) \in \mathbb{R}^q$ being the output vector and t being the time.

First, the states, inputs and outputs of the regarded system are determined:

$$\underline{x}(t) = \begin{pmatrix} p(t) \\ z(t) \\ \dot{z}(t) \end{pmatrix} \tag{4.19}$$

$$u(t) = U(t) \tag{4.20}$$

$$y(t) = z(t) \tag{4.21}$$

with $p(t)$ being the pressure inside the PMA, $z(t)$ the length of the PMA, $\dot{z}(t)$ the time derivative of the length of the PMA and $U(t)$ the command voltage to the valve.

The regarded system is autonomous, which means that on different times with the same input and at the same states the system yields the same output. Following, the model equations do not

depend explicit on the time. Also, the system is linear in $u(t)$ and there is no direct feedthrough, which means that the output $\underline{y}(t)$ does not depend directly on the input $\underline{u}(t)$. Therefore, Equation 4.17 can be rewritten as

$$\dot{\underline{x(t)}} = f(\underline{x(t)}) + g(\underline{x(t)})u(t) \tag{4.22}$$

$$y(t) = h(\underline{x}(t)) \tag{4.23}$$

The modeled properties of the PMA system are substituted, simplified and brought into state space form in Appendix A.2. The physical parameters of the model are assembled to the constant parameters α_i which are also defined in Appendix A.2. The resulting state space form is

$$\dot{m}_g(t) = \alpha_1 u(t)\sqrt{\alpha_2 x_1(t)^{\alpha_4} - \alpha_3 x_1(t)^{\alpha_5}} \tag{4.24}$$

$$\dot{x}_1(t) = \frac{\alpha_7 \dot{m}_g(t) - \chi x_1(t)\left(\alpha_8 - \alpha_{10} x_2^2(t)\right) x_3(t)}{\alpha_8 x_2(t) - \alpha_9 x_2^3(t)} \tag{4.25}$$

$$\dot{x}_2(t) = x_3(t) \tag{4.26}$$

$$\dot{x}_3(t) = \frac{1}{m_s}\left[F_{ext}(t) - (x_1(t) - p_0)\left(\alpha_8 - \alpha_{10} x_2^2(t)\right) - K x_2(t) - F_f(t)\right] \tag{4.27}$$

$$y(t) = x_2(t) \tag{4.28}$$

whereas Equation 4.24 is no state space equation, but written separately for a better readability of the equations.

In the slipping mode the friction force is substituted with Equation 4.15:

$$F_f(t) = C x_3(t) \tag{4.29}$$

In the sticking mode the state $x_2(t)$ is constant and following $x_3(t)$ is zero. Also $\dot{x}_3$ is zero. Therefore, the state space model is reduced to

$$\dot{x}_1(t) = \frac{\alpha_7 \alpha_1 u(t)\sqrt{\alpha_2 x_1(t)^{\alpha_4} - \alpha_3 x_1(t)^{\alpha_5}}}{\alpha_8 x_2 - \alpha_9 x_{2,stick}^3} \tag{4.30}$$

$$\dot{x}_{2,stick} = 0 \tag{4.31}$$

$$F_f(t) = F_{ext}(t) - (x_1(t) - p_0)\left(\alpha_8 - \alpha_{10} x_{2,stick}^2\right) - K x_{2,stick} \tag{4.32}$$

$$y_{stick} = x_{2,stick} \tag{4.33}$$

whereas $F_f(t)$ causes no change in the actual output y_{stick}, but is necessary for the change to the slipping mode.

4.3 Extension of the model to a joint driven by PMAs

In this thesis a joint driven by PMAs is modeled. Therefore, several experimental setups are possible. One possibility is the setup of two PMAs which act antagonistically, illustrated in Figure 2.3.b). A second possible setup is one PMA which works antagonistically to the weight of the moved link. This setup is illustrated in Figure 4.5. There are two links of the limb which are connected by a mechanical joint. The PMA affects the links in their center of gravity. One of the links is fixed. The moving link is lifted by the contraction of the PMA and lowered by its weight. The weight is assumed to be concentrated in the affecting point of the PMA at the moved link. This setup is adequate to the physiological setup where the muscles which actuate a joint affect at the bones which are connected by the joint.

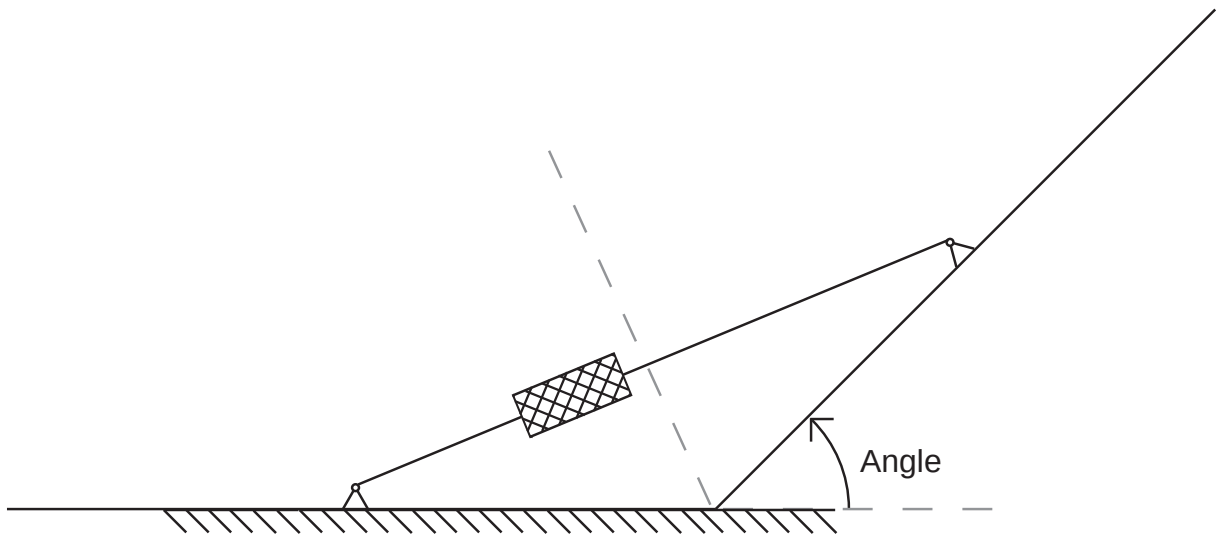

Figure 4.5: Joint driven by one PMA

The geometry of the joint is illustrated in Figure 4.6.

$$s_1 = \frac{L}{2} - z_0 \tag{4.34}$$

$$s_2(t) = \frac{L}{2} - \big(z_0 - z(t)\big) \tag{4.35}$$

$$h(t) = \frac{L}{2}\sin\left(\frac{\alpha(t)}{2}\right) \tag{4.36}$$

$$\beta(t) = \frac{1}{2}(\pi - \alpha(t)) \tag{4.37}$$

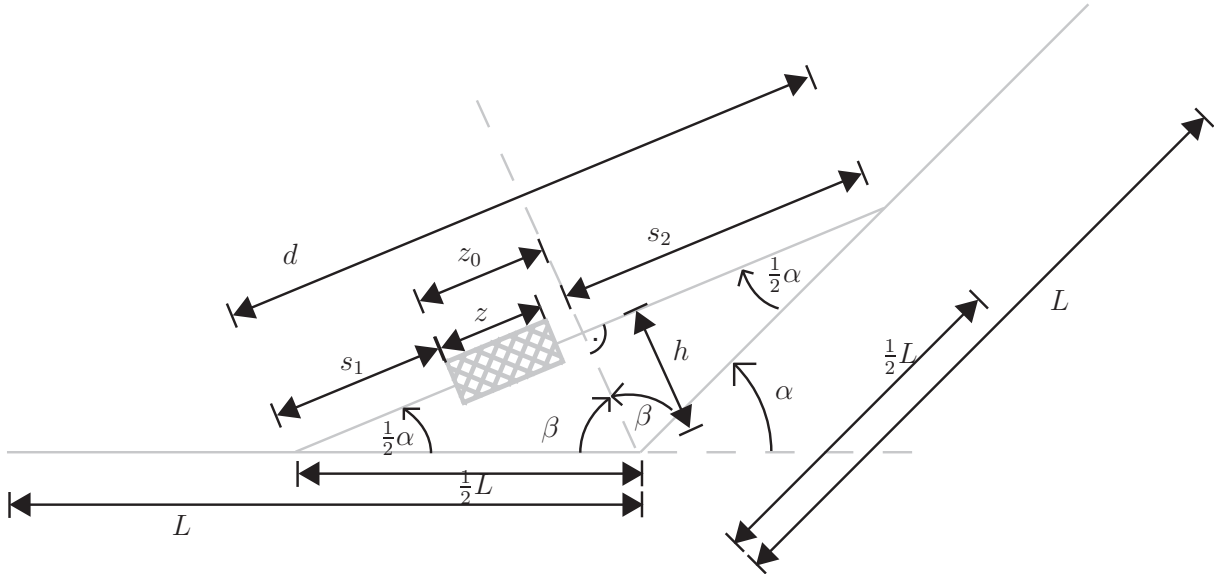

Figure 4.6: Geometry of the joint

L	[m]	-	length of the link
$z(t)$	[m]	-	actual length of the PMA
z_0	[m]	-	resting length of the PMA
$\alpha(t)$	[rad]	-	angle of the joint

Now the geometrical relationship between the joint angle $\alpha(t)$ and the PMA length $z(t)$ can be derived by expressing $d(t)$ trigonometric and by adding the lengthes. It has to be regarded that the direction of the movement is defined opposite, because a longer PMA corresponds to a smaller joint angle.

$$d(t) = 2 \cdot \frac{L}{2} \cos\left(\frac{\alpha(t)}{2}\right) \tag{4.38}$$

$$d(t) = s_1 + z_0 + s_2(t) \tag{4.39}$$

Setting the expressions equal yields

$$L \cos\left(\frac{\alpha(t)}{2}\right) = \frac{L}{2} - z_0 + z_0 + \frac{L}{2} - \big(z_0 - z(t)\big) \tag{4.40}$$

This expression is simplified to

$$\cos\left(\frac{\alpha(t)}{2}\right) = 1 + \frac{z(t) - z_0}{L} \tag{4.41}$$

The resulting relationships for both directions of converting are:

$$\alpha(t) = 2 \cdot \cos^{-1}\left(1 + \frac{z(t) - z_0}{L}\right) \tag{4.42}$$

$$z(t) = L \cdot \cos\left(\frac{\alpha(t)}{2} - 1\right) + z_0 \tag{4.43}$$

In Figure 4.7 this relationship is plotted for three different lengthes of the link. The shorter the links are the greater is the range of the angle, but this is limited by the length of the PMA which has to be shorter than the link length L.

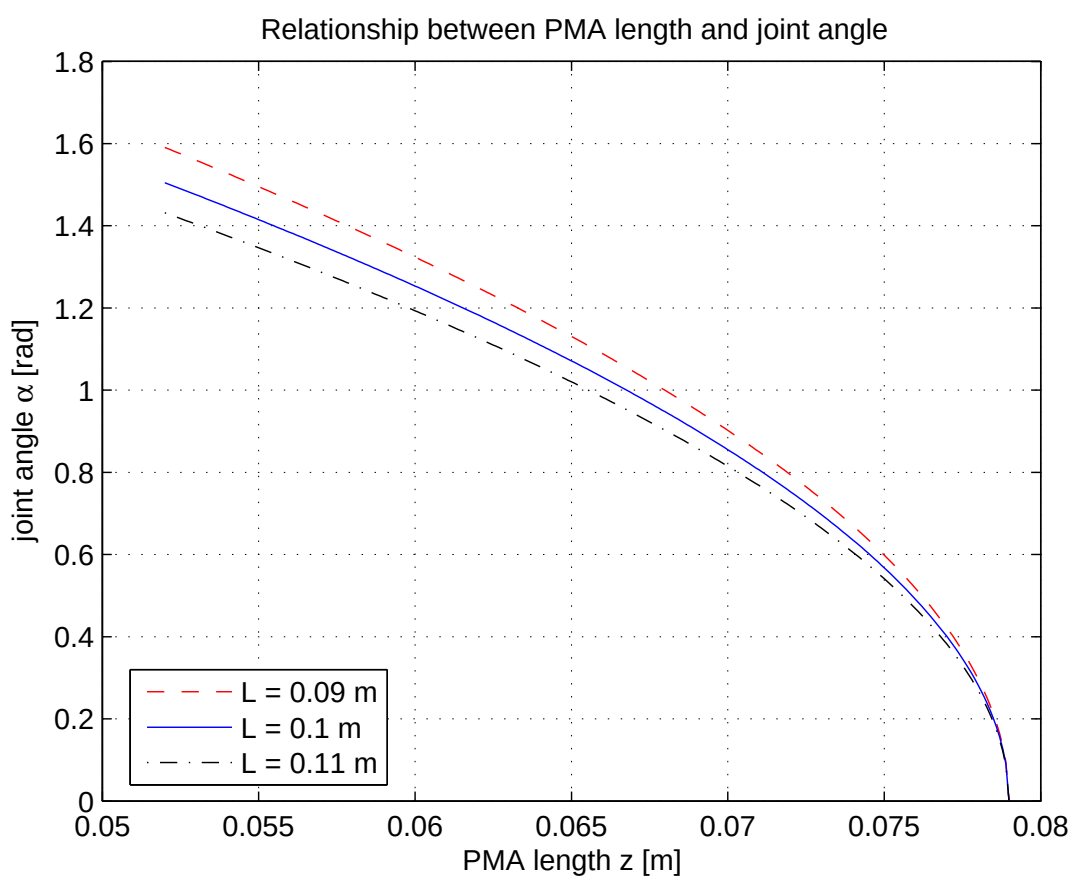

Figure 4.7: Relationship between PMA length and joint angle for different lengthes of the links

The affecting forces and torques are drawn in Figure 4.8. The gravitational force F_g induces a torque T_g in the joint:

$$T_g(t) = F_g \cdot \frac{L}{2} \cos\alpha(t) \tag{4.44}$$

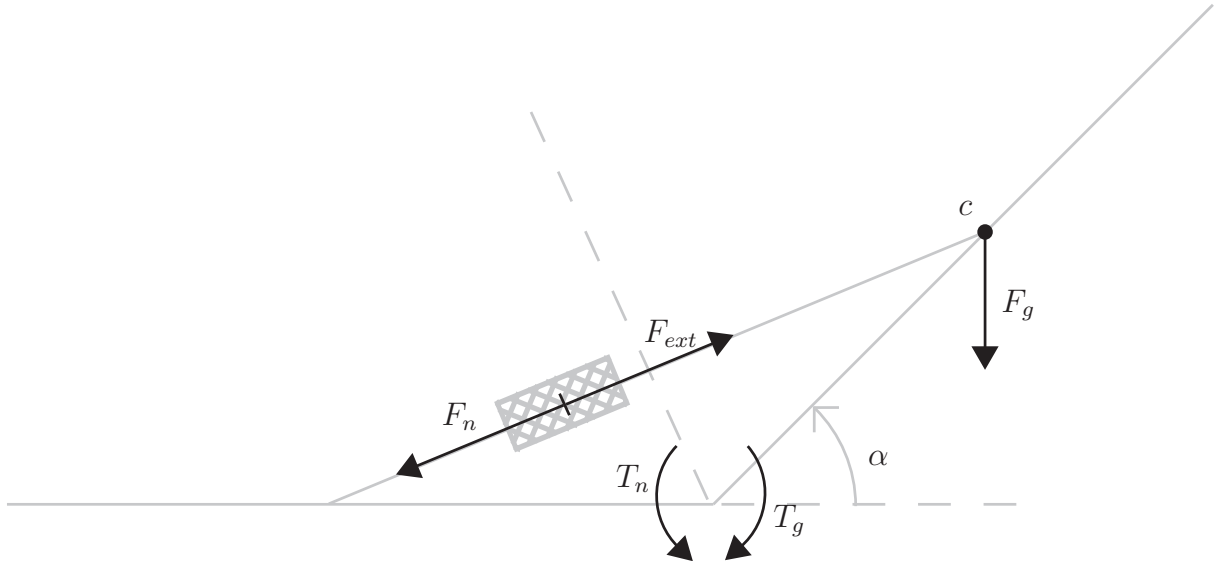

Figure 4.8: Affecting forces and torques

The torque $T_n(t)$ is the torque which is necessary to compensate $T_g(t)$. It is induced by the PMA.

$$T_n(t) = F_n(t) \cdot h(t) \tag{4.45}$$

$$= F_n(t) \cdot \frac{L}{2} \sin\left(\frac{\alpha(t)}{2}\right) \tag{4.46}$$

With $T_n(t) = T_g(t)$ the necessary force $F_n(t)$ is

$$F_n(t) = F_g \cdot \frac{\cos\alpha(t)}{\sin\frac{\alpha(t)}{2}} \tag{4.47}$$

This necessary force $F_n(t)$ is the external force F_{ext} in the balance of forces of the PMA (Equation 4.9). Because of the assumption that all mass is concentrated in the gravitation center c of the driven load there is no additional gravitation force. Some friction occurs in the joint. It is modeled identical to the friction of the vertically driven load before.

In Figure 4.9 the relationship between the joint angle and the external force is plotted for different masses. The external force is very high for a small angle which is the case if the moved link lies on the ground. Also at $\alpha = 0$ the external force is not defined. Because of this the initial angle is greater than zero.

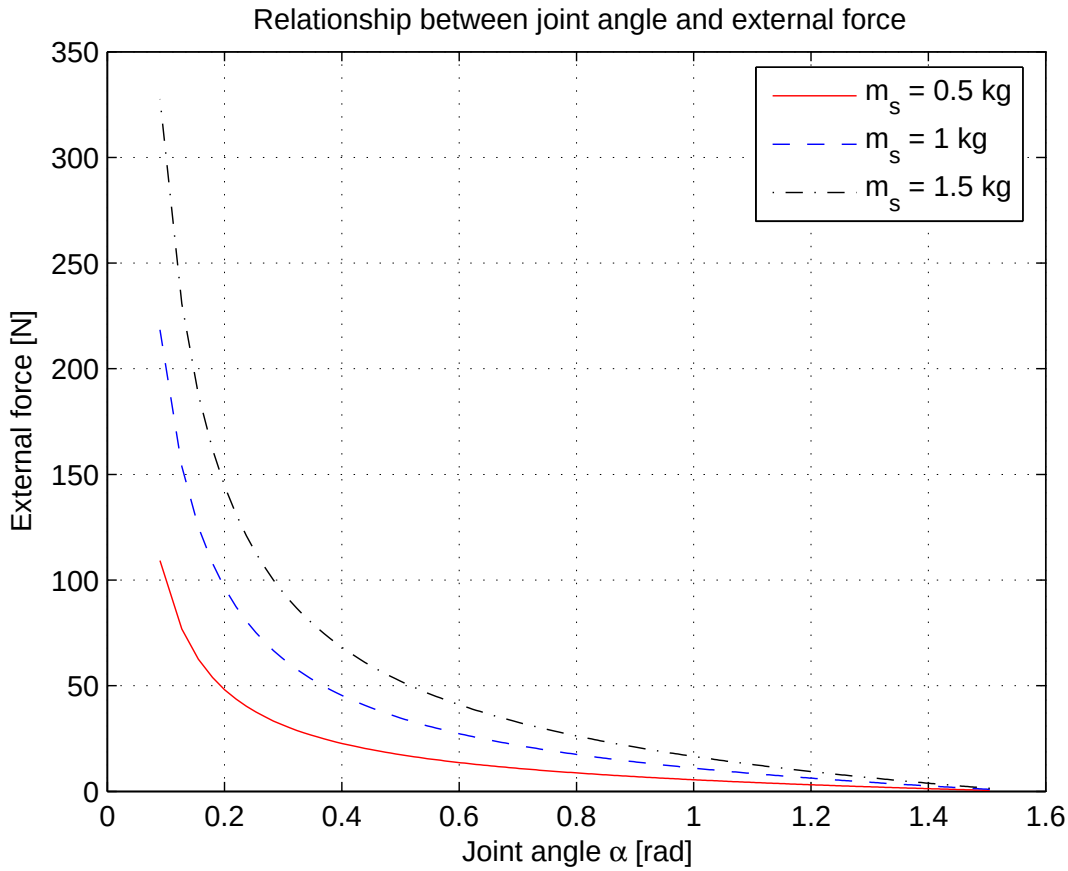

Figure 4.9: Relationship between joint angle and external force for different driven masses

4.4 Implementation of the model in MATLAB/ Simulink

The described model of the PMA is implemented in Simulink. It is implemented in signal flow form with several different levels. For single equations 'Embedded Matlab Functions' are used. The different implementation variants are printed in Appendix B.2. By opening the control loop experiments with the model can be performed.

There are three different model variants implemented. Two of the variants simulate the PMA driving vertically a load; one of them uses the Karnopp friction model and one uses a simple proportional friction law. The third variant simulates the joint driven by one PMA.

The input into the PMA is the command voltage $U(t)$, and the output is the PMA length $z(t)$ respectively the joint angle $\alpha(t)$.

The parameters driven mass m_s, temperature T and supply pressure p_s can be changed during the simulation.

4.4.1 Actual values of the model parameters

The actual parameters used in the simulations are assembled in Table 4.1. The PMA parameters are taken from Caldwell et al. [2].

4.4.2 Simulation results of the model

The modeled system behaves very unstable. Therefore, the only possible simulated experiments are to record the step response and the impulse response to the input. At time $t = 0$ s the input $u(t)$ is set from 0 to 0.02 V.

In Figure 4.10 the simulated pressure and length values to the input step are plotted with different friction models. The first friction model is a simple proportional law, the second model is the model of Karnopp. The driven mass is $m_s = 1$ kg. The threshold force is $F_{f,stick,thr} = 0.5$ N, and the threshold velocity is $\dot{z}_{thr} = 0.0001\ \frac{\mathrm{m}}{\mathrm{s}}$.

As expected, with the Karnopp friction model the PMA length remains constant for a longer time with nevertheless rising pressure. Due to this pressure rising the characteristics of the PMA

Table 4.1: Actual values of the model parameters

symbol	meaning	value	unit
R	gas constant of air	287	$\left[\frac{\text{J}}{\text{kg K}}\right]$
η	specific heat ratio	1.4	[-]
$T = T_s = T_0$	temperature	298	[K]
p_0	environment pressure	101325	$\left[\frac{\text{N}}{\text{m}^2}\right]$
p_s	supply pressure	303975	$\left[\frac{\text{N}}{\text{m}^2}\right]$
c	constant of proportionality of the valve	10^{-7}	$\left[\frac{\text{m}^2}{\text{V}}\right]$
χ	polytrophic exponent	1.26	[-]
h	helical fiber length	0.152	[m]
f	diametric distance parameter	0.0145	[m]
m_s	mass	$0.5 \ldots 1.5$	[kg]
g	gravitational constant	9.81	$\left[\frac{\text{m}}{\text{s}^2}\right]$
C	slipping friction constant	20	$\left[\frac{\text{kg}}{\text{s}}\right]$
K	elastic force constant	40	$\left[\frac{\text{m}}{\text{s}^2}\right]$
$\dot{z}_{thr}$	velocity threshold	0.0001	$\left[\frac{\text{m}}{\text{s}}\right]$
F_{thr}	force threshold	0.5	[N]
L	length of the link	0.1	[m]
z_0	relaxation length of the PMA	0.079	[m]
$z_m in$	length of the PMA at maximum contraction	0.052	[m]
$z_m ax$	length of the PMA at maximum elongation	0.143	[m]

length is not exactly time-shifted.

In Figure 4.11 the experiment is repeated with the impulse input. The input is set again to 0 V at time $t = 0.25$ s. The difference to the step response is very small.

In Figure 4.12 the characteristics of the PMA length and the pressure over the time are plotted for different driven masses. For the friction the Karnopp model is used. The step in the input occurs at time zero, and the initial value of the PMA length is fixed. The initial value of the inner pressure is calculated with the static relationship

$$\bar{x}_1 = \frac{F_{ext} - K\bar{x}_2}{\alpha_8 - \alpha_{10}\bar{x}_2^2} + p_0 \tag{4.48}$$

As expected in Subsection 4.1.2 the inner pressure of the PMA is higher for a heavier driven mass. Also, the pressure behaves inverse to the length, that means that a rising pressure causes a shortening of the PMA.

In Figure 4.13 the experiment is repeated with the impulse input. The input is set again to 0 V at time $t = 0.35$ s. Also here the difference to the step response is very small.

The same experiment is performed with the joint angle. In Figure 4.14 the step response is simulated. As described in Section 4.3, the joint angle behaves inverse to the PMA length and following in equal direction to the pressure.

In Figure 4.15 the impulse response of the joint angle is simulated. Also here the valve is closed at time $t = 0.35$ s. Also here the difference is minimal. Following, the model behaves very unstable.

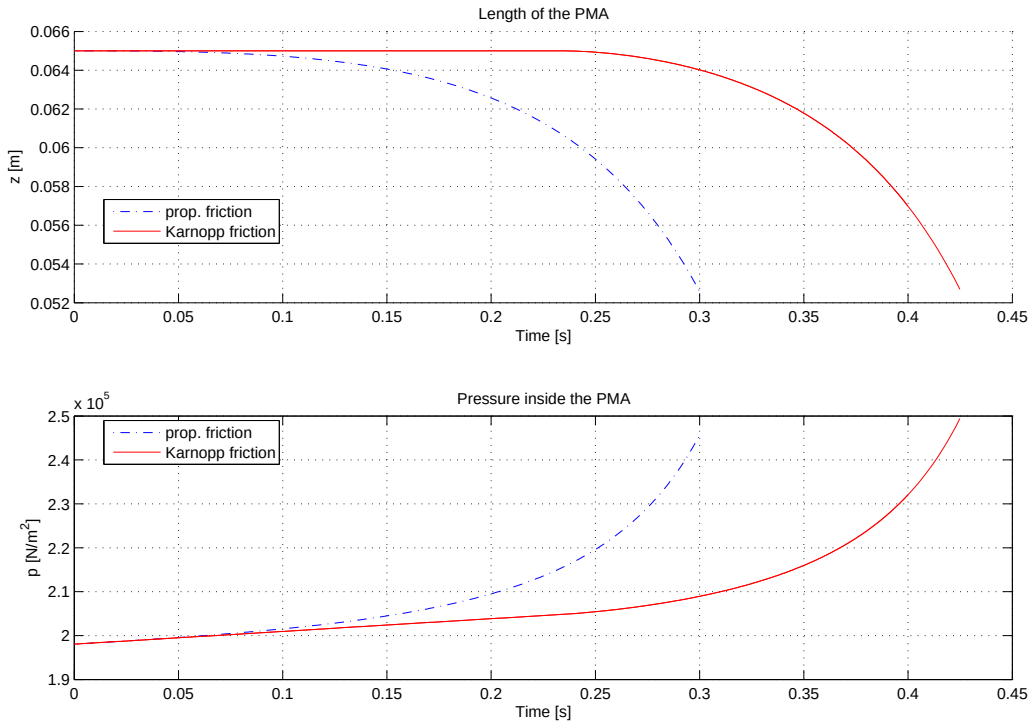

Figure 4.10: Step response of length and pressure for different friction models

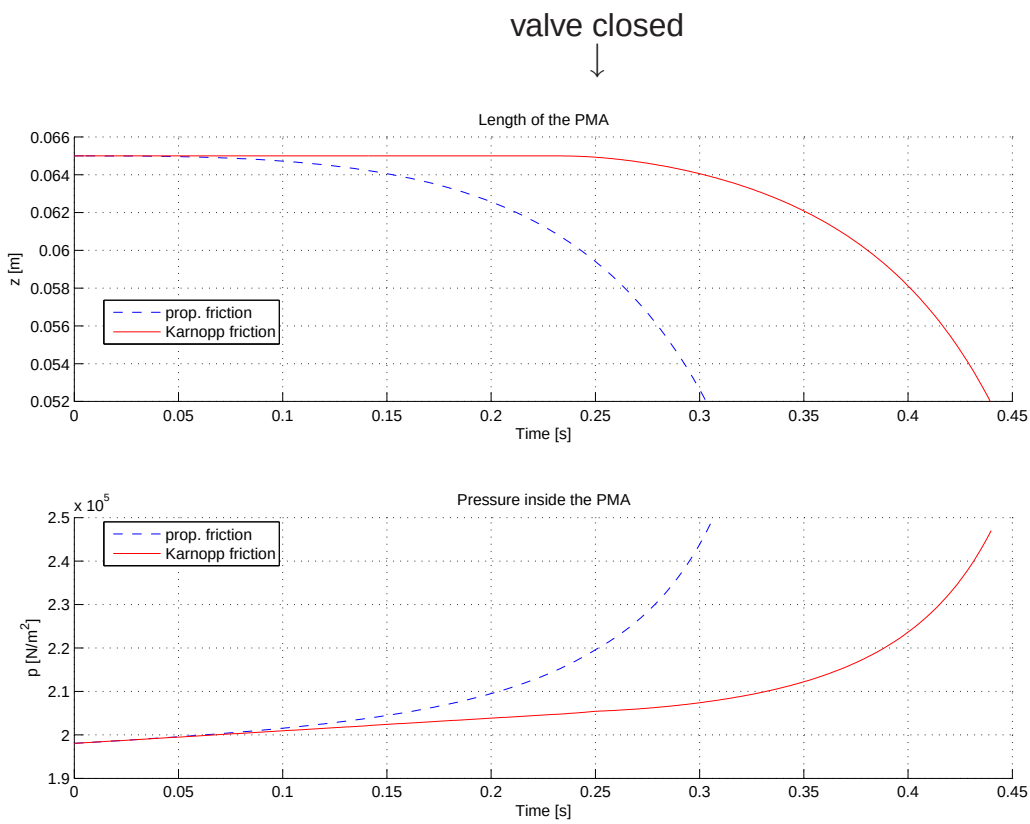

Figure 4.11: Impulse response of length and pressure for different friction models

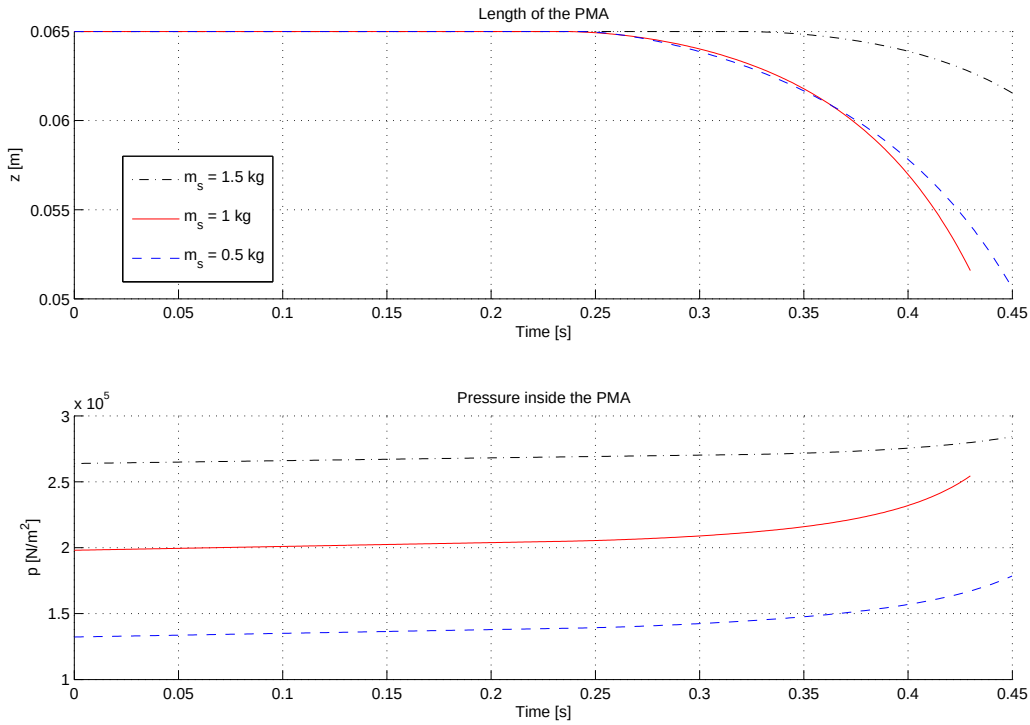

Figure 4.12: Step response of length and pressure for different driven masses

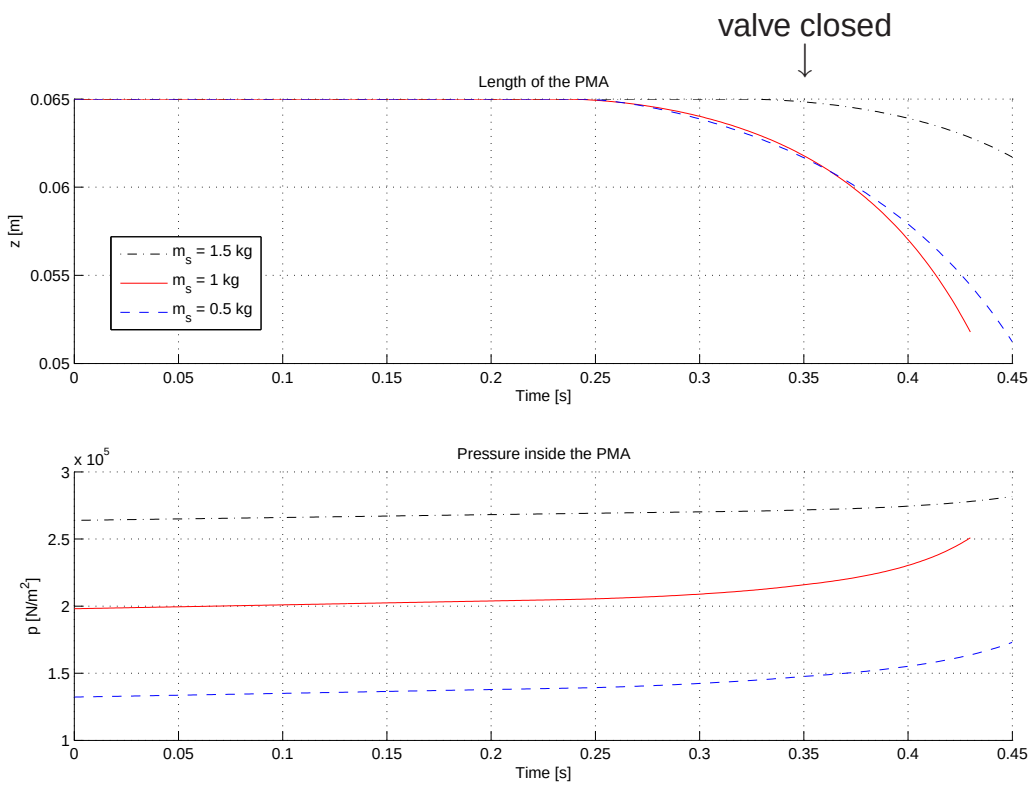

Figure 4.13: Impulse response of length and pressure for different driven masses

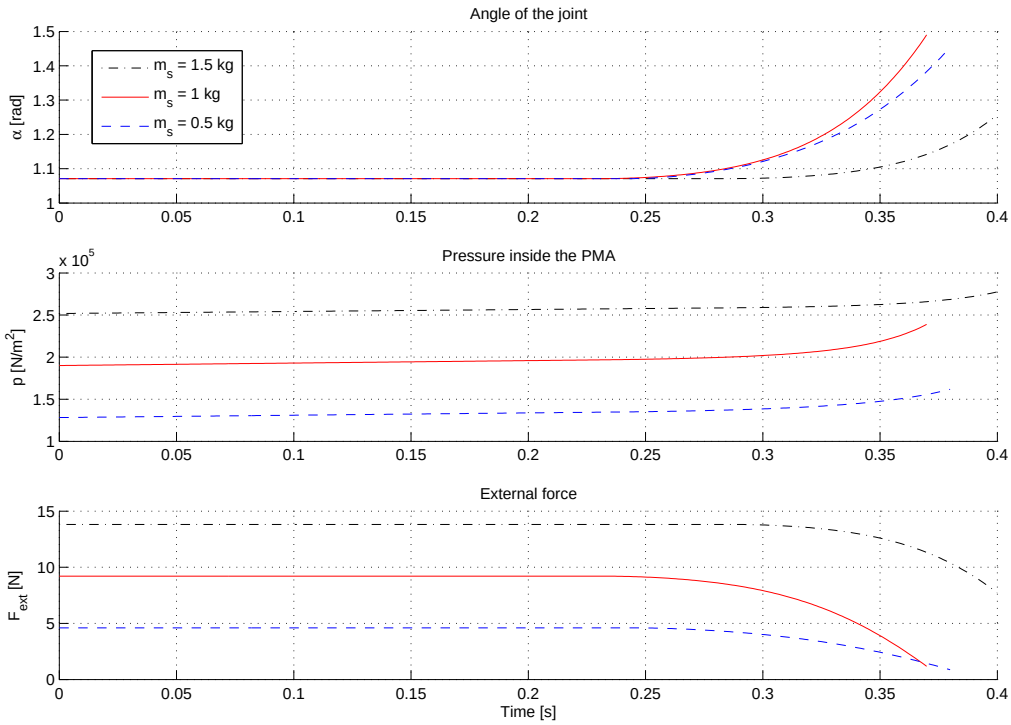

Figure 4.14: Step response of joint angle and pressure for different driven masses

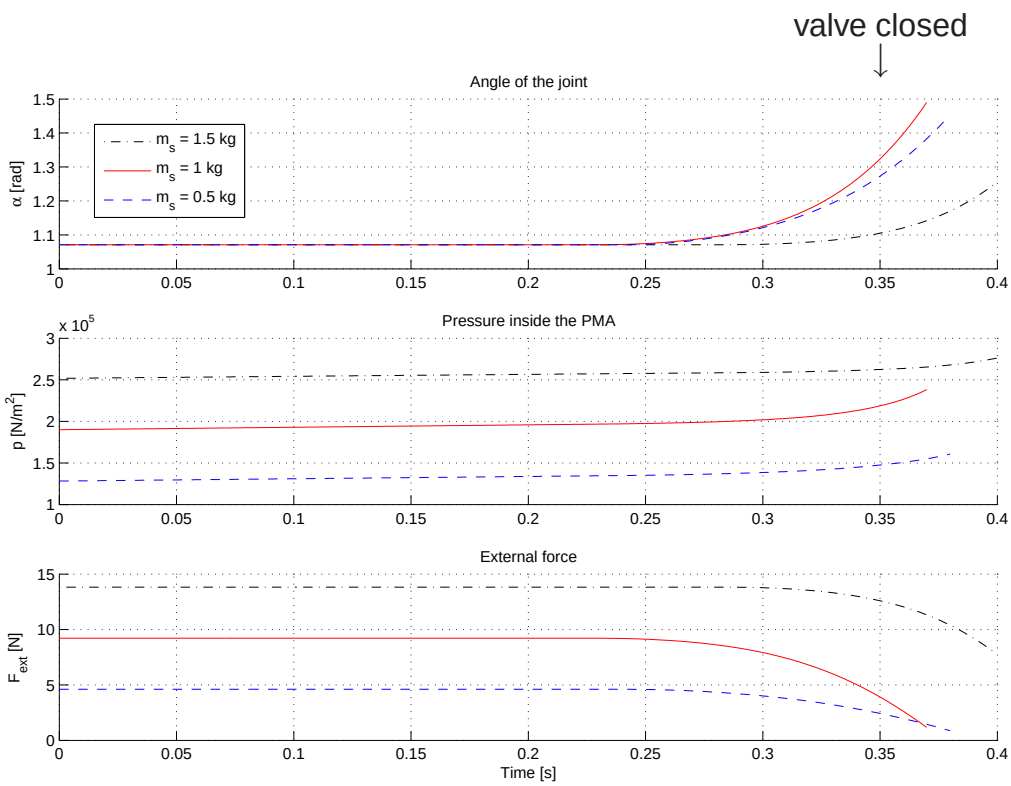

Figure 4.15: Impulse response of joint angle and pressure for different driven masses

Chapter 5

Closed-loop control

In this chapter the controller for the model is described. As controller a flatness based controller is chosen and introduced in Section 5.1. In Section 5.2 the application on the PMA driving vertically a load is described. In Section 5.3 the control system is extended to the control of the joint angle. The implementation of the controller in MATLAB/ Simulink and the performed experiments are described and discussed in Section 5.4.

5.1 Flatness based control

The model of the PMA behaves unstable, so it is necessary to stabilize it. Also it is desired that the PMA follows a given trajectory. So a closed loop tracking controller has to be designed. The model is strongly nonlinear, so the controller has to be able to deal with the nonlinearities. Some basic working principles are described in Section 2.3, and some performed designs are reviewed in Section 3.2. The main approaches are the dynamical linearization of the model in order to design a linear controller and the design of a nonlinear controller. In general, linearization methods combined with linear controller designs are numerically easier to deal with. In the actual model there are no uncertainties in the parameters, so it is not necessary to design an adaptive controller. So a linearization method can be used. Feedback linearization means that the nonlinearities of the model are canceled by the model input. Following, the nonlinearities appear in the input. This is a general drawback of feedback linearization, because due to physical limits of the actuator this could cause problems [17].

There are different possible designs of a feedback linearization, described in 3.2.1. Here the input-output linearization is more interesting than the input-state-linearization, because in a

tracking control system the output is more important than the state. There are also the classifications 'exact feedback linearization' and 'approximated feedback linearization'. This depends on the observability and the controllability of the system. If the system is both, it is exactly linearizable.

5.1.1 Basic idea of the controller

The structure of a flatness based controller is printed in Figure 5.1. This controller works with exact feedback linearization. The basic idea is to generate an input into the plant which cancels the nonlinearities of the plant. Therefore the plant is inverted, so that the inverse system and the plant together set up a linear system. This system can be controlled by a linear tracking controller.

The actual output $y(t)$ of the nonlinear plant is fed into the tracking control. According to the desired trajectory $y_d(t)$ the tracking controller generates an input $\nu(t)$ into the linear plant system. In the inverse system this input $\nu(t)$ is transformed into the input $u(t)$ into the nonlinear plant. With this input $u(t)$ the nonlinear plant is driven onto the desired trajectory.

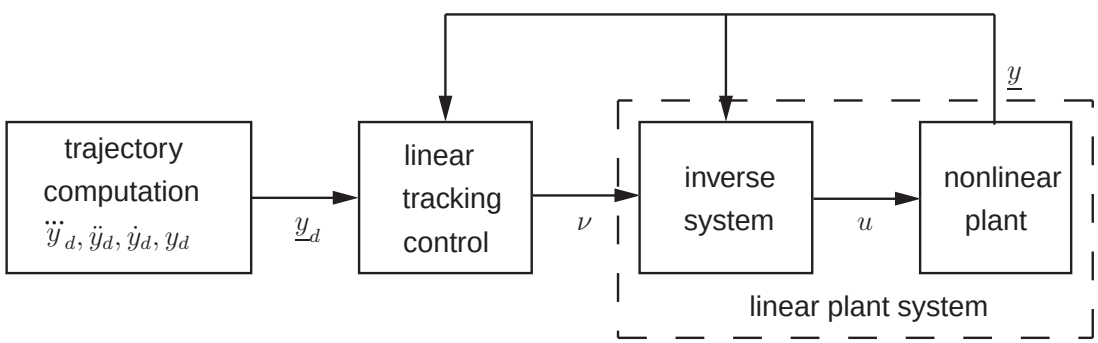

Figure 5.1: Structure of the control system

5.1.2 Prerequisites and necessary tools

Differential flatness of the model

One prerequisite for applying a flatness based controller is that the model is differential flat. This concept is described in [9] and [33]. Differential flatness means that there is one output of the plant (or a set of outputs) which can be described by terms depending on the state vector and

the input and a finite number of its derivatives. The states and the input have to be describable by terms depending on this flat output and a finite number of its derivatives:

$$y = y(x, u, \dot{u}, \ldots, u^{(l)}) \tag{5.1}$$

$$x = x(y, \dot{y}, \ldots, y^{(q)}) \tag{5.2}$$

$$u = u(y, \dot{y}, \ldots, y^{(q)}) \tag{5.3}$$

This property is necessary for inverting the plant, because in the inverse system all nonlinearities of the plant have to be included in the output of the nonlinear plant to obtain the exact cancelation. Also the states of the nonlinear plant have to be describable by the output, because if not the generated input into the nonlinear plant cannot cancel all the nonlinearities.

Relative degree

Differential flatness is a concept of exact feedback linearization. A system is exact linearizable if it is controllable and observable, which means that there are no internal (zero) dynamics. This requirement is fulfilled if the relative degree r of the system is equal to the order n of the system. If the system is controllable, but not observable, it is exact input-state linearizable, but not exact input-output linearizable. Otherwise the desired linearization has to be approximated. The effectiveness of the approximated linearization depends on the stability of the unobservable or uncontrollable parts of the system.

The relative degree r is the number of times the output equation has to be derived until the input appears.

Following, the relative degree is also the number of derivatives which have to be regarded in the calculations to cover all nonlinearities. That means that the trajectory error and r derivatives have to be compensated by the tracking controller. Because of that the desired trajectory has to be derivable r times.

5.2 Length control of the single PMA

In this section the controller is developed for the PMA driving a load vertically. Therefore the controller of Hildebrandt et al. [13] is modified. First the controller is designed for a proportional friction law and then the Karnopp friction model is applied.

5.2.1 Fulfilment of the prerequisites

In this subsection it is shown that the flatness based controller can be used for controlling the model of the PMA. First the relative degree of the model is obtained and therewith the possibility of exact linearization is shown. Next, the differential flatness of the model is shown.

Identification of the relative degree

For obtaining the relative degree, the output equation is derived with respect to the time until the input appears.

For a better readability of the equations the dependencies on time are not notated here. y, u, all x_i and the external force F_{ext} depend on the time. Following, also all ψ_i depend on the time.

First some abbreviations which also include the states and its derivatives are introduced to simplify the differential equation of the pressure (Equation 4.24 and 4.25):

$$\psi_1(x_1) = a_1\sqrt{a_2 x_1^{a_4} - a_3 x_1^{a_5}} \tag{5.4}$$

$$\psi_2(x_1, x_2) = \frac{a_7}{V(x_2)}\psi_1(x_1) \tag{5.5}$$

$$\psi_3(x_1, x_2, x_3) = \frac{\chi}{V(x_2)}x_1(a_8 - a_{10}x_2^2)x_3 \tag{5.6}$$

The abbreviated equation is:

$$\dot{x}_1(t) = \psi_2(x_1, x_2)u(t) - \psi_3(x_1, x_2, x_3) \tag{5.7}$$

Next the output equation (Equation 4.28) is derived.

$$
\begin{aligned}
y &= x_2 && (5.8)\\
\dot{y} &= x_3 = \dot{x}_2 && (5.9)\\
\ddot{y} &= \frac{1}{m_s}(F_{ext} + F_g - F_m - F_e - F_f) \\
&= \frac{1}{m_s}\left(F_{ext} + m_s g - (x_1 - p_0)(a_8 - a_{10}x_2^2) - Kx_2 - Cx_3\right) \\
&= \frac{1}{m_s}\left(F_{ext} + m_s g - a_8 x_1 + a_{10}x_1 x_2^2 + a_8 p_0 - a_{10}p_0 x_2^2 - Kx_2 - Cx_3\right) && (5.10)\\
\dddot{y} &= \frac{1}{m_s}\left(-a_8\dot{x}_1 + a_{10}\dot{x}_1 x_2^2 + 2a_{10}(x_1 - p_0)x_2 x_3 + \dot{F}_{ext} - K\dot{x}_2 - C\dot{x}_3\right) && (5.11)
\end{aligned}
$$

Also here some abbreviations are introduced to simplify the third derivative of the output (Equation 5.11):

$$
\begin{aligned}
\psi_4(x_1, x_2, x_3, \dot{x}_3) &= \frac{2}{m_s}a_{10}(x_1 - p_0)x_2 x_3 + \frac{1}{m_s}\dot{F}_{ext} - \frac{K}{m_s}\dot{x}_2 - \frac{C}{m_s}\dot{x}_3 && (5.12)\\
\psi_5(x_1, x_2) &= -\frac{1}{m_s}(a_8 - a_{10}x_2^2)\psi_2(x_1, x_2) && (5.13)\\
\psi_6(x_1, x_2, x_3, \dot{x}_3) &= \frac{1}{m_s}(a_8 - a_{10}x_2^2)\psi_3(x_1, x_2, x_3) + \psi_4(x_1, x_2, x_3, \dot{x}_3) && (5.14)
\end{aligned}
$$

The abbreviated equation is

$$
\begin{aligned}
\dddot{y} &= \frac{1}{m_s}(a_{10}x_2^2 - a_8)\dot{x}_1 + \psi_4(x_1, x_2, x_3, \dot{x}_3) \\
&= \frac{1}{m_s}(a_{10}x_2^2 - a_8)(\psi_2(x_1, x_2)u - \psi_3(x_1, x_2, x_3)) + \psi_4(x_1, x_2, x_3, \dot{x}_3) \\
&= \psi_5(x_1, x_2)u + \psi_6(x_1, x_2, x_3, \dot{x}_3) && (5.15)
\end{aligned}
$$

The input u appears in the third derivative of the output equation, so the relative degree of the system is $r = 3$. The order n of the system is the number of states which is also $n = 3$. So the system is controllable and observable which means that there are no internal (zero) dynamics. Following, the desired exact input-output linearization is possible.

Also, the desired trajectory has to be at least three times differentiable.

Differential flatness of the PMA model

The PMA can be in several different states and modi. It can be in relaxed, elongated or contracted state. Another criterion is whether the driven load is sticking or slipping. The latter

criterion concerns the modeled friction force. First, the slipping modus is discussed.

According to Equation 5.8 Equation 5.1 is fulfilled.

$$x_1 = \frac{F_{ext} - Ky - C\dot{y} - m_s\ddot{y}}{a_8 - a_{10}y^2} + p_0 \quad \text{(from Equation 4.27)} \tag{5.16}$$

$$x_2 = y \tag{5.17}$$

$$x_3 = \dot{x_2} = \dot{y} \tag{5.18}$$

Equation 5.2 is mainly fulfilled, the only problem occurs as a pole at $y = \sqrt{\frac{a_8}{a_{10}}}$. In this case the PMA is in elongated state.

With Equation 4.24, 4.25, 5.4, 5.5 and 5.6 the state derivative $\dot{x}_1$ is expressed as

$$\dot{x}_1 = \psi_2(x_1)u - \psi_3(x_1, x_2, x_3) \tag{5.19}$$

and with Equations 5.16, 5.17 and 5.18 the input u can be described as

$$u = \frac{\dot{x}_1(y, \dot{y}, \ddot{y}, \dddot{y}) + \psi_3(y, \dot{y}, \ddot{y})}{\psi_2(y, \dot{y}, \ddot{y})} \tag{5.20}$$

Also Equation 5.3 is fulfilled with the exception inner pressure = supply pressure. This is uncritical, because the parameters like the driven mass can be chosen so that the problem does not occur in the possible range of length values. So in contracted and relaxed state the model of the plant is differential flat.

During the sticking mode the velocity and the acceleration of the PMA are set to zero. Therefore, the balance of forces (Equation 4.9) is in sticking mode no differential equation, but reduced to an algebraic equation (Equation 4.16). So in sticking mode Equation 5.16 is reduced to

$$x_1 = \frac{F_{ext} - Ky}{a_8 - a_{10}y^2} + p_0 \tag{5.21}$$

which is nevertheless differential flat with the described exception in elongated state.

In sticking mode the input equation (Equation 5.20) is

$$u = \frac{\dot{x}_1(y)}{\psi_2(y)} \tag{5.22}$$

which is also flat with the exception inner pressure = supply pressure. The other equations are identical to the equations for the slipping mode.

Therefore, the plant is differential flat with the two described exceptions, one pole in elongated state and one pole at $x_1 = p_s$.

Following, if the PMA is also driven in elongated state another controller has to be used or other solutions have to be found. In this thesis the PMA is only driven in contracted and relaxed state, so inside the used range of values the problem does not occur.

Summarizing, the required prerequisites are fulfilled, so the PMA can be controlled by a flatness based controller.

5.2.2 Controller equations

In this subsection the equations for the controller are derived. Therefore the tracking control and the inverse system have to be developed.

Tracking control

The PMA shall be driven along a given trajectory. For this tracking control a simple linear approach can be used, here a pole placement controller. The order of the controller has to be the relative degree r of the system. Following, the desired trajectory $y_d(t)$ has to be at least $r = 3$ times differentiable.

The tracking error $e(t)$ and its derivatives are defined as

$$e(t) := -(y(t) - y_d(t)) \tag{5.23}$$

$$\dot{e}(t) := -(\dot{y}(t) - \dot{y}_d(t)) \tag{5.24}$$

$$\ddot{e}(t) := -(\ddot{y}(t) - \ddot{y}_d(t)) \tag{5.25}$$

$$\dddot{e}(t) := -(\dddot{y}(t) - \dddot{y}_d(t)) \tag{5.26}$$

whereas the minus is due to the negative relation between the computed input $u(t)$ into the model and the model output $y(t)$, which means that a positive model input leads to a smaller

model output.

The differential equation

$$0 = \dddot{e}(t) + K_2\ddot{e}(t) + K_1\dot{e}(t) + K_0 e(t) \qquad \forall K_i \geq 0 \tag{5.27}$$

guarantees an asymptotic tracking.

The controller parameters K_i are calculated from the desired poles P_i of the closed loop control system. Therefore the error differential equation is Laplace transformed and divided by $E(s)$.

$$0 = s^3E(s) + K_2s^2E(s) + K_1sE(s) + K_0E(s) \tag{5.28}$$

$$0 = s^3 + K_2s^2 + K_1s + K_0 \tag{5.29}$$

With

$$s^3 + K_2s^2 + K_1s + K_0 = (s - P_1)(s - P_2)(s - P_3) \tag{5.30}$$

$$= s^3 - (P_1 + P_2 + P_3)s^2 + (P_1P_2 + P_2P_3 + P_1P_3)s - P_1P_2P_3 \tag{5.31}$$

the controller parameters are obtained as:

$$K_2 = -(P_1 + P_2 + P_3) \tag{5.32}$$

$$K_1 = P_1P_2 + P_2P_3 + P_1P_3 \tag{5.33}$$

$$K_0 = -P_1P_2P_3 \tag{5.34}$$

with $P_i \leq 0$.

The computed input $\nu(t)$ into the linear plant system is set to the third derivative of the real trajectory [13]:

$$\nu(t) =: \dddot{y}(t) \tag{5.35}$$

With Equation 5.23 - 5.26 follows

$$\nu(t) = -\dddot{y}_d(t) + K_2\ddot{e}(t) + K_1\dot{e}(t) + K_0 e(t) \tag{5.36}$$

Inverse system

The inverse system transforms the computed input into the linear system $\nu(t)$ into the input $u(t)$ into the nonlinear plant. Therefore, Equation 5.15 and Equation 5.35 are put together to

$$\nu(t) = \psi_5\Big(y(t), \dot{y}(t), \ddot{y}(t)\Big)u(t) + \psi_6\Big(y(t), \dot{y}(t), \ddot{y}(t)\Big) \tag{5.37}$$

and transformed to

$$u(t) = \frac{\nu(t) - \psi_6\Big(y(t), \dot{y}(t), \ddot{y}(t)\Big)}{\psi_5\Big(y(t), \dot{y}(t), \ddot{y}(t)\Big)} \tag{5.38}$$

This input $u(t)$ into the nonlinear system contains the linear compensation of the trajectory error and the exact cancelation of the nonlinearities. Following, with this input $u(t)$ the PMA is driven along the desired trajectory.

5.2.3 Application of the Karnopp friction

The friction force is modeled at first proportional to the velocity of the movement. In a second step the model is extended by the model of Karnopp [16], described in Subsection 3.1.1. Here the mode of the PMA is split into a slipping mode where the PMA is moving and the friction is described by a simple model and a sticking mode where the PMA is resting. This sticking friction force is modeled to depend on the other forces while the length of the PMA is constant. For the resting a region is defined where the velocity of the PMA is near to zero and the sticking friction force is also small. Inside this region the velocity and also the acceleration are set to zero. This occurs in the model, so the controller itself does not switch between the different modi.

The controller is dimensioned for the slipping mode. The accurate control depends on the knowledge and the correctness of the velocity and the acceleration at every time. During sticking mode the knowledge is assured, so the model is still differential flat and the controller can work. The velocity and acceleration values are not correct during sticking mode, so the accuracy of the tracking and the smoothness of the control signal will be reduced. Following, also the smoothness of the state characteristics will be reduced.

5.3 Extension to the control of the joint

The desired trajectory is given as joint angle. With Equation 4.43 the trajectory is transformed into the desired length trajectory. The simulated model output is computed for the PMA length and then transformed with Equation 4.42 into the joint angle. The tracking error is computed with the length values. Also in the inverse system the calculations takes place with the PMA length, but there the joint angle is needed explicitly. In Equation 5.12 the derivative of the external force $\dot{F}_{ext}$ occurs. In the control of the PMA length with a vertically driven mass the external force F_{ext} is the gravitational force which is constant. In the control of the joint angle the external force $F_{ext}(t)$ depends on the time-dependent angle $\alpha(t)$ which depends nonlinear geometrical on the PMA length. Therefore, the time derivatives of the external force and the joint angle have to be calculated by using Equation 4.47 and Equation 4.42.

$$\begin{aligned}
\alpha(t) &= 2 \cdot \cos^{-1}\left(1 + \frac{z(t) - z_0}{L}\right) \qquad \text{for } z(t) \neq z_0 \\
\dot{\alpha}(t) &= -\frac{2\dot{z}(t)}{L\sqrt{1 - \left(1 + \frac{z(t)-z_0}{L}\right)^2}} \qquad (5.39) \\
F_{ext}(t) &= F_g \cdot \frac{\cos\alpha(t)}{\sin\frac{\alpha(t)}{2}} \\
\dot{F}_{ext}(t) &= -F_g \cdot \frac{\dot{\alpha}(t)\sin\alpha(t)\sin\frac{\alpha(t)}{2} + \frac{\dot{\alpha}(t)}{2}\cos\frac{\alpha(t)}{2}\cos\alpha(t)}{\sin^2\frac{\alpha(t)}{2}} \qquad (5.40)
\end{aligned}$$

The other necessary equations are taken from the PMA length control.

5.4 Implementation of the controller in MATLAB/ Simulink

The described controller is implemented in Simulink. It is included into the implementation of the model. The controller implementations for the different model variants are printed in Appendix B.2. There also the handling of the control is explained.

The concrete experiments which are performed with the closed-loop control of the PMA are described and their results are discussed in Subsection 5.4.1, the properties and the values of the varied parameters are given in Subsection 5.4.2, and the plotted characteristics are given in Subsection 5.4.3.

5.4.1 Performed experiments with the closed loop control system

To test the performance of the implemented controller several different experiments are simulated. Mainly the experiments are performed as follows: At $t = 0$ s the load is applied. The initial value of the PMA length respectively the joint angle differs from the desired value. At $t = 3$ s the investigated parameter is changed abruptly, and at $t = 6$ s it is changed back to the initial value. The desired trajectory cannot be changed abruptly, because the controller requires that it has to be three times differentiable. So the investigated desired trajectories are constant and sinusoidal.

Control of the vertically driven load, Karnopp friction model

At first the onset behavior of the control of the vertically driven mass is tested for different loads. It is shown in Figure 5.2.

The tracking occurs fast. After 0.3 s the desired value is achieved for the medium and the heavy load. It is noticeable that for the lightweight load the variables oscillate slightly, so the desired length is achieved after 0.5 s.

The controller also works quite accurate, the maximum error after achieving the desired trajectory is in the order of 10^{-5} m for the medium and the heavy load and 10^{-4} m for the lightweight load. The maximum error occurs at the sticking mode.

The control signal is smooth during the slipping mode. In the sticking mode, there are abrupt peaks and little chatters caused by the Karnopp friction model (see Subsection 5.2.3). As expected, the magnitude of the command voltages corresponds to the weight of the driven load. A heavier load requires a higher pressure, so for the same speed of the controller a higher mass flow which depends proportional on the command voltage is required.

The second experiment investigates the performance of the controller with abrupt changes in the load. The desired trajectory is a constant value. The load is applied at $t = 0$ s, reduced at

$t = 3$ s and raised at $t = 6$ s. The simulated characteristics are given in Figure 5.3.

At the reduction of the load the PMA shortens 2 mm and at the raising the PMA elongates 1.3 mm, but after 0.35 s the disturbance is compensated by reducing respectively raising the pressure.

The control signal is smaller at the reduction of the load than at the rising, also at the reduction the error is greater than at the raise. This signifies that the elongation of the PMA and therewith the pressure release occurs faster than the contraction and therewith the pressure generation.

The third experiment is the same experiment as the second one but with a sinusoidal desired trajectory. Here the disturbances occur during slipping mode. The characteristics are given in Figure 5.4.

In the slipping mode the trajectory error is smaller and the control signal is smoother, because the controller can react more adequate. The trajectory errors and the compensation time at the load variations are not significant smaller than with the constant trajectory. Also the magnitude of the control signal is not significant different, but the control signal is smoother.

It is noticeable that the pressure behaves within the direction of the PMA length. Due to the characteristics of the PMA force a shorter PMA requires a lower pressure for inducing the same force, so the controller generates an adequate mass flow.

Control of the vertically driven load, proportional friction law

To investigate the influence of the friction model the second and the third experiment are repeated with a simple proportional friction law. In the forth experiment the desired trajectory is constant. The characteristics are plotted in Figure 5.5.

Here the tracking is nearly perfect, the error after onset and after compensating the disturbances in the load is in the order of 10^{-8} m. The trajectory errors at the disturbances, the magnitudes of the control signal and the compensation times are not significant different from the values with

the Karnopp friction model, but the control signal and the pressure and length characteristics are very smooth and the changes due to the disturbances are very clear.

In the fifth experiment the desired trajectory is sinusoidal. The characteristics are given in Figure 5.6. Also here the significant differences are the smoothness and clearness of the control signal, pressure and length characteristics.

Control of the joint angle, Karnopp friction model

In the next experiments the performance of the joint angle controller is tested. The friction force is modeled with the Karnopp model. In the working range of the angle the external force is higher than the gravitation force (see Figure 4.9), so the driven mass has to be reduced for the joint angle experiments. Alternatively, the length of the links could be reduced, but this is limited by the length of the PMA, because the link has to be longer than the PMA in relaxed state.

The second and third experiment are repeated with the control of the joint angle which means that the reaction of the controller to an abrupt change of the load is investigated. The load is applied at $t = 0$ s, reduced at $t = 3$ s and raised at $t = 6$ s.

In the sixth experiment the desired trajectory is a constant value. The characteristics are plotted in Figure 5.7.

The joint angle behaves inverse to the PMA length and following inverse to the pressure. The observed variables oscillate slightly with the reduced mass.

The control signal is quite smooth, it contains no peaks, the deviations are waves started with a small chatter.

The trajectory error at the mass reduction is 0.15 rad, at the mass raise 0.07 rad and without the disturbances maximal 0.02 rad. The compensation times are similar to the compensation time of the length control. The onset time is with 0.25 s shorter, but the initial error is smaller than in the length control.

The seventh experiment is the same experiment as the sixth one but with a sinusoidal desired trajectory. The characteristics are plotted in Figure 5.8.

Here the trajectory error at the load reduction is with 0.1 rad significant smaller than in the experiment before, but the compensation time is with 0.7 s longer.

During the slipping mode the characteristics of the variables are smooth.

In the next experiments the controller performance at fluctuations in the supply pressure is investigated. It has to be remarked that the supply pressure cannot be reduced under the actual pressure value, because this causes numerical problems.

In the eights experiment, shown in Figure 5.9, the supply pressure is reduced abruptly at $t = 3$ s and raised at $t = 6$ s to the initial value. The expected result of a lower supply pressure is a higher magnitude of the command voltage, because due to the smaller pressure difference the orifice area of the valve has to be greater for obtaining the same mass flow. This effect can be seen in the plot. In the characteristics of the angle and the pressure there is no significant difference.

In the ninth experiment the supply pressure is raised at $t = 3$ s and reduced at $t = 6$ s. In Figure 5.10 the described effect occurs in the other direction, which means that the magnitude of the command voltage is smaller during the higher supply pressure.

In Figure 5.11 the tenth experiment is plotted. There the ninth experiment is performed with a sinusoidal desired trajectory. Also here the magnitude of the command voltage is smaller at a higher supply pressure. In the other variables there is no significant difference.

Changes in the temperature are investigated in the eleventh experiment, given in Figure 5.12. The temperature is raised at $t = 3$ s and reduced at $t = 6$ s to the initial value. There is no significant change in the characteristics. Following, the controller seems to be robust for changes in the temperature.

Effects of the threshold parameters for the Karnopp friction model

The Karnopp friction model requires two threshold parameters, the threshold velocity $\dot{z}_{thr}$ and the threshold friction force F_{thr}. In the next experiments the effects of changes in these parameters are investigated. Therefore the driven mass is varied. It is applied at $t = 0$ s, reduced at $t = 3$ s and raised at $t = 6$ s. In the experiments the joint angle is controlled, and the desired trajectory is sinusoidal.

The twelfth experiment is identical to the seventh, but plotted again for comparison in Figure 5.13. The velocity threshold is low and the force threshold is medium-sized.

In the thirteenth experiment, printed in Figure 5.14, the velocity threshold is high and the force threshold is medium-sized. Here the control signal chatters more than with the lower threshold. Also there are more oscillations for the smaller weight. Especially for the smaller weight the tracking error is higher than with the lower threshold. In the Karnopp friction model the velocity near to zero shall be regarded as zero, so the lower threshold with $\dot{z}_{thr} = 0.1 \left[\frac{\text{mm}}{\text{s}}\right]$ is chosen as parameter.

The threshold force is reduced in the fourteenth experiment. The characteristics are given in Figure 5.15. In the fifteenth experiment, given in Figure 5.16, the threshold force is raised. During the slipping mode, there are no differences. At the sticking mode there are wavelike deviations in the angle, the pressure and the command voltage which raise with raising threshold force. Also the tracking error is higher during the sticking mode. With the threshold force it is described which force has to be generated to start a movement of the joint or load. The medium-sized threshold force is $F_{thr} = 0.5$ N which corresponds to a load of 50 g. With a mass range of $m_s = 0.5$ to 1.5 kg this seems to be realistic. So the medium-sized threshold force is

used as parameter for the simulations.

The experiments show that with a supply pressure of 3 bar which is the working range also postulated in the literature the single PMA used in this thesis can carry loads in the range of 0.5 to 1.5 kg. In the described joint design the range of the weight is between 0.5 and 1 kg with the range of the angle between 0.75 rad respectively 0.9 rad and 1.5 rad. These ranges could be extended by raising the supply pressure, but it is questionable if the material of the PMA can withstand the higher pressure for longer time. The controller can deal with fluctuations of the driven mass and the supply pressure. The temperature has no influence on the experiments.

5.4.2 Actual parameters for the closed-loop control experiments

Actual values of the controller parameters

The actual controller parameters are given in Table 5.1.

Table 5.1: Actual values of the controller parameters

symbol	meaning	value	unit
P_1, P_2, P_3	applied poles	-25	[-]
K_2	controller parameter	75	[-]
K_1	controller parameter	1875	[-]
K_0	controller parameter	15625	[-]

Values of the varied model parameters

The parameter values which are used in the single experiments are assembled in Table 5.2.

5.4.3 Results of the experiments

In the first subplot the command voltage as input into the model is given. In the second subplot the simulated and the desired trajectory are plotted. The trajectory error is given in the third subplot as $y(t) - y_d(t)$, and the pressure characteristics are plotted in the forth subplot.

Table 5.2: Properties and values of the varied parameters

number of exp.	driven mass m_s [kg]			supply pressure p_s [$\frac{N}{m^2}$]			temperature T [K]			threshold velocity $\dot{z}_{thr}$ [$\frac{m}{s}$]	threshold force $F_{thr}[N]$	Figure
1	0.5, 1 and 3			303975			298			0.0001	0.5	5.3
2	1.5	1	1.5	303975			298			0.0001	0.5	5.3
3	1.5	1	1.5	303975			298			0.0001	0.5	5.4
4	1.5	1	1.5	303975			298			-	-	5.5
5	1.5	1	1.5	303975			298			-	-	5.6
6	0.75	0.5	0.75	303975			298			0.0001	0.5	5.7
7	0.75	0.5	0.75	303975			298			0.0001	0.5	5.8
8	0.75			303975	202488	303975	298			0.0001	0.5	5.9
9	0.75			303975	506625	303975	298			0.0001	0.5	5.10
10	0.75			303975	506625	303975	298			0.0001	0.5	5.11
11	0.75			303975			298	318	298	0.0001	0.5	5.12
12	0.75	0.5	0.75	303975			298			0.0001	0.5	5.13
13	0.75	0.5	0.75	303975			298			0.02	0.5	5.14
14	0.75	0.5	0.75	303975			298			0.0001	0.15	5.15
15	0.75	0.5	0.75	303975			298			0.0001	1	5.16

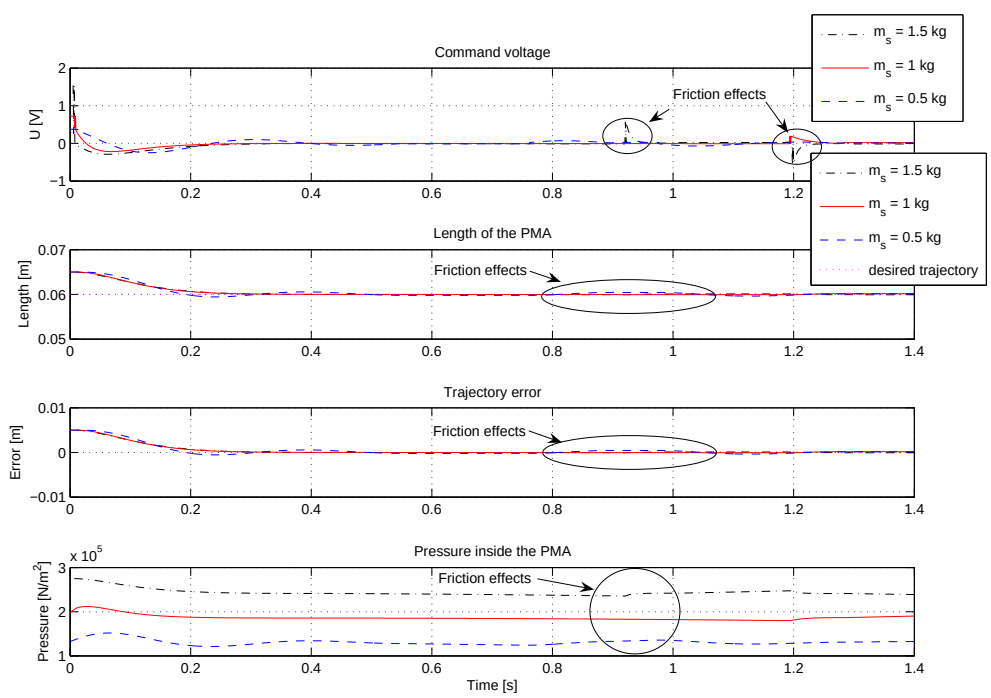

Figure 5.2: Onset behavior of the length control with different driven loads and constant desired trajectory

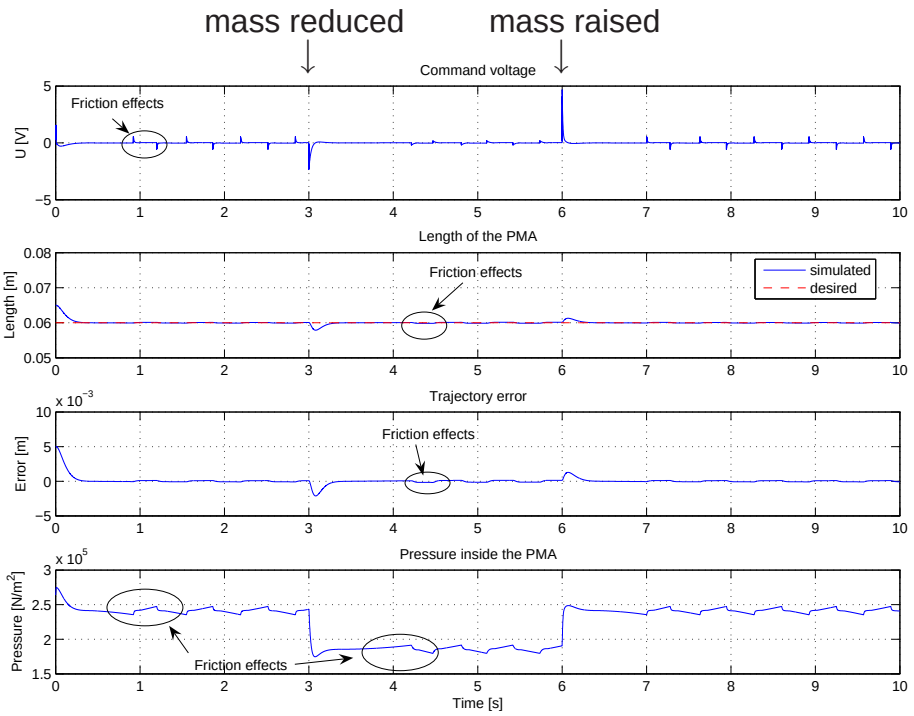

Figure 5.3: Length control with abruptly changed driven mass, Karnopp friction model and constant desired trajectory

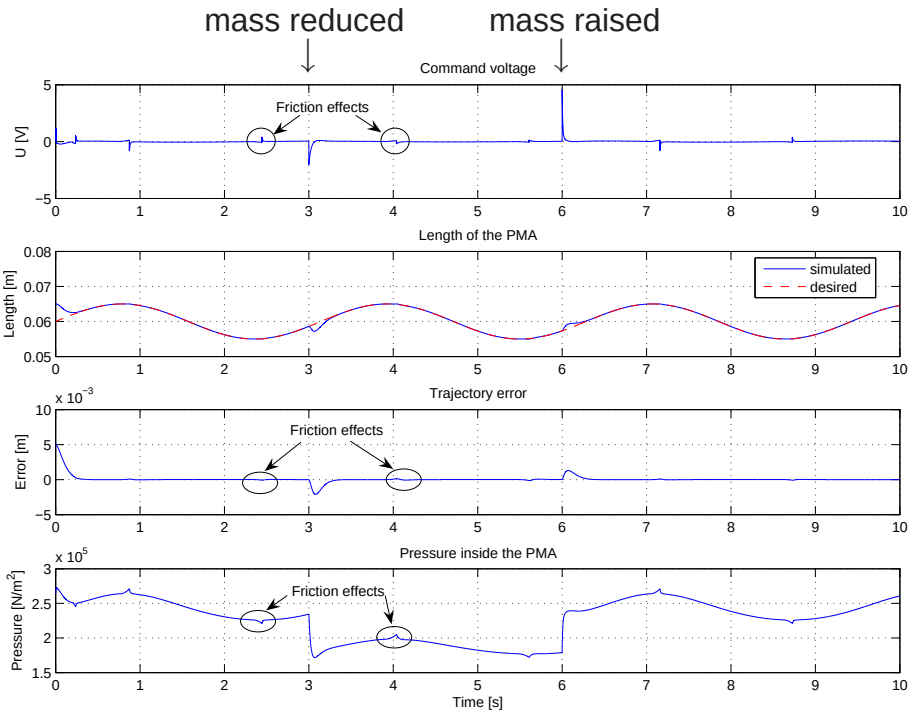

Figure 5.4: Length control with abruptly changed driven mass, Karnopp friction model and sinusoidal desired trajectory

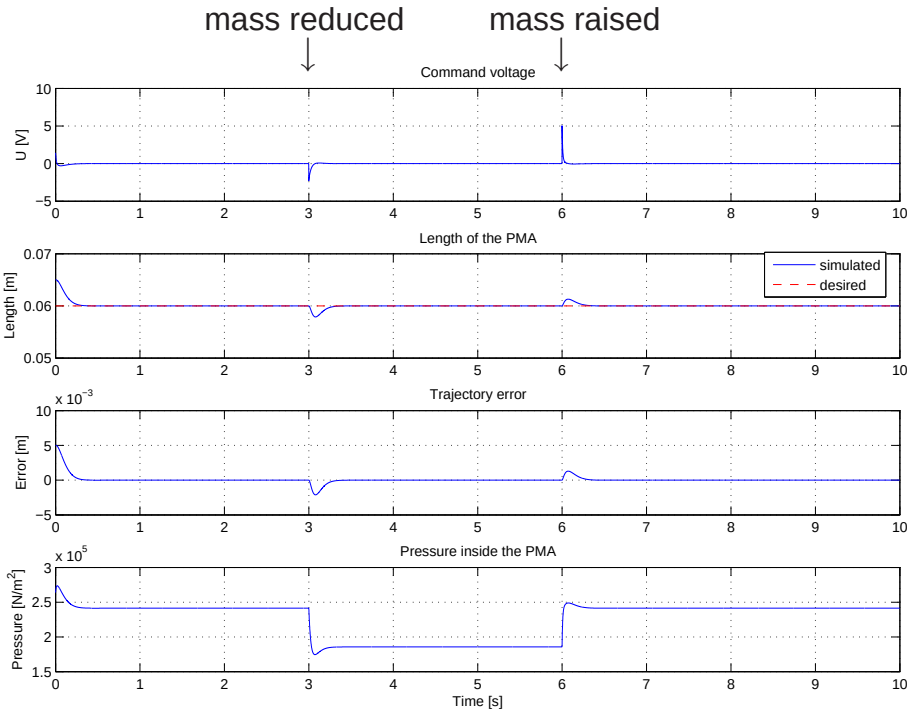

Figure 5.5: Length control with abruptly changed driven mass, proportional friction law and constant desired trajectory

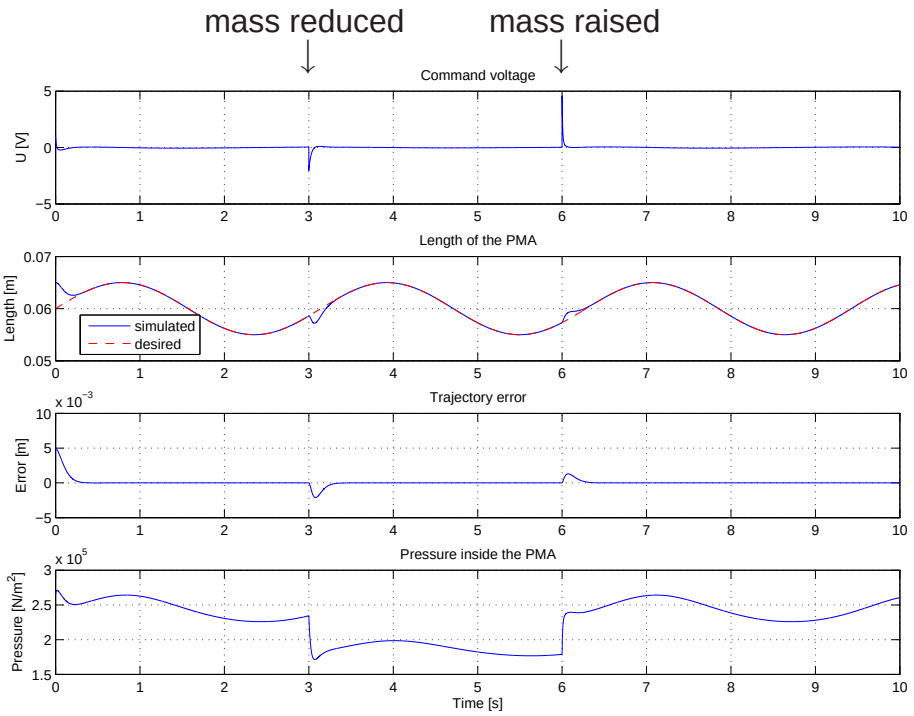

Figure 5.6: Length control with abruptly changed driven mass, proportional friction law and sinusoidal desired trajectory

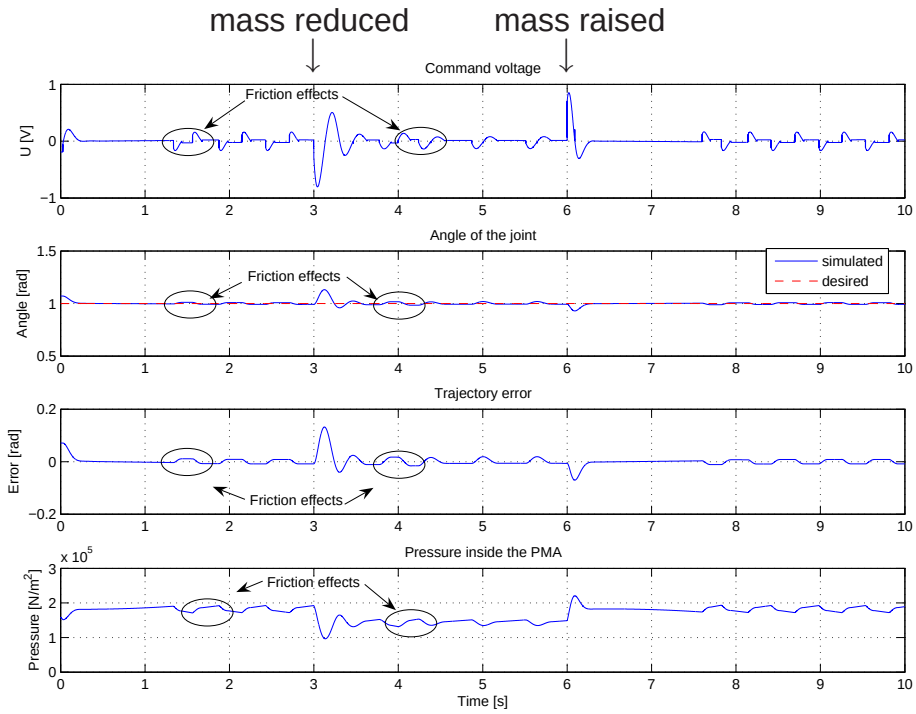

Figure 5.7: Angle control with abruptly changed driven mass and constant desired trajectory

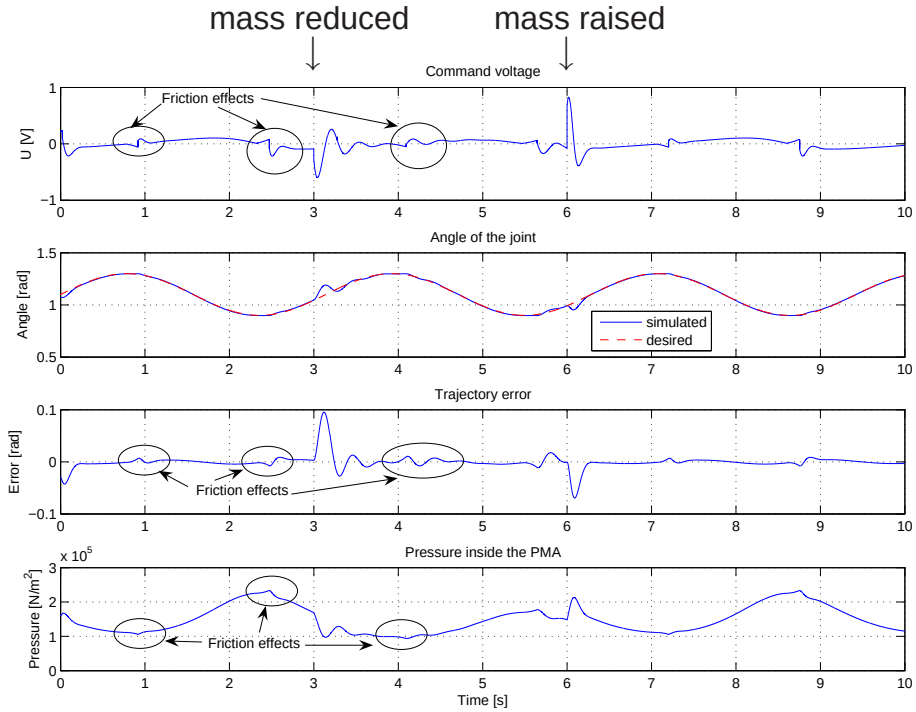

Figure 5.8: Angle control with abruptly changed driven mass and sinusoidal desired trajectory

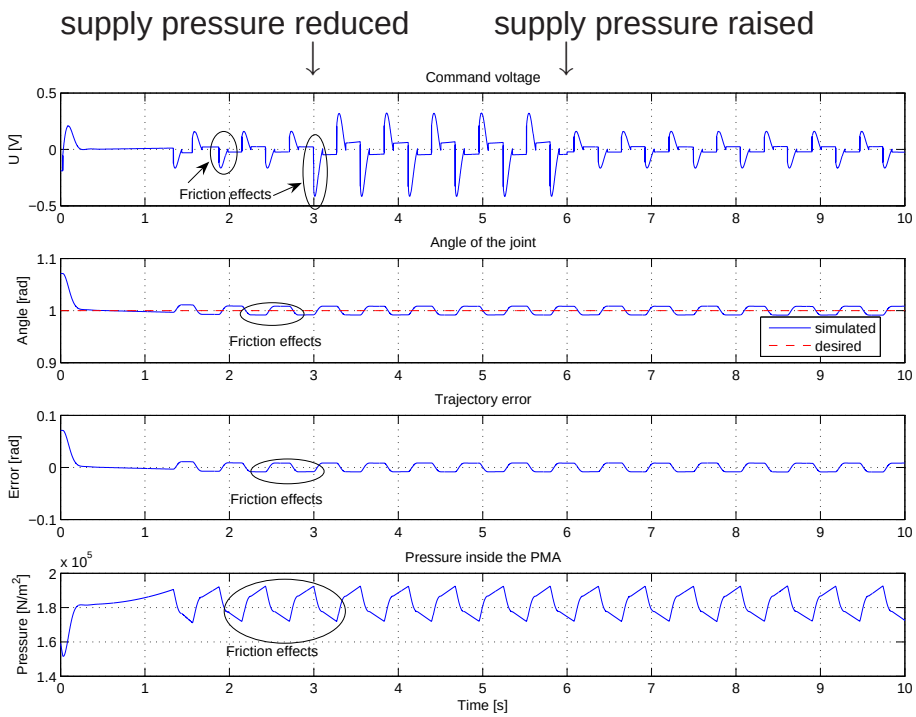

Figure 5.9: Angle control with abruptly decreasing and normalizing supply pressure and constant desired trajectory

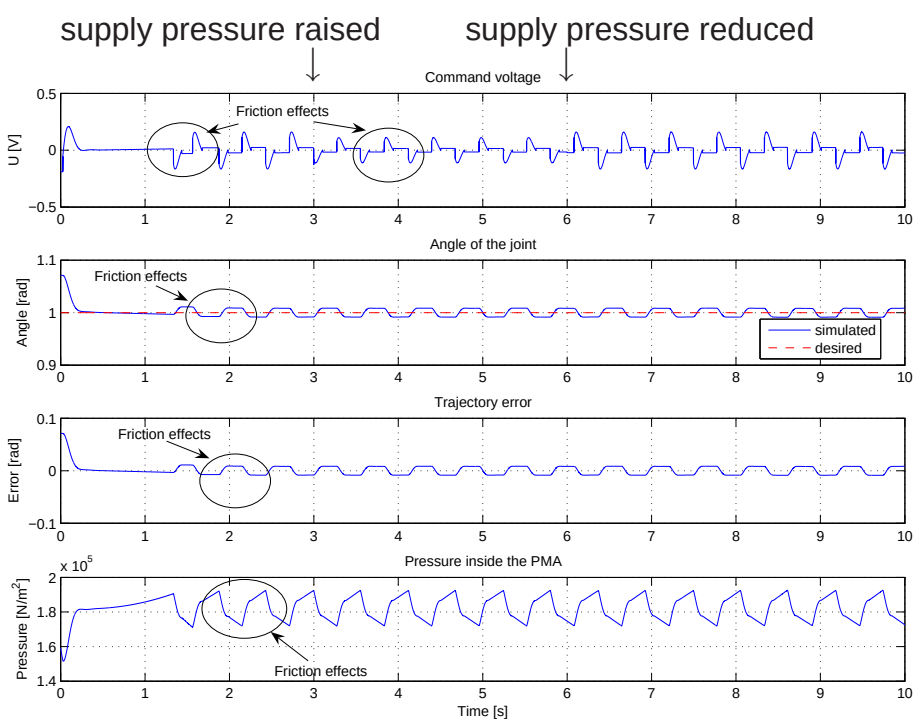

Figure 5.10: Angle control with abruptly increasing and normalizing supply pressure and constant desired trajectory

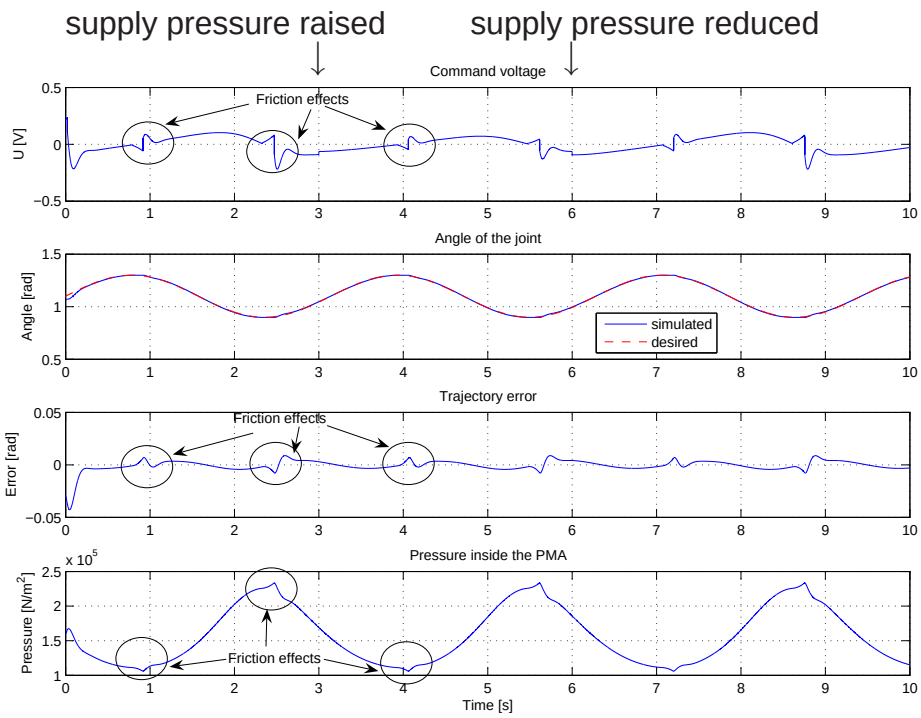

Figure 5.11: Angle control with abruptly increasing and normalizing supply pressure and sinusoidal desired trajectory

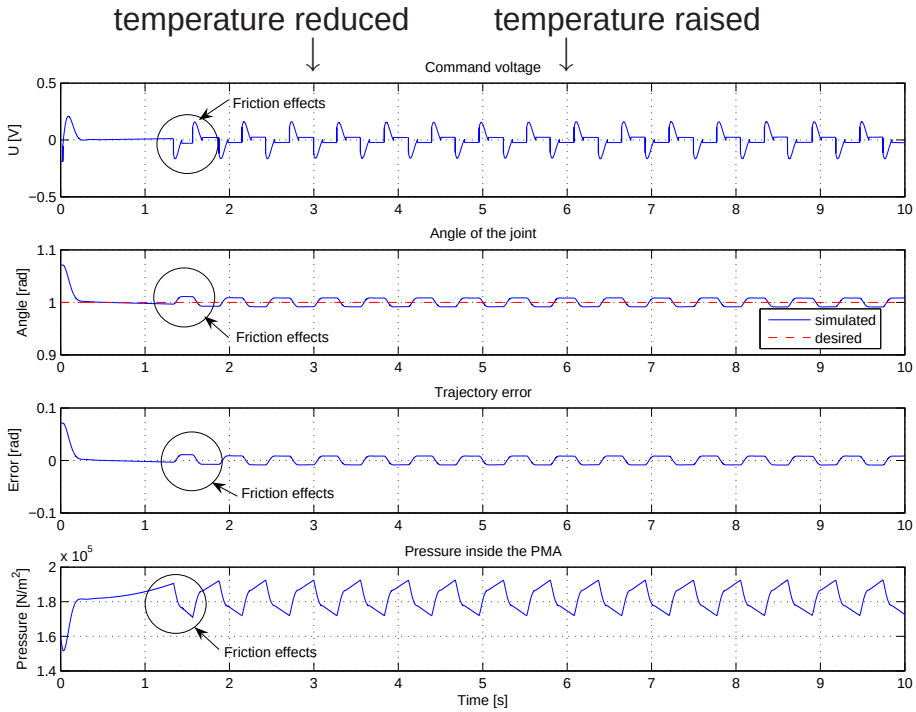

Figure 5.12: Angle control with abruptly changed temperature and constant desired trajectory

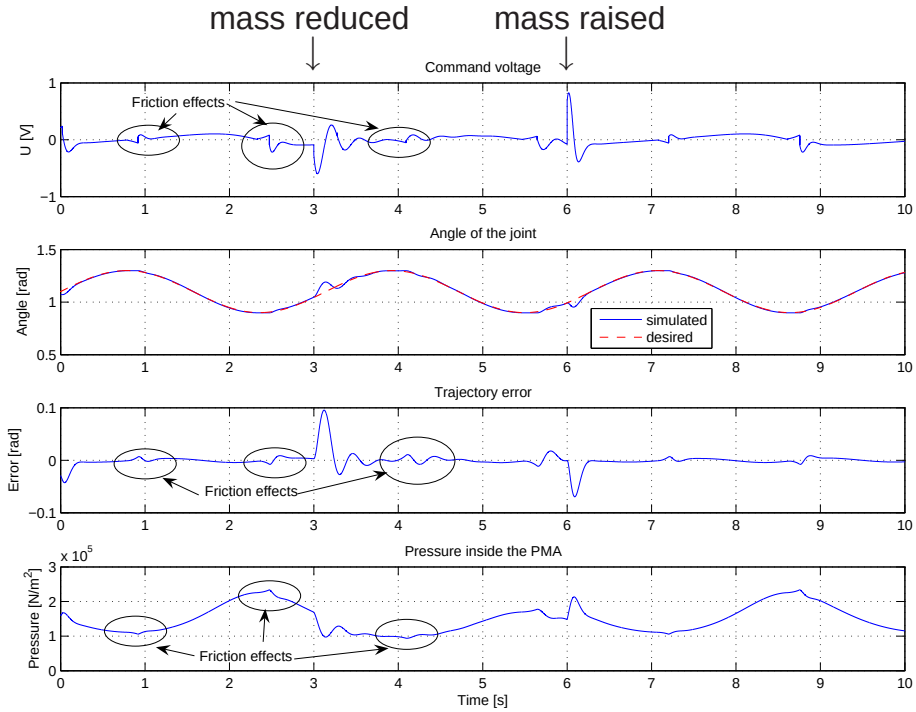

Figure 5.13: Angle control with low threshold velocity

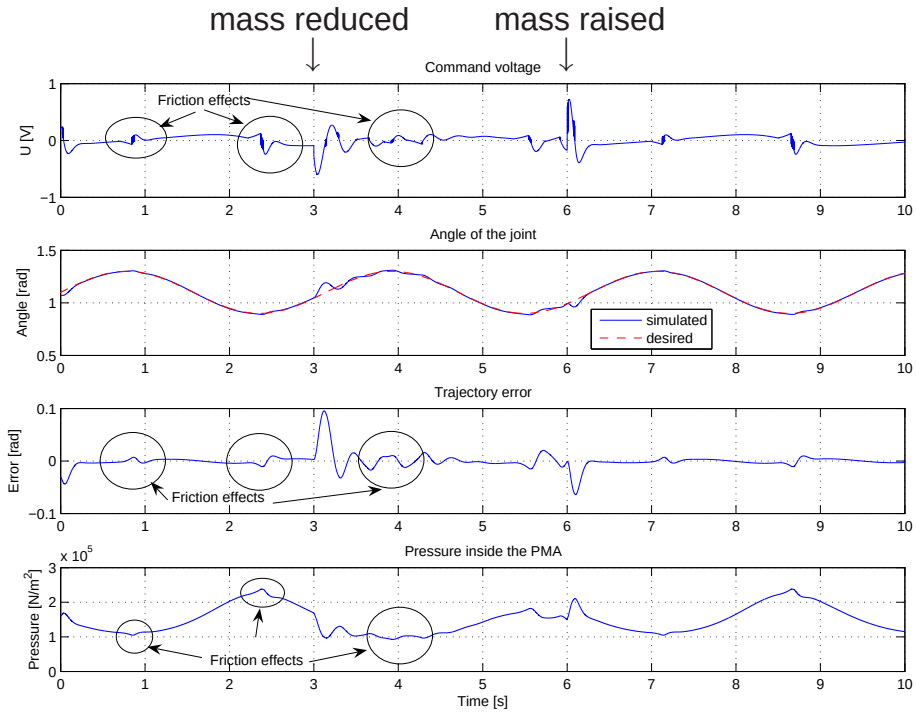

Figure 5.14: Angle control with high threshold velocity

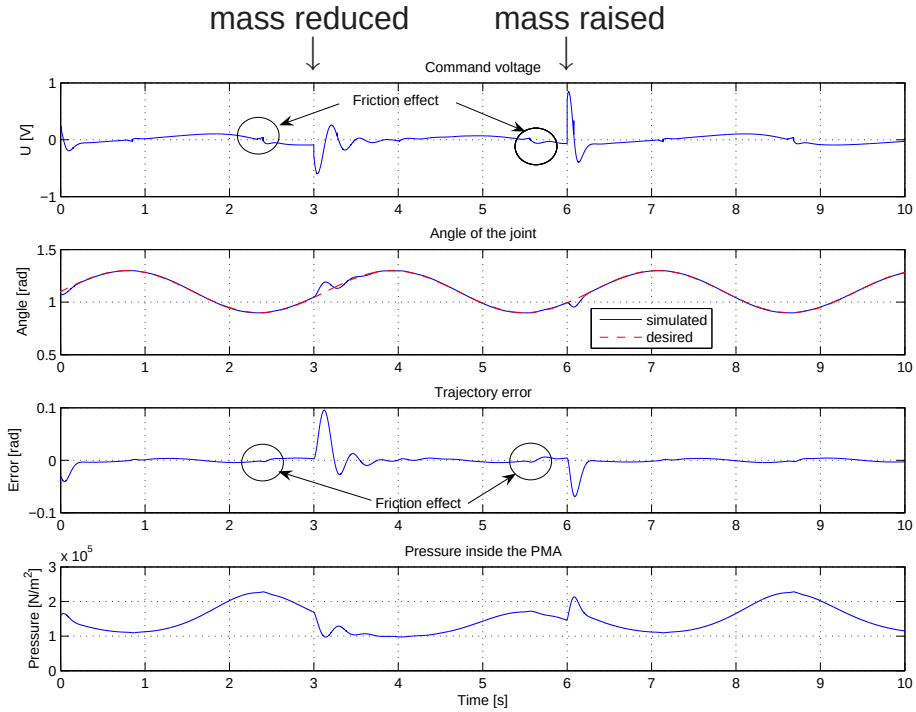

Figure 5.15: Angle control with low threshold force

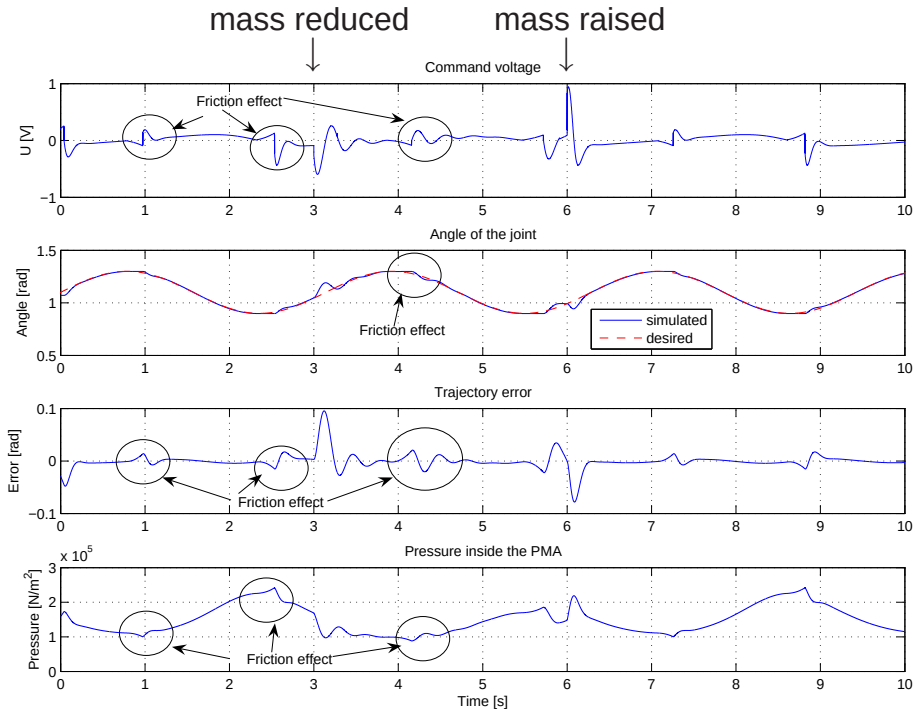

Figure 5.16: Angle control with high threshold force

Chapter 6

Conclusions and outlook

In this thesis a closed loop control of an artificial joint actuated by Pneumatic Muscle Actuators (PMA) was designed.

Starting from a detailed literature review a physical based model was developed and implemented in MATLAB/ Simulink. In simulated experiments the model was validated and its behavior was investigated. Physically the PMA contracts at rising inner pressure. This relation was also observed in the simulations. The PMA behaves very unstable.

There were two different friction models applied and compared. The friction model which distinguishes between the slipping and the sticking modus of the PMA represents the occurring friction more adequate than the simple proportional friction law.

The PMA was modeled and implemented in its basic form by driving a load vertically. For different applications the external force which affects the PMA has to be exchanged. This was done in the design of a mechanical joint. Also the model of the joint was validated simulative.

A possible further research topic is the validation of the PMA model by performing experiments with a real PMA.

Next a closed loop tracking control was applied. Therefore a flatness based controller combined with a pole placement tracking controller was designed. The prerequisites for applying this control method are fulfilled in relaxed and contracted state of the PMA. The performance of the closed loop control system was validated by MATLAB/ Simulink simulations. It was shown that

the controller can compensate abruptly mass changes and fluctuations in the supply pressure and in the temperature.

Also the controller performance was compared for the two different friction laws. It works very good for the proportional friction law. The control signal is smooth and the tracking occurs fast and exact. With the slip-stick model there occur some effects like a slightly chattering in the control signal and some roughnesses in the control signal and the state characteristics. These effects occur during sticking mode, but they are not very strong.

Two possible further research topic are the the control of a PMA in extended state and the validation of the closed loop control system by performing experiments with a real PMA.

Bibliography

[1] K.J. Åström and B. Wittenmark. *Adaptive Control*. Addison-Wesley Publishing Company Inc., 2. edition, 1995.

[2] D.G. Caldwell, G.A. Medrano-Cerda, and M. Goodwin. Control of pneumatic muscle actuators. *IEEE Control Systems*, 15(1):40–48, Feb. 1995.

[3] D.G. Caldwell, N. Tsagarakis, and G.A. Medrano-Cerda. Bio-mimetic actuators: polymeric Pseudo Muscular Actuators and pneumatic Muscle Actuators for biological emulation. *Mechatronics*, 10:499–530, 2000.

[4] P. Carbonell, Z.-P. Jiang, and D.W. Repperger. Nonlinear Control of a Pneumatic Muscle Actuator System. *http://ctrl.poly.edu/visitors/pjcarbon/pdf/nolcos01.pdf*, 2001.

[5] W. Chester. *Mechanics*. Chapman & Hall, 1991.

[6] C.-P. Chou and B. Hannaford. Measurement and Modeling of McKibben Pneumatic Artificial Muscles. *IEEE Transactions on Robotics and Automation*, 12(1):90–102, 1996.

[7] W.E. Dixon, A. Behal, D.M. Dawson, and S.P. Nagarkatti. *Nonlinear Control of Engineering Systems : A Lyapunov-Based Approach*. Birkhäuser, 2003.

[8] C.L. Dym and E.S. Ivey. *Principles of Mathematical Modeling*. Academic Press, Harcourt Brace and Company, 1980.

[9] M. Fliess, J. Lévine, P. Martin, and P. Rouchon. Flatness and defect of non-linear systems: introductory theory and examples. *International Journal of Control*, 61(6):1327–1361, 1995.

[10] R.A. Freeman, M. Krstić, and P.V. Kokotović. Robustness of Adaptive Nonlinear Control to Bounded Uncertainties. *Automatica*, 34(10):1227–1230, 1998.

[11] R. Van Ham, F. Daerden, B. Verrelst, and D. Lefeber. Control of a joint actuated by two Pneumatic Artificial Muscles with fast switching ON-OFF Valves. In *6th National congress on theoretical and applied mechanics*, Ghent, May 2003. CD-ROM, Paper no. 075.

[12] B. Hannaford, K. Jaax, and G. Klute. Bio-Inspired Actuation and Sensing. *Autonomous Robots*, 11:267–272, 2001.

[13] A. Hildebrandt, O. Sawodny, R. Neumann, and A. Hartmann. A Flatness Based Design for Tracking Control of Pneumatic Muscle Actuators. In *Seventh International Conference on Control, Automation, Robotics and Vision (ICARCV'02)*, Singapore, Dec 2002.

[14] A. Isidori. *Nonlinear Control Systems II*. Springer, London, 1999.

[15] Z.-P. Jiang and L. Praly. Design of Robust Adaptive Controllers for Nonlinear Systems with Dynamic Uncertainties. *Automatica*, 34(7):825–840, 1998.

[16] D. Karnopp. Computer Simulation of Stick-Slip Friction in Mechanical Dynamic Systems. *Journal of Dynamic Systems, Measurement, and Control*, 107:100–103, March 1985.

[17] H.J. Marquez. *Nonlinear Control Systems : Analysis and Design*. Wiley, 2003.

[18] G.A. Medrano-Cerda, C.J. Bowler, and D.G. Caldwell. Adaptive Position Control of Antagonistic Pneumatic Muscle Actuators. In *Proceedings of the International Conference on Intelligent Robots and Systems-Volume 1*, volume 1, pages 378–383, Washington, DC, 1995. IEEE Computer Society.

[19] K. Osuka, T. Kimura, and T. Ono. H^{∞} Control of a Certain Nonlinear Actuator. In *Proceedings of the 29th IEEE Conference on Decision and Control 1990*, pages 370–371, Honolulu, Hawaii, Dec. 1990.

[20] N.-C. Park, H.-S. Yang, H.-W. Park, and Y.-P. Park. Position/vibration control of two-degree-of-freedom arms having one flexible link with artificial pneumatic muscle actuators. *Robotics and Autonomous Systems*, 40:239–253, 2002.

[21] G. Puschmann and R. Drath. *Technische Wärmelehre*. Technik-Tabellen-Verlag Fikentscher und Co., Darmstadt, 25 edition, 1980.

[22] J. Raisch. *Mehrgrößenregelung im Frequenzbereich*. Oldenbourg, München, 1994.

[23] D.W. Repperger, K.R. Johnson, and C.A. Phillips. A VSC Position Tracking System Involving a large Scale Pneumatic Muscle Actuator. In *Proceedings of the 37th IEEE Conference on Decision and Control 1998*, pages 4302–4307, Tampa, Florida, Dec. 1998.

[24] D.W. Repperger, K.R. Johnson, and C.A. Phillips. Nonlinear Feedback Controller Design of A Pneumatic Muscle Actuator System. In *Proceedings of the American Control Conference 1994*, pages 1525–1529, San Diego, California, Jun. 1999.

[25] R. Resnick, D. Halliday, and K.S. Krane. *Physics*. Wiley and Sons, Inc., New York, 4 edition, 1992.

[26] D.B. Reynolds, D.W. Repperger, C.A. Phillips, and G. Bandry. Modeling the Dynamic Characteristics of Pneumatic Muscle. *Annals of Biomedical Engineering*, 31(3):310–317, 2003.

[27] R.Y. Rubinstein and B. Melamed. *Modern Simulation and Modeling*. Wiley and Sons, Inc., New York, 1998.

[28] E. Shafai. Einführung in die Adaptive Regelung. Technical report, Institut für Mess- und Regeltechnik, Eidgenössische Technische Hochschule, Zürich, April 2003.

[29] T. Takuma, S. Nakajima, K. Hosoda, and M. Asada. Design of Self-Contained Biped Walker with Pneumatic Actuators. In *SICE Annual Conference 2004*, 2004. WPI-2-4.

[30] G. Tao. *Adaptive Control Design and Analysis*. Wiley, 2003.

[31] H. Unbehauen. *Regelungstechnik III*. Friedr. Vieweg und Sohn Verlagsgesellschaft mbH, Braunschweig / Wiesbaden , 2000. Sechste Auflage.

[32] R.Q. van der Linde. Design, Analysis, and Control of a Low Power Joint for Walking Robots, by Phasic Activations of McKibben Muscles. *IEEE Transactions on Robotics and Automation*, 15(4):599–604, 1999.

[33] M. van Nieuwstadt, M. Rathinam, and R.M. Murray. Differential Flatness and Absolute Equivalence of Nonlinear Control Systems . *SIAM Journal on Control and Optimization*, 36(4):1225–1239, 1998.

List of Figures

2.1 Braided Pneumatic Muscle Actuator (PMA) 12
2.2 Possible antagonistic designs of a PMA 13
2.3 Angle formed by PMAs 14
2.4 Control system of a model reference adaptive controller (MRAC) 18
2.5 Control system of a self-tuning controller (STC) 19

3.1 Illustration of the interweave angle 24
3.2 Pleated Pneumatic Muscle Actuator (PMA) 29
3.3 Characteristics of the Karnopp friction force model 31

4.1 Main structure of the model 45
4.2 Scheme of the affecting forces on the PMA 48
4.3 Static relation between the PMA length respectively the inner pressure and the PMA force 50
4.4 General view of a system 52
4.5 Joint driven by one PMA 54
4.6 Geometry of the joint 55
4.7 Relationship between PMA length and joint angle for different lengthes of the links 56
4.8 Affecting forces and torques 57
4.9 Relationship between joint angle and external force for different driven masses 58
4.10 Step response of length and pressure for different friction models 62
4.11 Impulse response of length and pressure for different friction models 62
4.12 Step response of length and pressure for different driven masses 63
4.13 Impulse response of length and pressure for different driven masses 63
4.14 Step response of joint angle and pressure for different driven masses 64
4.15 Impulse response of joint angle and pressure for different driven masses 64

5.1 Structure of the control system 66
5.2 Onset behavior of the length control with different driven loads and constant desired trajectory 81
5.3 Length control with abruptly changed driven mass, Karnopp friction model and constant desired trajectory 82
5.4 Length control with abruptly changed driven mass, Karnopp friction model and sinusoidal desired trajectory 82
5.5 Length control with abruptly changed driven mass, proportional friction law and constant desired trajectory 83
5.6 Length control with abruptly changed driven mass, proportional friction law and sinusoidal desired trajectory 83
5.7 Angle control with abruptly changed driven mass and constant desired trajectory 84
5.8 Angle control with abruptly changed driven mass and sinusoidal desired trajectory 84
5.9 Angle control with abruptly decreasing and normalizing supply pressure and constant desired trajectory 85
5.10 Angle control with abruptly increasing and normalizing supply pressure and constant desired trajectory 85
5.11 Angle control with abruptly increasing and normalizing supply pressure and sinusoidal desired trajectory 86
5.12 Angle control with abruptly changed temperature and constant desired trajectory 86
5.13 Angle control with low threshold velocity 87
5.14 Angle control with high threshold velocity 87
5.15 Angle control with low threshold force 88
5.16 Angle control with high threshold force 88

A.1 Illustration of the geometric variables of the PMA 99

B.1 Main level of the control of a driven load with proportional friction law 108
B.2 Init block of the control of a driven load with proportional friction law 109
B.3 Input generation for the control of a driven load with proportional friction law . 110
B.4 Desired trajectory for the control of a driven load with proportional friction law 110
B.5 PMA model for the control of a driven load with proportional friction law . . . 111
B.6 Intrinsic PMA model in the control of a driven load with proportional friction law 112
B.7 Internal pressure in the control of a driven load with proportional friction law . 113

B.8 Volume in the control of a driven load with proportional friction law 113
B.9 PMA length in the control of a driven load with proportional friction law 113
B.10 PMA force in the control of a driven load with proportional friction law 114
B.11 Other forces in the control of a driven load with proportional friction law 114
B.12 Valve in the control of a driven load with proportional friction law 114
B.13 Controller of a driven load with proportional friction law 115
B.14 Trajectory computation for the control of a driven load with proportional friction law 115
B.15 Tracking control for a driven load with proportional friction law 115
B.16 Inverse system for the control of a driven load with proportional friction law . . 116
B.17 Main level of the control of a driven load with Karnopp friction model 117
B.18 Init block of the control of a driven load with Karnopp friction model 118
B.19 Input generation for the control of a driven load with Karnopp friction model . 119
B.20 Desired trajectory for the control of a driven load with Karnopp friction model . 119
B.21 PMA model for the control of a driven load with Karnopp friction model 120
B.22 Intrinsic PMA model in the control of a driven load with Karnopp friction model 121
B.23 Internal pressure in the control of a driven load with Karnopp friction model . . 122
B.24 Volume in the control of a driven load with Karnopp friction model 122
B.25 PMA length in the control of a driven load with Karnopp friction model 123
B.26 PMA force in the control of a driven load with Karnopp friction model 123
B.27 Other forces in the control of a driven load with Karnopp friction model 124
B.28 Valve in the control of a driven load with Karnopp friction model 124
B.29 Controller of a driven load with Karnopp friction model 125
B.30 Trajectory computation for the control of a driven load with Karnopp friction model 125
B.31 Tracking control for a driven load with Karnopp friction model 125
B.32 Inverse system for the control of a driven load with Karnopp friction model . . 126
B.33 Main level of the control of a driven joint with Karnopp friction model 127
B.34 Conversion length to angle in the control of a driven joint with Karnopp friction model 128
B.35 Init block of the control of a driven joint with Karnopp friction model 128
B.36 Input generation for the control of a driven joint with Karnopp friction model . 129
B.37 Desired trajectory for the control of a driven joint with Karnopp friction model 129

B.38 PMA model for the control of a driven joint with Karnopp friction model . . . 130
B.39 Intrinsic PMA model in the control of a driven joint with Karnopp friction model 131
B.40 Internal pressure in the control of a driven joint with Karnopp friction model . . 132
B.41 Volume in the control of a driven joint with Karnopp friction model 132
B.42 PMA length in the control of a driven joint with Karnopp friction model 133
B.43 PMA force in the control of a driven joint with Karnopp friction model 133
B.44 Other forces in the control of a driven joint with Karnopp friction model 134
B.45 Valve in the control of a driven joint with Karnopp friction model 135
B.46 Controller of a driven joint with Karnopp friction model 135
B.47 Trajectory computation for the control of a driven joint with Karnopp friction model 136
B.48 Conversion of the angle to the length in the control of a driven joint with Karnopp friction model 136
B.49 Tracking control for a driven joint with Karnopp friction model 137
B.50 Inverse system for the control of a driven joint with Karnopp friction model . . 137

List of Tables

3.1 Parameters and variables of Hildebrandt et al. [13] 23
3.2 Parameters and variables of Caldwell et al. [2] 27
3.3 Parameters and variables of Repperger et al. [23, 24] 32
3.4 Parameters and variables of Reynolds et al. [26] 34

4.1 Actual values of the model parameters 60

5.1 Actual values of the controller parameters 80
5.2 Properties and values of the varied parameters 81

Appendix A

Mathematical derivations

A.1 Derivation of the volume of the PMA

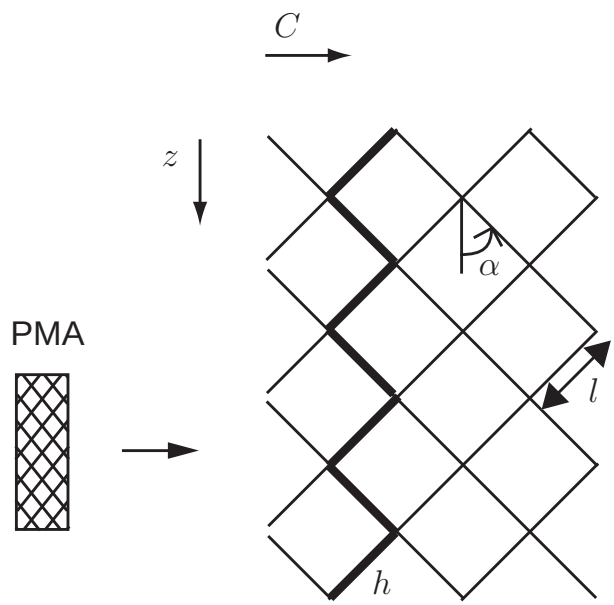

Figure A.1: Illustration of the geometric variables of the PMA

For the volume model equation the shell of the PMA is 'opened'. It is presented schematic in Figure A.1. The shell consists mainly of a braid which forms many little trapezoids. The angle of the single braid fibers with respect to the longitudinal axis is called interweave angle α. It changes during the contraction and extension of the PMA. In dependency of this interweave

angle $\alpha(t)$ the length $z(t)$ and the circumference $C(t)$ of the PMA are expressed. The diameter $D(t)$ of the PMA is proportional to the circumference.

$$z(t) = 2 \cdot A \cdot l \cdot \cos\alpha(t) \tag{A.1}$$

$$C(t) = 2 \cdot B \cdot l \cdot \sin\alpha(t) \tag{A.2}$$

$$D(t) = \frac{1}{\pi} \cdot C(t) \tag{A.3}$$

A	[-]	-	number of trapezoids in z-direction (longitudinal)
B	[-]	-	number of trapezoids in y-direction (radial)
l	[m]	-	side length of the trapezoids

The constant parameters of these equations are assembled for simplifying and included into the Equations A.1 - A.3.

$$h = 2 \cdot A \cdot l \tag{A.4}$$

$$f = \frac{1}{\pi} \cdot 2 \cdot B \cdot l \tag{A.5}$$

$$z(t) = h \cdot \cos\alpha \tag{A.6}$$

$$D(t) = f \cdot \sin\alpha \tag{A.7}$$

h	[m]	-	helical fiber length of the PMA
f	[m]	-	diametric distance parameter of the PMA

The surface area $S(t)$ of the PMA is derived as

$$S(t) = C(t) \cdot z(t) = \pi \cdot D(t) \cdot z(t) \tag{A.8}$$

The volume $V(t)$ of the PMA is determined as

$$V(t) = \frac{\pi}{4} \cdot D^2(t) \cdot z(t) \tag{A.9}$$

Next the Equations A.6 and A.7 are included:

$$V(t) = \frac{\pi}{4} \cdot f^2 \cdot \sin^2\alpha(t) \cdot h \cdot \cos\alpha(t) \tag{A.10}$$

The interweave angle α cannot be measured online, so it is replaced by a function of the length of the PMA. According to Equation A.6 $\cos\alpha$ can be replaced directly. To replace $\sin^2\alpha$ Equation A.6 is squared and the trigonometric law

$$\sin^2\alpha + \cos^2\alpha = 1 \tag{A.11}$$

is applied:

$$z^2(t) = h^2(1 - \sin^2 \alpha) \tag{A.12}$$

which yields

$$\sin^2 \alpha = \frac{h^2 - z^2(t)}{h^2} \tag{A.13}$$

with

$$0 \leq \sin \alpha \leq 1 \tag{A.14}$$

which means

$$0 \leq \alpha \leq \frac{\pi}{2} \tag{A.15}$$

Now Equation A.10 can be rewritten as:

$$V(t) = \frac{\pi f^2}{4h^2} \cdot \left(h^2 - z^2(t)\right) \cdot z(t) \tag{A.16}$$

respectively

$$V(t) = \frac{\pi f^2}{4} \cdot z(t) - \frac{\pi f^2}{4h^2} \cdot z^3(t) \tag{A.17}$$

The first derivative with respect to the length is

$$\frac{dV(t)}{dz(t)} = \frac{\pi f^2}{4} - \frac{3\pi f^2}{4h^2} \cdot z^2(t) \tag{A.18}$$

respectively

$$\frac{dV(t)}{dz(t)} = \frac{\pi f^2}{4h^2} \cdot \left(h^2 - 3z^2(t)\right) \tag{A.19}$$

A.2 Development of the state space form

A.2.1 Assembling and simplification of the modeled properties:

The mass flow through the valve is described by Equation 4.2 and Equation 4.3. The physical parameters are summarized for simplification:

$$\alpha_1 := c \cdot p_s \tag{A.20}$$

$$\alpha_2 := \frac{2\eta}{RT(\eta - 1)} \cdot p_s^{-\frac{2}{\eta}} \tag{A.21}$$

$$\alpha_3 := \frac{2\eta}{RT(\eta - 1)} \cdot p_s^{-\frac{\eta+2}{\eta}} \tag{A.22}$$

$$\alpha_4 := \frac{2}{\eta} \tag{A.23}$$

$$\alpha_5 := \frac{\eta + 2}{\eta} \tag{A.24}$$

$$\tag{A.25}$$

The simplified equation for the mass flow is:

$$\dot{m}_g(t) = \alpha_1 \cdot U(t) \cdot \sqrt{\alpha_2 \cdot p(t)^{\alpha_4} - \alpha_3 \cdot p(t)^{\alpha_5}} \tag{A.26}$$

The inner pressure, derived from ideal gas equation (Equation 4.4) is with

$$\alpha_6 := \frac{1}{RT} \tag{A.27}$$

summarized to

$$m_g(t) = \alpha_6 p(t) V(t) \tag{A.28}$$

Also the polytrophic gas law is important:

$$pV^{\chi} = \text{constant} \tag{A.29}$$

The differential equation for the pressure (Equation 4.6) is simplified with

$$\alpha_7 \quad := \quad \chi RT \tag{A.30}$$

$$\tag{A.31}$$

to:

$$\dot{p}(t) = \alpha_7 \cdot \frac{\dot{m}_g(t)}{V(t)} - \chi \cdot \frac{p(t)\dot{V}(t)}{V(t)} \tag{A.32}$$

whereas

$$\dot{V}(t) = \frac{dV(t)}{dt} = \frac{dV(t)}{dz} \cdot \dot{z}(t) \tag{A.33}$$

The equation for the volume (Equation 4.8) is summarized with

$$\alpha_8 \quad := \quad \frac{\pi}{4} f^2 \tag{A.34}$$

$$\alpha_9 \quad := \quad \frac{\pi f^2}{4h^2} \tag{A.35}$$

to

$$V(t) = \alpha_8 z(t) - \alpha_9 z^3(t) \tag{A.36}$$

The derivative of the volume with respect to the PMA length (Equation 4.13) is simplified with

$$\alpha_{10} \quad := \quad \frac{3\pi f^2}{4h^2} \tag{A.37}$$

to

$$\frac{dV(t)}{dz} = \alpha_8 - \alpha_{10} z^2(t) \tag{A.38}$$

The second main equation is the balance of forces:

$$m_s \ddot{z}(t) = m_s g + F_{ext} - F_m(t) - F_e(t) - F_f(t) \tag{A.39}$$

The generated PMA force $F_m(t)$ is modeled as

$$F_m(t) = (p(t) - p_0) \cdot \frac{dV(t)}{dz} \tag{A.40}$$

the elastic force $F_e(t)$ depends linear on the PMA length

$$F_e(t) = K \cdot z(t) \tag{A.41}$$

and the friction force depends linear on the velocity.

$$F_f(t) = C \cdot \dot{z}(t) \tag{A.42}$$

A.2.2 Overall system

$$\dot{m}_g(t) = \alpha_1 U(t) \sqrt{\alpha_2 p(t)^{\alpha_4} - \alpha_3 p(t)^{\alpha_5}} \tag{A.43}$$

$$\dot{p}(t) = \frac{\alpha_7 \dot{m}_g(t) - \chi p(t) \left(\alpha_8 - \alpha_{10} z^2(t)\right) \dot{z}(t)}{\alpha_8 z(t) - \alpha_9 z^3(t)} \tag{A.44}$$

$$\ddot{z}(t) = \frac{1}{m_s} \left[m_s g + F_{ext} - (p(t) - p_0) \left(\alpha_8 - \alpha_{10} z^2(t)\right) - K z(t) - C \dot{z}(t) \right] \tag{A.45}$$

A.2.3 State space form

First, the input, output and state variables are determined:

$$\underline{x}(t) = \begin{pmatrix} p(t) \\ z(t) \\ \dot{z}(t) \end{pmatrix} \tag{A.46}$$

$$u(t) = U(t) \tag{A.47}$$

$$y(t) = z(t) \tag{A.48}$$

Substituting into the model of the overall system yields the following set of equations. For simplicity, the weight force of the load, $m_s g$, is integrated into the external force F_{ext}. Also, the gas mass is no state, but the equation for the mass flow (Equation A.49) is written separately for a better readability of the equations.

$$\dot{m}_g(t) = \alpha_1 u(t)\sqrt{\alpha_2 x_1(t)^{\alpha_4} - \alpha_3 x_1(t)^{\alpha_5}} \tag{A.49}$$

$$\dot{x}_1(t) = \frac{\alpha_7 \dot{m}_g(t) - \chi x_1(t)\left(\alpha_8 - \alpha_{10} x_2^2(t)\right) x_3(t)}{\alpha_8 x_2(t) - \alpha_9 x_2^3(t)} \tag{A.50}$$

$$\dot{x}_2(t) = x_3(t) \tag{A.51}$$

$$\dot{x}_3(t) = \frac{1}{m_s}\left[F_{ext} + (x_1(t) - p_0)\left(\alpha_8 - \alpha_{10} x_2^2(t)\right) - K x_2(t) - C x_3(t)\right] \tag{A.52}$$

Appendix B

Programs

In this chapter the Simulink models of the closed loop control are printed and their handling is explained. At first the control of the driven load with proportional friction is described, second the control of the driven load with Karnopp friction model. Last, the implementation of the control of the joint with Karnopp friction model is described. In every implementation the loop can be opened so that the model can be simulated separately.

B.1 Initialization

In the init-file the parameters and initial conditions of the simulink model are set. It is called as callback function from the 'init'-block in the model. This file is used by all implementations; for the control of the angle the external force has to be changed.

```
% init.m
% initializes the simulink model PMA_system.mdl: sets sample time,
% parameters and initial conditions for the ODEs
% is automatically called by the block 'Init' in the highest system level
% author: Sabine Haumann


clear all;
clc;
close all;

% Sample time
ts          = 0;            %[s]        sample time

%%%
```

```
% Air properties
param.R      = 287;          %[J/kgK]    gas constant for air
param.eta    = 1.41;         %[-]        specific heat ratio of air

% Environment properties
param.T      = 298;          %[K]        temperature
param.p_0    = 101325;       %[N/m^2]    environment pressure

% Supply properties
param.p_s    = 5*101325;     %[N/m^2]    supply pressure

% Valve properties
param.c      = (1e-7);       %[m^2/V]    valve constant of proportionality

% PMA properties
param.chi    = 1.26;         %[-]        polytrophic exponent
param.h      = 0.152;        %[m]        helical fiber length of the PMA
param.f      = 0.0145;       %[m]        diametric distance parameter
a8           = pi/4 * param.f*param.f;
                             %[m^2]      summarized parameter
a10          = 3/4 * pi*param.f*param.f/(param.h*param.h);
                             %[-]        summarized parameter


% Load properties
param.M      = 1;            %[kg]       driven mass
param.g      = 9.81;         %[m/s^2]    gravitation constant
param.C      = 20;           %[kg/s]     friction coefficient
param.K      = 40;           %[kg/s^2]   elastic coefficient

% Joint properties
param.L      = 0.1;          %[m]        length of one link
param.z0     = 0.079;        %[m]        relaxation length of the PMA


% Switching thresholds (whether system is slipping or sticking)
param.F_thr  = 0.5;          %[N]        threshold sticking friction force
param.zdot_thr = 0.0001;     %[m/s]      threshold velocity


% Initial conditions
% x        = [p z zdot]

z0         = 0.065;          %[m]        initial PMA length
alpha0     = 2*acos(1+(z0-param.z0)/param.L);
                             %[rad]      initial joint angle

F_ext0     = param.M*param.g %[N]        external force for a vertically
                             %           driven load (=gravitational force)
% F_ext0 = param.M*param.g*cos(alpha0)./sin(alpha0/2);
```

```
                                %[N]        external force for a joint

p0        = (F_ext0 - param.K*z0) ./ (a8 - a10*z0.*z0) + param.p_0;
                                %[N/m^2]    initial inner pressure

xinit     = [p0 z0 0];


%%%
```

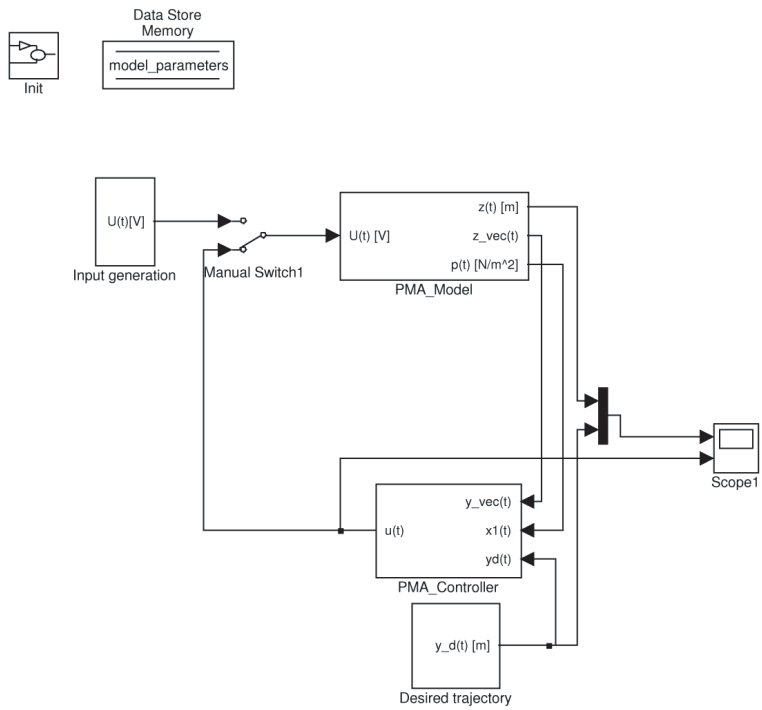

Figure B.1: Main level of the control of a driven load with proportional friction law

```
function [a1,a2,a3,a4,a5,a6,a7,a8,a9,a10] = summarize(p_s,T,c,R,eta,chi,h,f,M,g,C,K)
a1=c*p_s;
a2=2*eta/(R*T*(eta-1)) * p_s^(-2/eta);
a3=2*eta/(R*T*(eta-1)) * p_s^(-(eta+2)/eta);
a4=2/eta;
a5=(eta+2)/eta;
a6=1/(R*T);
a7=chi*R*T;
a8=pi/4 * f*f;
a9=pi/4 * f*f/(h*h);
a10=3/4 * pi*f*f/(h*h);
```

The input generation (Figure B.3) is only necessary for the model experiments, here the valve can be closed and opened. This can occur constant or as step or as impulse. The input data is saved in the Matlab workspace.

In the subsystem 'Desired_trajectory' (Figure B.4) the desired trajectory can be chosen between a constant and a sinusoidal trajectory. The desired trajectory data is saved in the Matlab workspace.

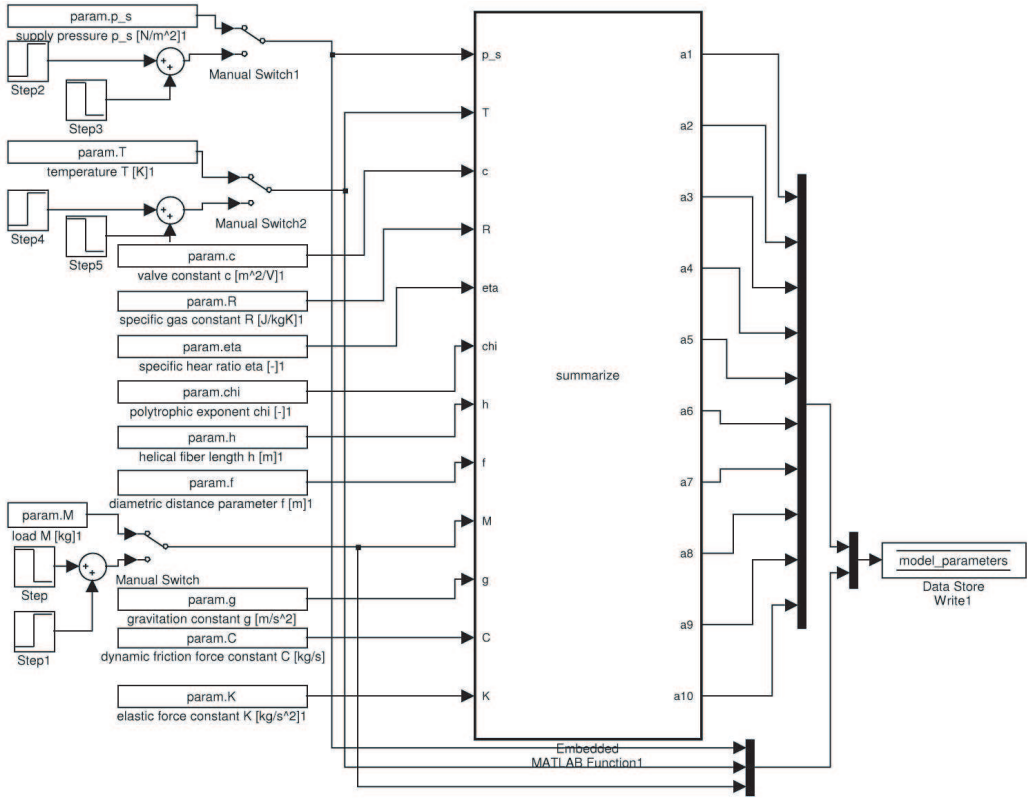

Figure B.2: Init block of the control of a driven load with proportional friction law

In the subsystem 'PMA_model' (Figure B.5) the PMA is modeled with the valve and the intrinsic PMA.

In the subsystem 'PMA' (Figure B.6) the intrinsic PMA is modeled. The main parts are the calculation of the inner pressure and the length of the PMA.

In the subsystem 'Internal pressure of the PMA' (Figure B.7) the internal pressure of the PMA is calculated by integrating the model equation. The pressure data is saved in the Matlab workspace. The model equation is implemented as:

```
% Embedded Matlab function: pressure
% calculates the derivative of the pressure
function pdot = pressure(mdot_g,p,V,dVdz,z,zdot,chi,a7)
pdot = 1/V * (a7*mdot_g - chi*p*dVdz*zdot);
```

One necessary variable is the volume of the PMA which is calculated in the subsystem 'PMA volume' (Figure B.8) and in the function:

```
% Embedded Matlab function
% calculates the PMA volume
% and the derivative with respect to the length
```

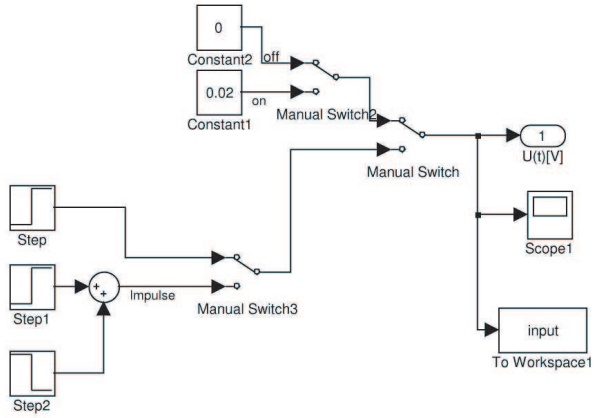

Figure B.3: Input generation for the control of a driven load with proportional friction law

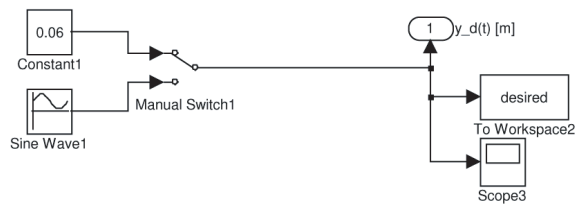

Figure B.4: Desired trajectory for the control of a driven load with proportional friction law

```
function [V,dVdz]= volume(z,a8,a9,a10)
    V = a8*z - a9*z*z*z;
dVdz = a8 - a10*z*z;
```

In the subsystem 'PMA length' (Figure B.9) the length of the PMA is calculated. Mainly the affecting forces are calculated in two subsystems, added and integrated two times. The length data is saved in the Matlab workspace.

In the subsystem 'PMA force' (Figure B.10) the longitudinal PMA force is calculated. The Embedded Matlab function is:

```
% Embedded Matlab function: PMA_force
% calculates the longitudinal PMA force
function F_m= PMA_force(p,z,p_0,a8,a10)
dVdz = (a8 - a10*z*z);
F_m = (p - p_0) * dVdz;
```

In the subsystem 'Other forces' (Figure B.11) the other affecting forces (elastic force, proportional friction force and gravitational force) are calculated.

In the subsystem 'valve' (Figure B.12) the valve is modeled. The Embedded function is:

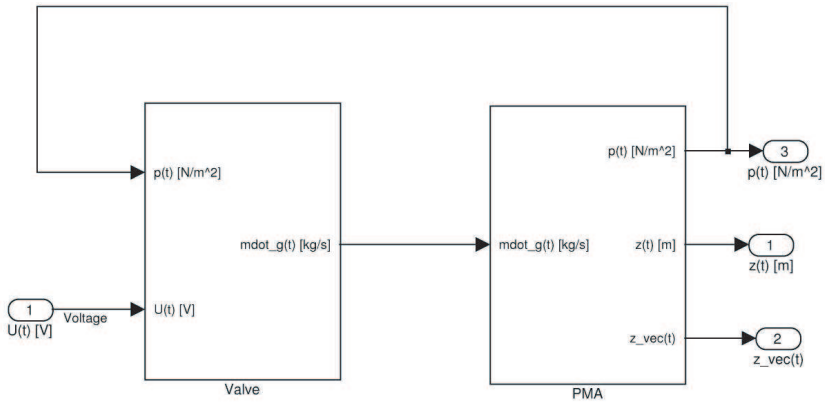

Figure B.5: PMA model for the control of a driven load with proportional friction law

```
% Embedded Matlab function: valve
                % models the valve
function mdot_g = valve(p,U,a1,a2,a3,a4,a5)
abb = a2*p^a4 - a3*p^a5;
if abb < 0
    mdot_g = - a1 * U * sqrt(-abb);
else
    mdot_g = a1 * U * sqrt(abb);
end
```

Next the controller implementation is presented. In the subsystem 'PMA_Controller' (Figure B.13) the controller with trajectory computation, tracking control and the inverse system is given.

In the subsystem 'Trajectory computation' (Figure B.14) the derivatives of the desired trajectory are computed. Because of the numerical problems the derivations are calculated manually. For the constant desired trajectory the constants zero and for the sinusoidal desired trajectory the sinus generators have to be chosen as derivatives.

In the subsystem 'Tracking control' (Figure B.15) the linear tracking control takes place. The Embedded function is:

```
% Embedded Matlab function: tracking
% linear tracking control
function ny = tracking(e,e_dot,e_2dot,yd_3dot,K2,K1,K0)
ny = yd_3dot + K2*e_2dot + K1*e_dot + K0*e;
```

In the subsystem 'Inverse system' (Figure B.16) the intrinsic control signal is computed. The Embedded function is

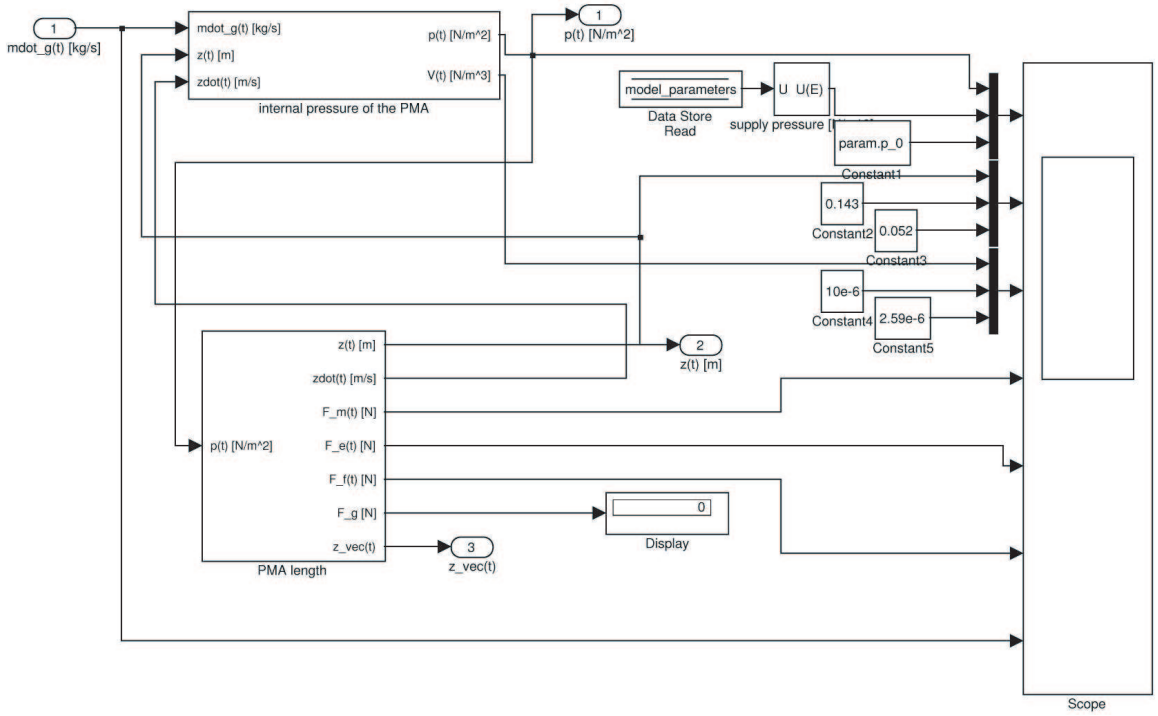

Figure B.6: Intrinsic PMA model in the control of a driven load with proportional friction law

```
% Embedded Matlab function: inv_sys
% Inverse system, generates input u(t) which cancels the nonlinearities of the system
                    function u = inv_sys(y,y_dot,y_2dot,x1,ny,a1,a2,a3,a4,a5,a6,a7,a8,a9,a10,g,m_s,p_0,K,C,chi)

% Abbrevations
V       = a8*y - a9*y*y*y;
psi_1   = a1*sqrt(a2*x1^a4 - a3*x1^a5);
psi_2   = a7/V*psi_1;
psi_3   = chi/V*x1*(a8-a10*y*y)*y_dot;
psi_4   = 2/m_s*a10*(x1-p_0)*y*y_dot - K/m_s*y_dot - C/m_s*y_2dot;
psi_5   = -1/m_s*(a8-a10*y*y)*psi_2;
psi_6   = 1/m_s*(a8-a10*y*y)*psi_3 + psi_4;

% Generation of the input
u=(ny-psi_6)/psi_5;
```

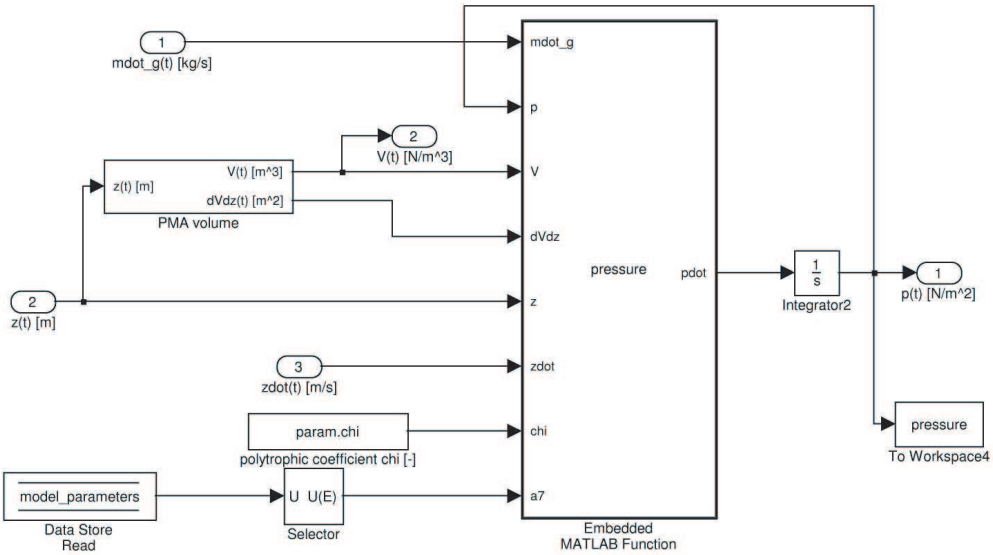

Figure B.7: Internal pressure in the control of a driven load with proportional friction law

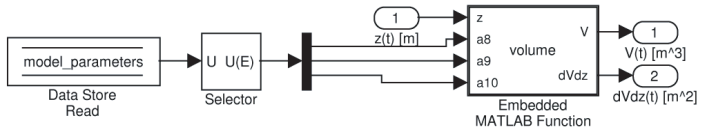

Figure B.8: Volume in the control of a driven load with proportional friction law

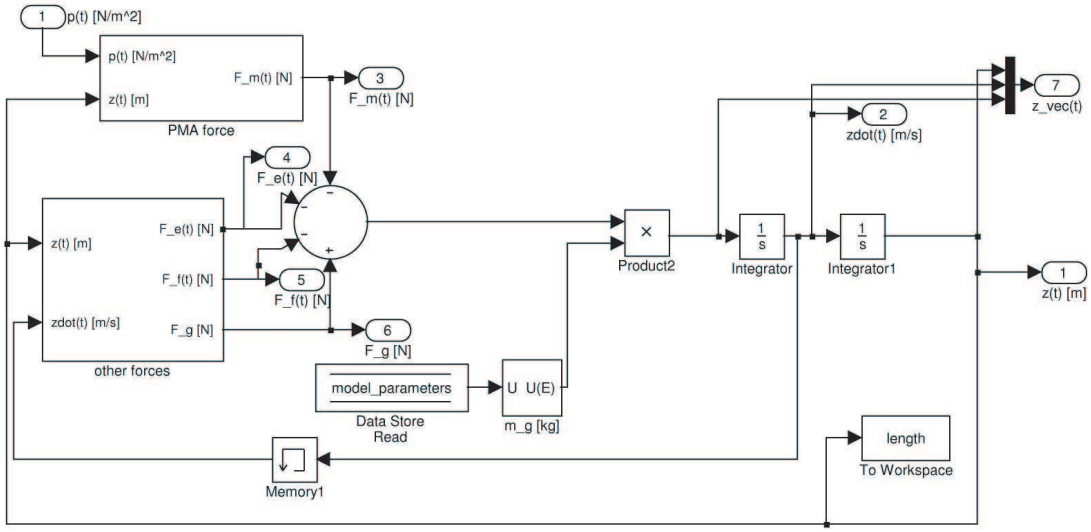

Figure B.9: PMA length in the control of a driven load with proportional friction law

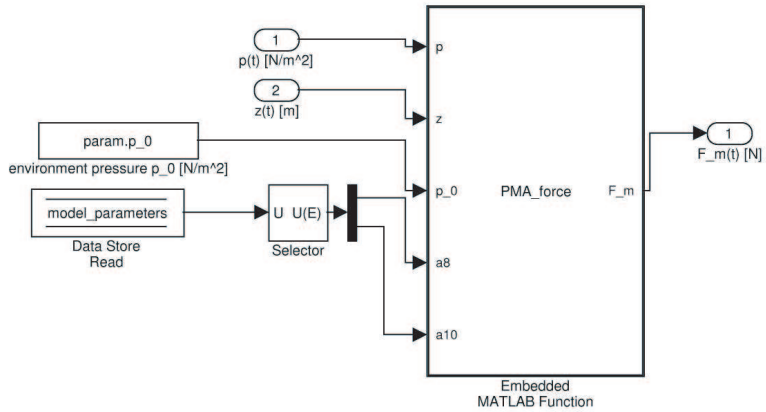

Figure B.10: PMA force in the control of a driven load with proportional friction law

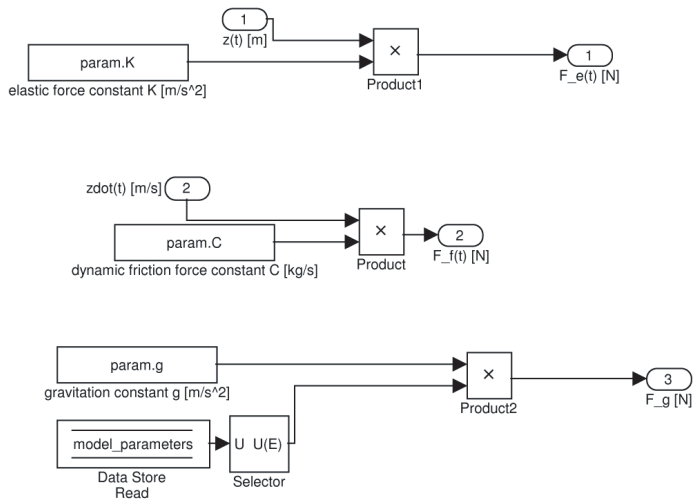

Figure B.11: Other forces in the control of a driven load with proportional friction law

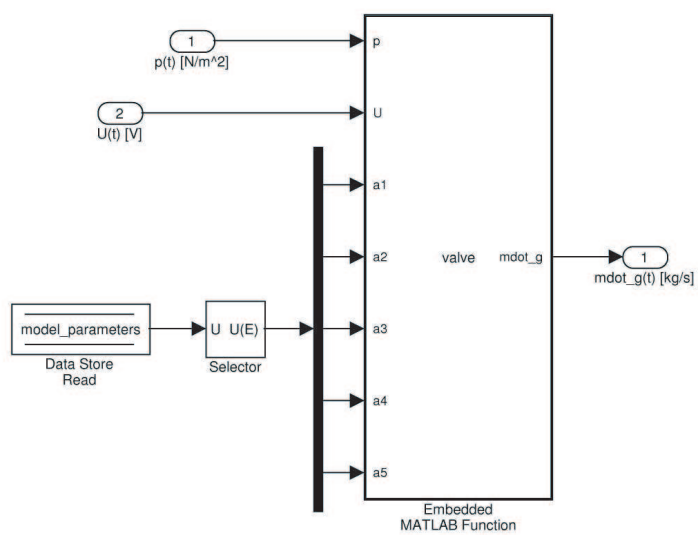

Figure B.12: Valve in the control of a driven load with proportional friction law

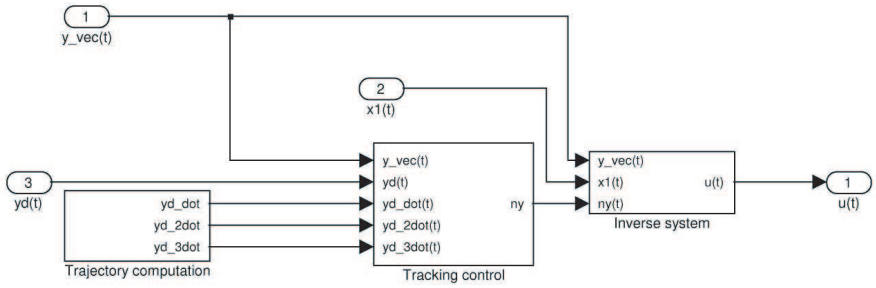

Figure B.13: Controller of a driven load with proportional friction law

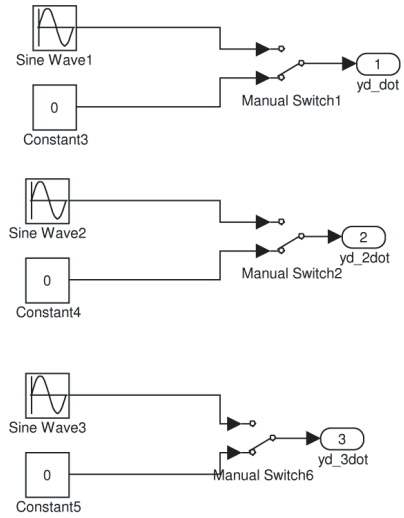

Figure B.14: Trajectory computation for the control of a driven load with proportional friction law

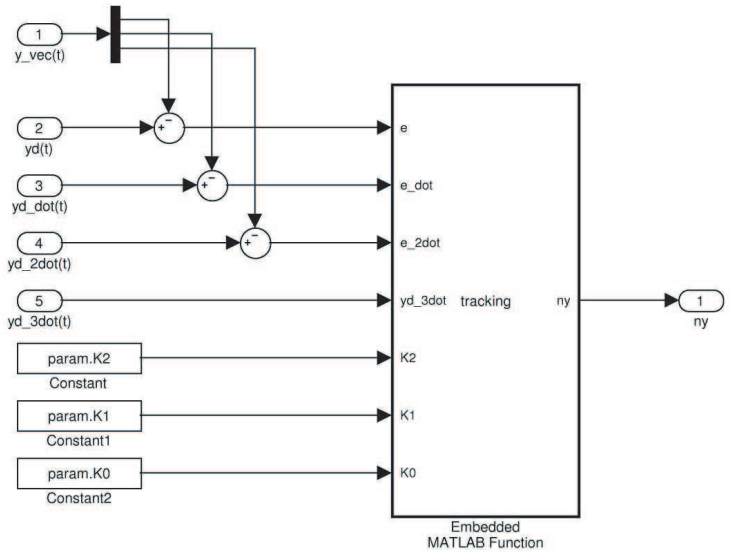

Figure B.15: Tracking control for a driven load with proportional friction law

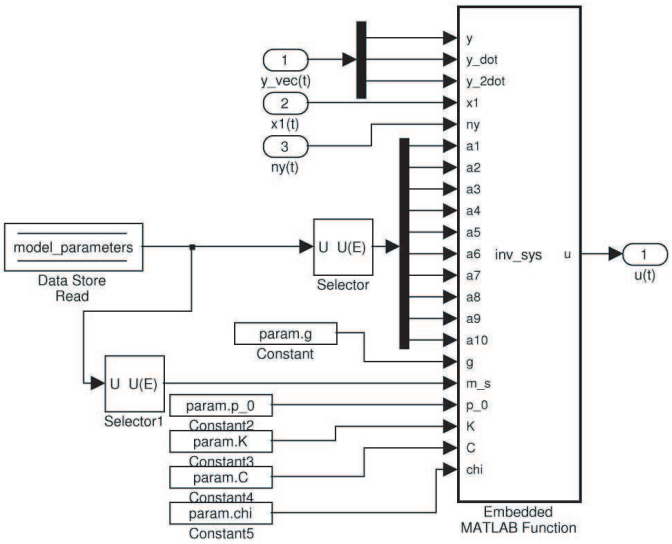

Figure B.16: Inverse system for the control of a driven load with proportional friction law

B.2.2 Control of the driven load with Karnopp friction law

In this subsection the implementation of the control of the driven load with the Karnopp friction model is presented. Most of the features are identical to the implementation with the simple proportional friction law. In Figure B.17 the main level is printed.

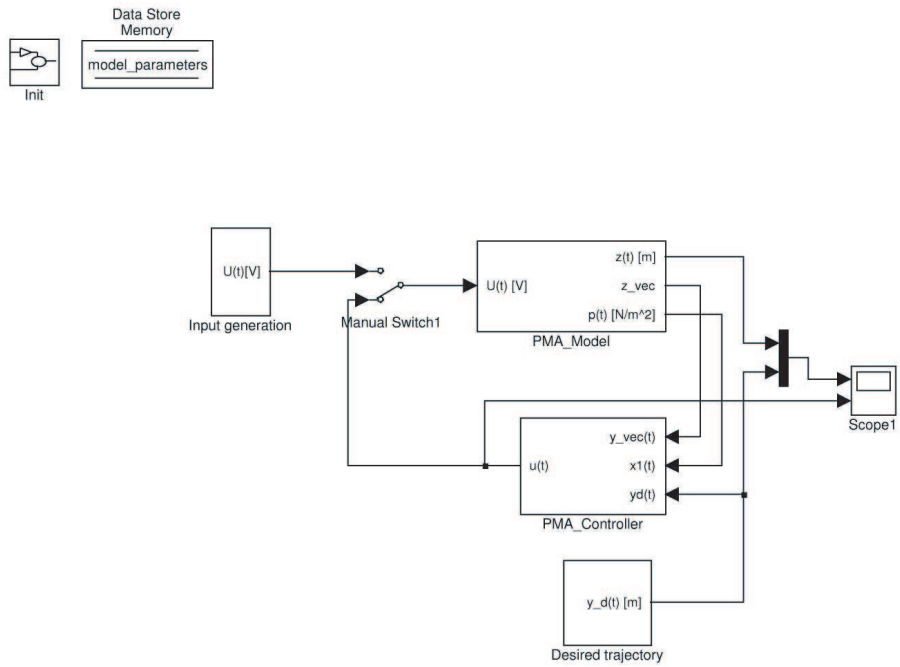

Figure B.17: Main level of the control of a driven load with Karnopp friction model

In Figure B.18 the init block is plotted. With the hand switch it can be decided whether the experiments are performed with the model of the PMA or with the closed loop control. The Embedded Matlab function is:

```
% Embedded Matlab function: summarize
% summarizes the physical parameters
function [a1,a2,a3,a4,a5,a6,a7,a8,a9,a10] = summarize(p_s,T,c,R,eta,chi,h,f,M,g,C,K)
a1=c*p_s;
a2=2*eta/(R*T*(eta-1)) * p_s^(-2/eta);
a3=2*eta/(R*T*(eta-1)) * p_s^(-(eta+2)/eta);
a4=2/eta;
a5=(eta+2)/eta;
a6=1/(R*T);
a7=chi*R*T;
a8=pi/4 * f*f;
a9=pi/4 * f*f/(h*h);
a10=3/4 * pi*f*f/(h*h);
```

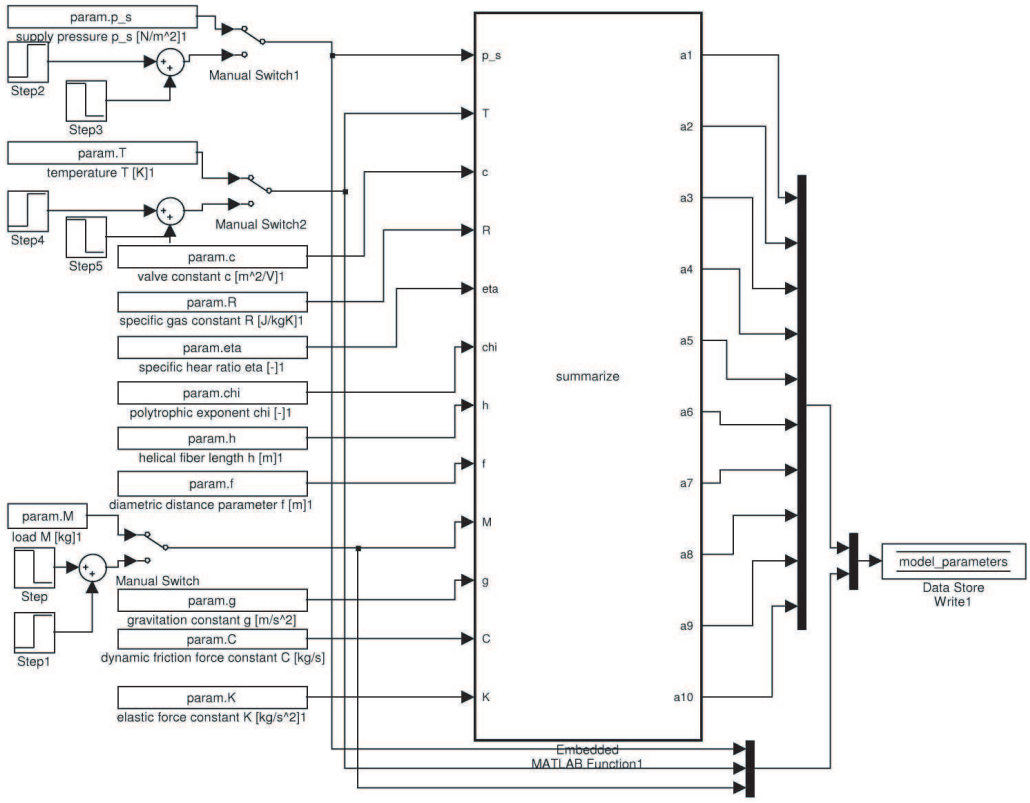

Figure B.18: Init block of the control of a driven load with Karnopp friction model

The input generation (Figure B.19) is only necessary for the model experiments. Here the valve can be closed and opened. This can occur constant or as step or as impulse. The input data is saved in the Matlab workspace.

In the subsystem 'Desired_trajectory' (Figure B.20) the desired trajectory can be chosen between a constant and a sinusoidal trajectory. The desired trajectory data is saved in the Matlab workspace.

In the subsystem 'PMA_model' (Figure B.21) the PMA is modeled with the valve and the intrinsic PMA.

In the subsystem 'PMA' (Figure B.22) the intrinsic PMA is modeled. The main parts are the calculation of the inner pressure and the length of the PMA.

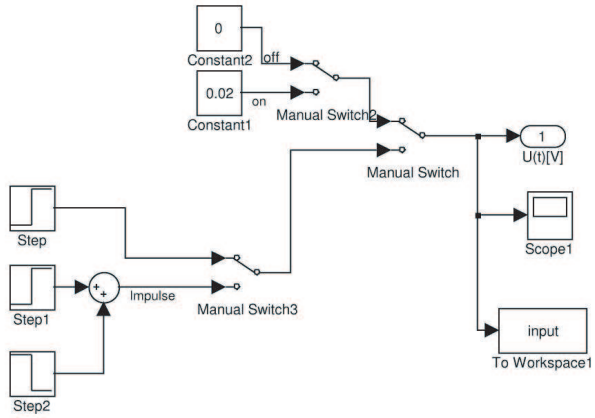

Figure B.19: Input generation for the control of a driven load with Karnopp friction model

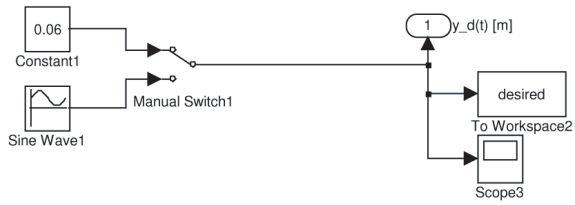

Figure B.20: Desired trajectory for the control of a driven load with Karnopp friction model

In the subsystem 'Internal pressure of the PMA' (Figure B.23) the internal pressure of the PMA is calculated by integrating the model equation. The pressure data is saved in the Matlab workspace. The model equation is implemented as:

```
% Embedded Matlab function: pressure
% calculates the derivative of the inner pressure
function pdot = pressure(mdot_g,p,V,dVdz,z,zdot,chi,a7)
pdot = 1/V * (a7*mdot_g - chi*p*dVdz*zdot);
```

One necessary variable is the volume of the PMA which is calculated in the subsystem 'PMA volume' (Figure B.24) and in the function:

```
% Embedded Matlab function
% calculates the PMA volume
% and the derivative with respect to the length
function [V,dVdz]= volume(z,a8,a9,a10)
V = a8*z - a9*z*z*z;
dVdz = a8 - a10*z*z;
```

In the subsystem 'PMA length' (Figure B.25) the length of the PMA is calculated. Mainly the affecting forces are calculated in two subsystems, added and integrated two times. The second derivative is multiplied by a state value which represents the sticking and the slipping mode of the PMA. For slipping this value is one, so the integrations occur as with the proportional

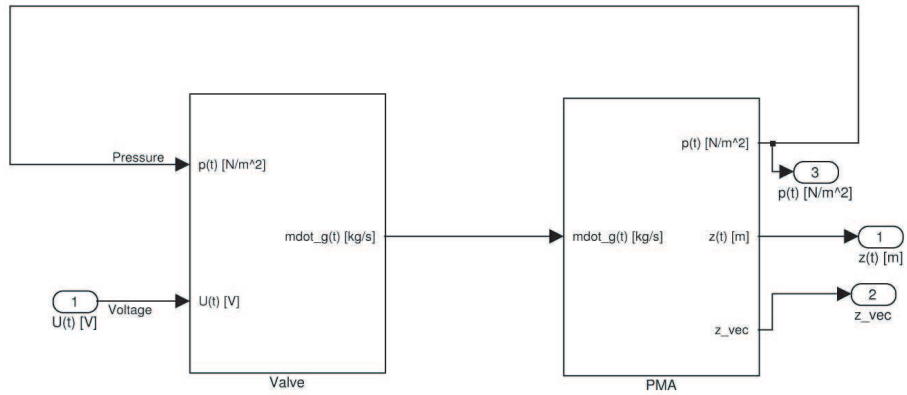

Figure B.21: PMA model for the control of a driven load with Karnopp friction model

friction. During sticking the state is zero, so the derivative is zero and the PMA length remains constant. The length data is saved in the Matlab workspace.

In the subsystem 'PMA force' (Figure B.26) the longitudinal PMA force is calculated. The Embedded Matlab function is:

```
% Embedded Matlab function: PMA_force
% calculates the longitudinal PMA force
function F_m = PMA_force(p,z,p_0,a8,a10)
dVdz = (a8 - a10*z*z);
F_m = (p - p_0) * dVdz;
```

In the subsystem 'Other forces' (Figure B.27) the other affecting forces are calculated. The elastic force, the gravitational force and the slipping friction force are calculated like before. The status is calculated in the Embedded function:

```
% Embedded matlab function
% detects whether the PMA is in slipping or in sticking mode
function status = stickslip(zdot,zdot_thr,F_s,F_thr)

if (abs(zdot) < zdot_thr) && (abs(F_s) < F_thr) %sticking
    status = 0;
else
    status = 1;                                 %slipping
end
```

The sticking friction force is calculated in the Embedded function:

```
% Embedded Matlab function: stick
% Calculates the sticking friction force
function F_s = stick(status,F_m,F_e,F_g)
if status == 1
    F_s = 0;
else
```

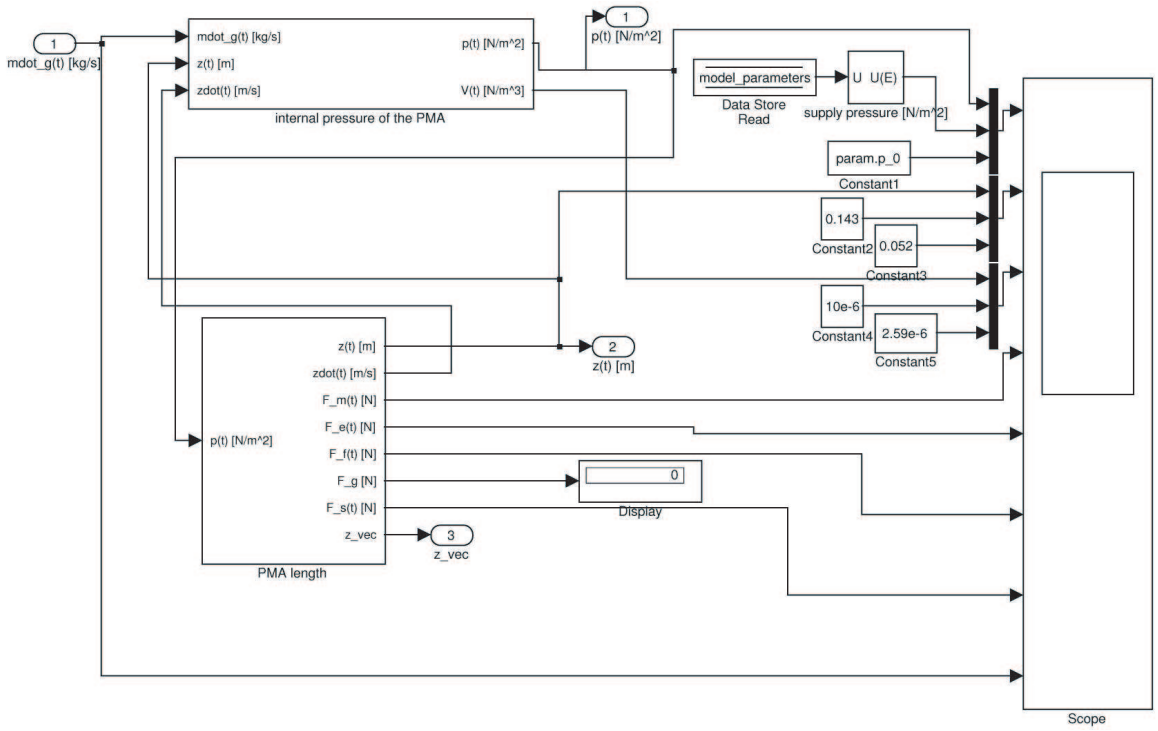

Figure B.22: Intrinsic PMA model in the control of a driven load with Karnopp friction model

```
F_s = F_g - F_e - F_m;
  end
```

In the subsystem 'valve' (Figure B.28) the valve is modeled. The Embedded function is:

```
% Embedded Matlab function: valve
% models the valve
function mdot_g = valve(p,U,a1,a2,a3,a4,a5)
abb = a2*p^a4 - a3*p^a5;
if abb < 0
    mdot_g = - a1 * U * sqrt(-abb);
else
    mdot_g = a1 * U * sqrt(abb);
end
```

Next the controller implementation is presented. In the subsystem 'PMA_Controller' (Figure B.29) the controller with trajectory computation, tracking control and the inverse system is given. It is identical to the controller of the system with the proportional friction law.

In the subsystem 'Trajectory computation' (Figure B.30) the derivatives of the desired trajectory are computed. For the constant desired trajectory the constants zero and for the sinusoidal desired trajectory the sinus generators have to be chosen as derivatives.

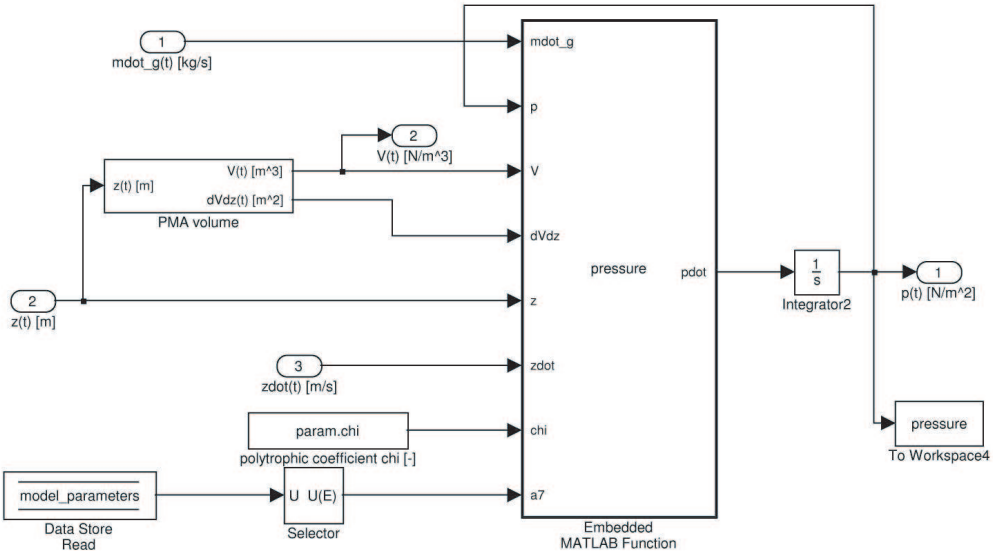

Figure B.23: Internal pressure in the control of a driven load with Karnopp friction model

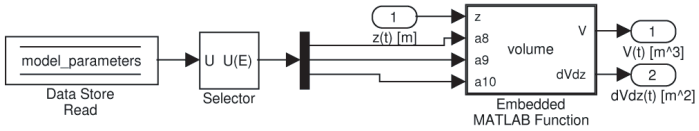

Figure B.24: Volume in the control of a driven load with Karnopp friction model

In the subsystem 'Tracking control' (Figure B.31) the linear tracking control takes place. The Embedded function is:

```
% Embedded Matlab function: tracking
% linear tracking control
function ny = tracking(e,e_dot,e_2dot,yd_3dot,K2,K1,K0)
ny = yd_3dot + K2*e_2dot + K1*e_dot + K0*e;
```

In the subsystem 'Inverse system' (Figure B.32) the intrinsic control signal is computed. The Embedded function is

```
% Embedded Matlab function: inv_sys
% Inverse system, generates input u(t) which cancels the nonlinearities of the system
function u = inv_sys(y,y_dot,y_2dot,x1,ny,a1,a2,a3,a4,a5,a6,a7,a8,a9,a10,g,m_s,p_0,K,C,chi)

% Abbrevations
V       = a8*y - a9*y*y*y;
psi_1   = a1*sqrt(a2*x1^a4 - a3*x1^a5);
psi_2   = a7/V*psi_1;
psi_3   = chi/V*x1*(a8-a10*y*y)*y_dot;
psi_4   = 2/m_s*a10*(x1-p_0)*y*y_dot - K/m_s*y_dot - C/m_s*y_2dot;
psi_5   = -1/m_s*(a8-a10*y*y)*psi_2;
psi_6   = 1/m_s*(a8-a10*y*y)*psi_3 + psi_4;
```

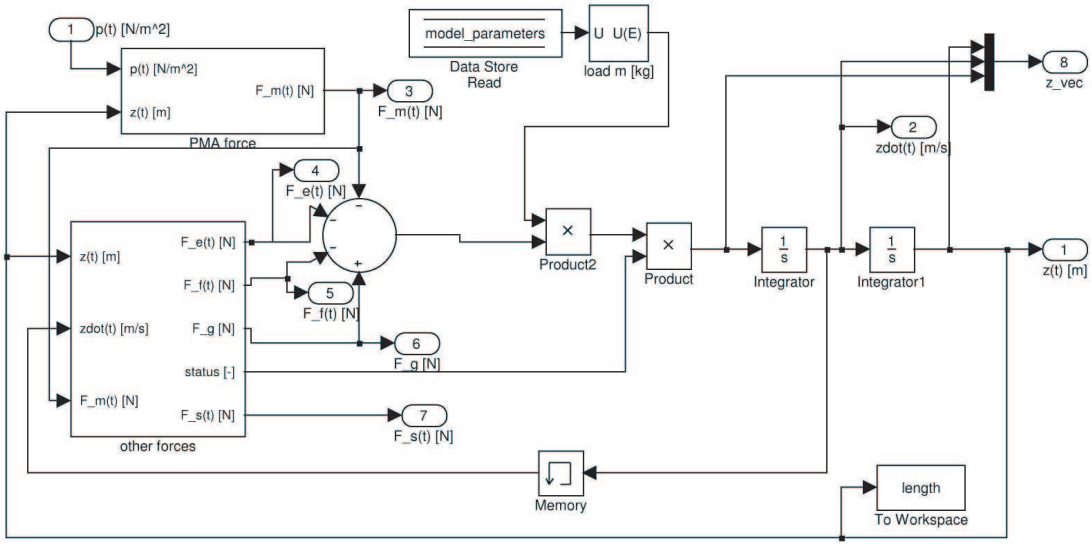

Figure B.25: PMA length in the control of a driven load with Karnopp friction model

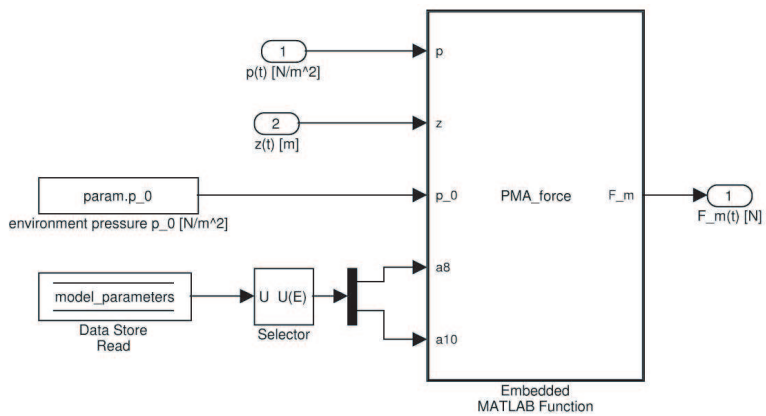

Figure B.26: PMA force in the control of a driven load with Karnopp friction model

```
% Generation of the input
u=(ny-psi_6)/psi_5;
```

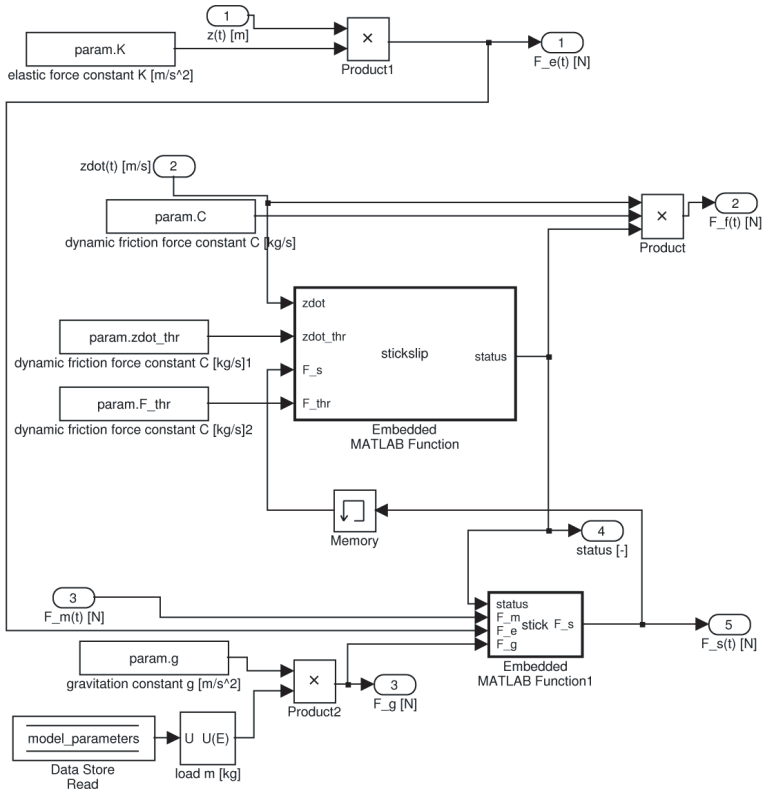

Figure B.27: Other forces in the control of a driven load with Karnopp friction model

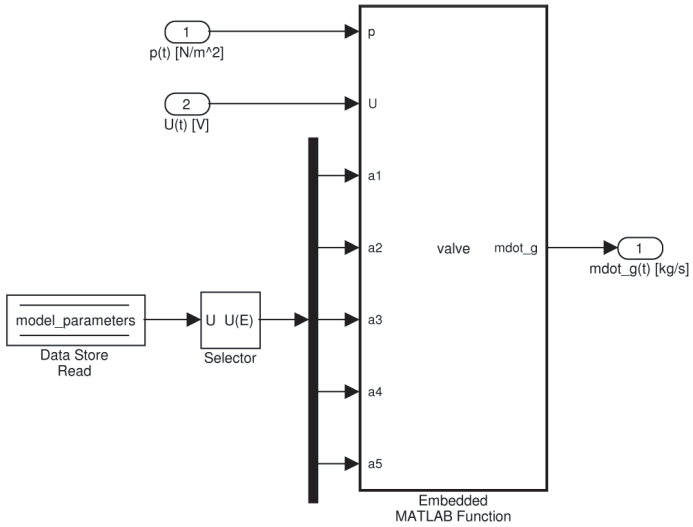

Figure B.28: Valve in the control of a driven load with Karnopp friction model

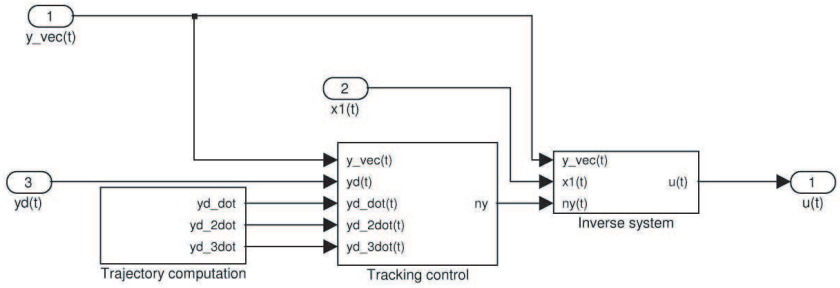

Figure B.29: Controller of a driven load with Karnopp friction model

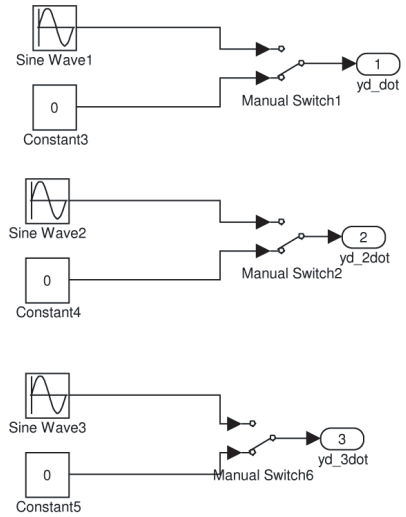

Figure B.30: Trajectory computation for the control of a driven load with Karnopp friction model

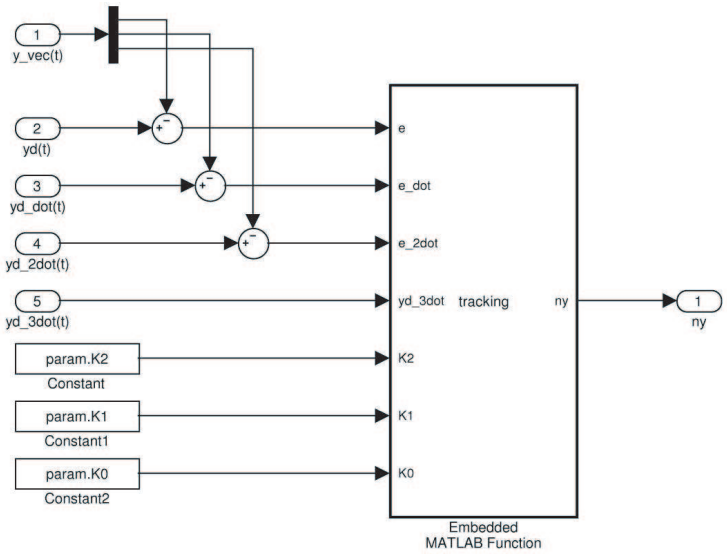

Figure B.31: Tracking control for a driven load with Karnopp friction model

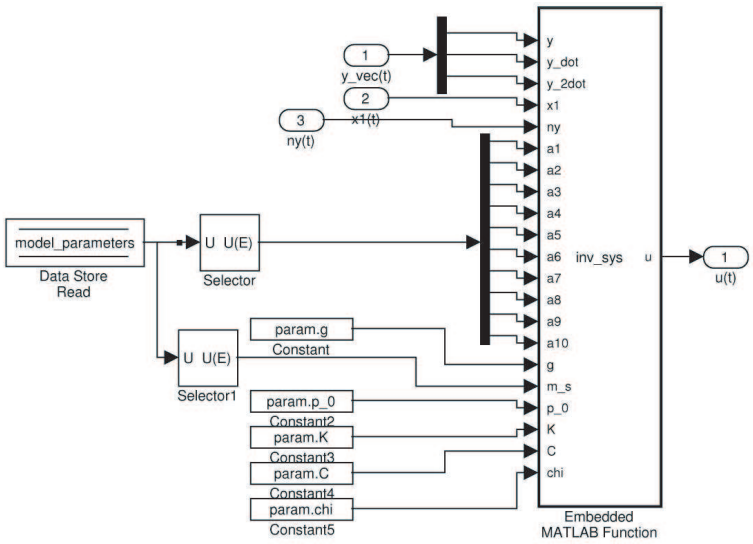

Figure B.32: Inverse system for the control of a driven load with Karnopp friction model

B.2.3 Control of the driven joint with Karnopp friction law

In this subsection the implementation of the control of the driven joint with the Karnopp friction model is presented. Most of the features are identical to the implementations of the driven load. In Figure B.33 the main level is printed. The intrinsic calculations take place with the PMA length.

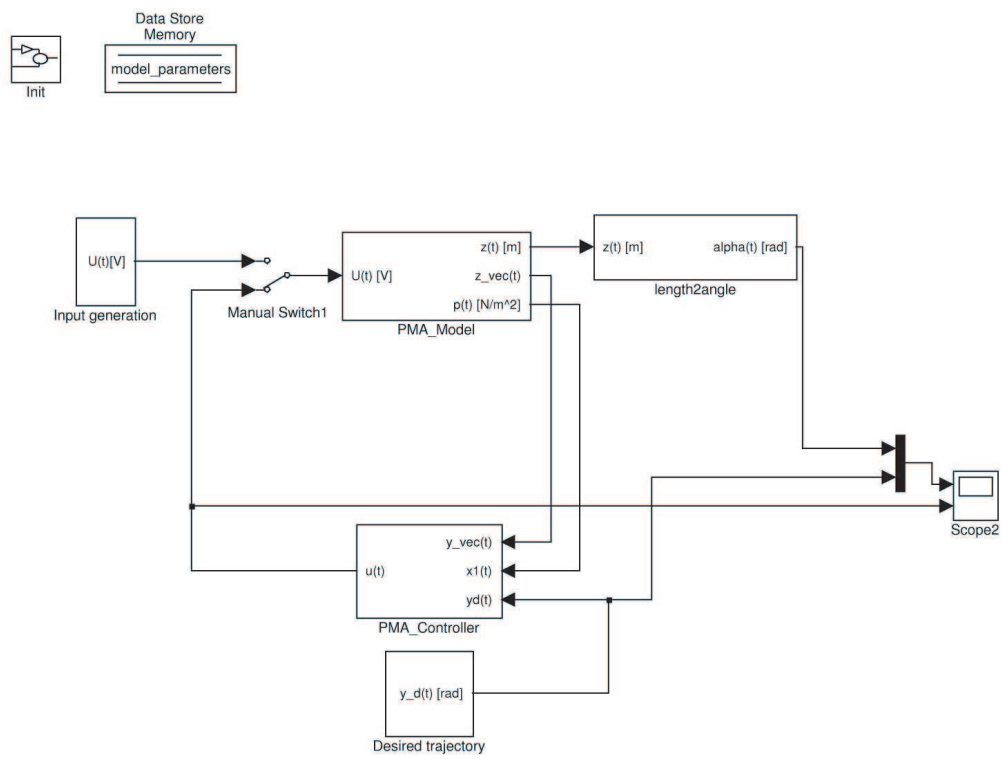

Figure B.33: Main level of the control of a driven joint with Karnopp friction model

With the subsystem 'length2ang' (Figure B.34) the length is converted to the joint angle. The angle and the length data are saved in the Matlab workspace. The Embedded function is

```
% Embedded Matlab function: length2ang
% converts the PMA length to the joint angle
function alpha = length2ang(z,L,z0)
alpha = 2*acos(1+(z-z0)/L);
```

In Figure B.35 the init block is plotted. With the hand switch it can be decided whether the experiments are performed with the model of the PMA or with the closed loop control. The Embedded Matlab function is:

```
% Embedded Matlab function: summarize
% summarizes the physical parameters
function [a1,a2,a3,a4,a5,a6,a7,a8,a9,a10] = summarize(p_s,T,c,R,eta,chi,h,f,M,g,C,K)
```

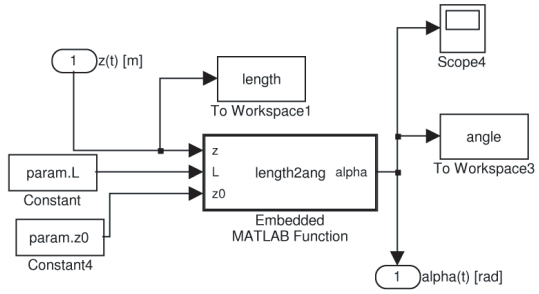

Figure B.34: Conversion length to angle in the control of a driven joint with Karnopp friction model

```
a1=c*p_s;
a2=2*eta/(R*T*(eta-1)) * p_s^(-2/eta);
a3=2*eta/(R*T*(eta-1)) * p_s^(-(eta+2)/eta);
a4=2/eta;
a5=(eta+2)/eta;
a6=1/(R*T);
a7=chi*R*T;
a8=pi/4 * f*f;
a9=pi/4 * f*f/(h*h);
a10=3/4 * pi*f*f/(h*h);
```

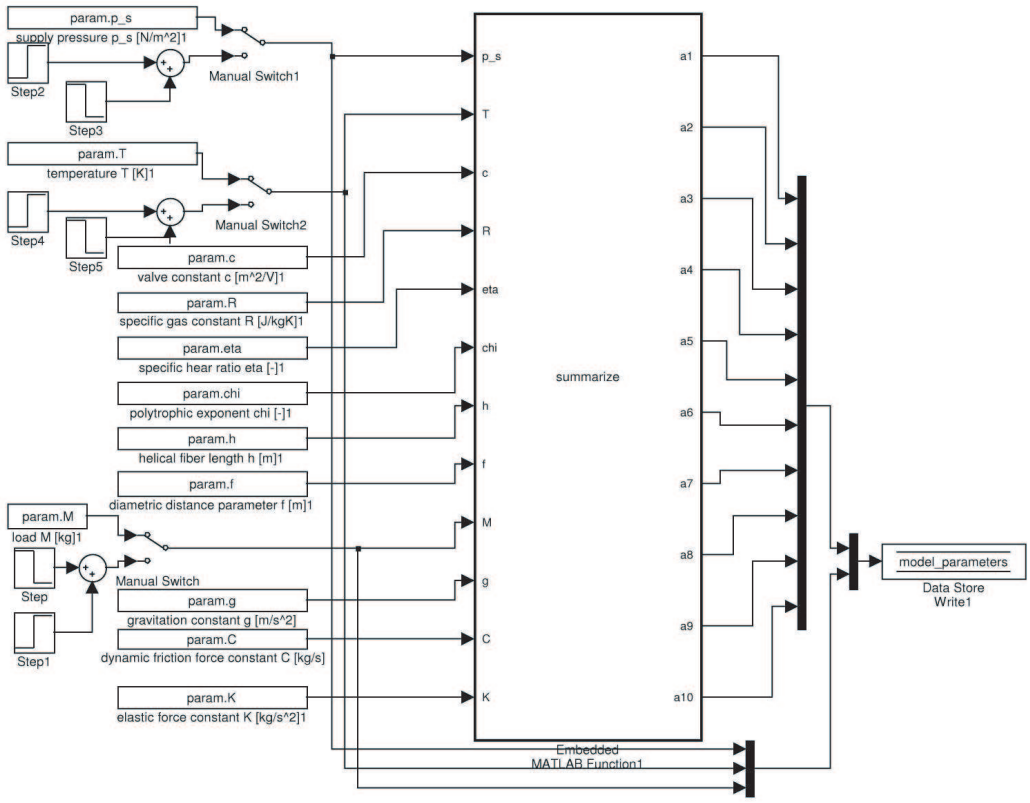

Figure B.35: Init block of the control of a driven joint with Karnopp friction model

The input generation (Figure B.36) is only necessary for the model experiments. Here the valve can be closed and opened. This can occur constant or as step or as impulse. The input data is saved in the Matlab workspace.

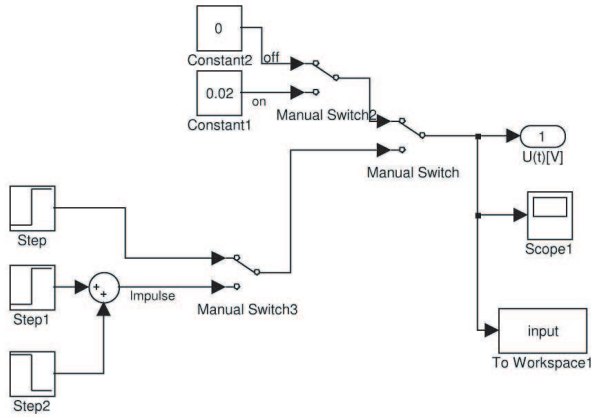

Figure B.36: Input generation for the control of a driven joint with Karnopp friction model

In the subsystem 'Desired_trajectory' (Figure B.37) the desired trajectory can be chosen between a constant and a sinusoidal trajectory. The desired trajectory data is saved in the Matlab workspace.

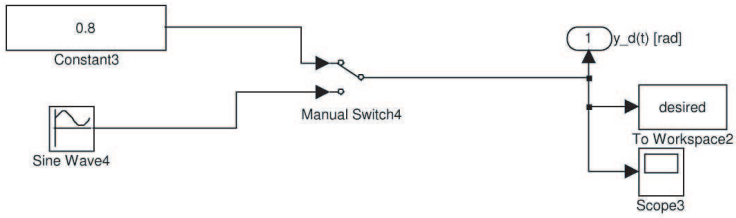

Figure B.37: Desired trajectory for the control of a driven joint with Karnopp friction model

In the subsystem 'PMA_model' (Figure B.38) the PMA is modeled with the valve and the intrinsic PMA.

In the subsystem 'PMA' (Figure B.39) the intrinsic PMA is modeled. The main parts are the calculation of the inner pressure and the length of the PMA.

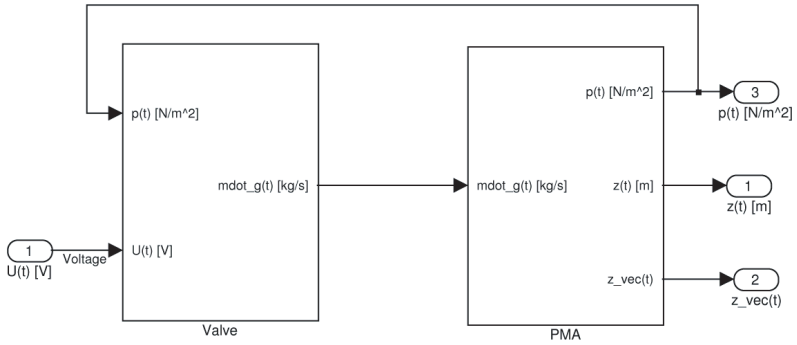

Figure B.38: PMA model for the control of a driven joint with Karnopp friction model

In the subsystem 'Internal pressure of the PMA' (Figure B.40) the internal pressure of the PMA is calculated by integrating the model equation. The pressure data is saved in the Matlab workspace. The model equation is implemented as:

```
% Embedded Matlab function: pressure
% calculates the first derivative of the inner pressure
function pdot = pressure(mdot_g,p,V,dVdz,z,zdot,chi,a7)
pdot = 1/V * (a7*mdot_g - chi*p*dVdz*zdot);
```

One necessary variable is the volume of the PMA which is calculated in the subsystem 'PMA volume' (Figure B.41) and in the function:

```
% Embedded Matlab function
% calculates the PMA volume
% and the derivative with respect to the length
function [V,dVdz]= volume(z,a8,a9,a10)
V = a8*z - a9*z*z*z;
dVdz = a8 - a10*z*z;
```

In the subsystem 'PMA length' (Figure B.42) the length of the PMA is calculated. Mainly the affecting forces are calculated in two subsystems, added and integrated two times. The second derivative is multiplied by a state value which represents the sticking and the slipping mode of the PMA. For slipping this value is one, so the integrations occur as with the proportional friction. During sticking the state is zero, so the derivative is zero and the PMA length remains constant.

In the subsystem 'PMA force' (Figure B.43) the longitudinal PMA force is calculated. The Embedded Matlab function is:

```
% Embedded Matlab function: PMA_force
% calculates the longitudinal PMA force
function F_m = PMA_force(p,z,p_0,a8,a10)
```

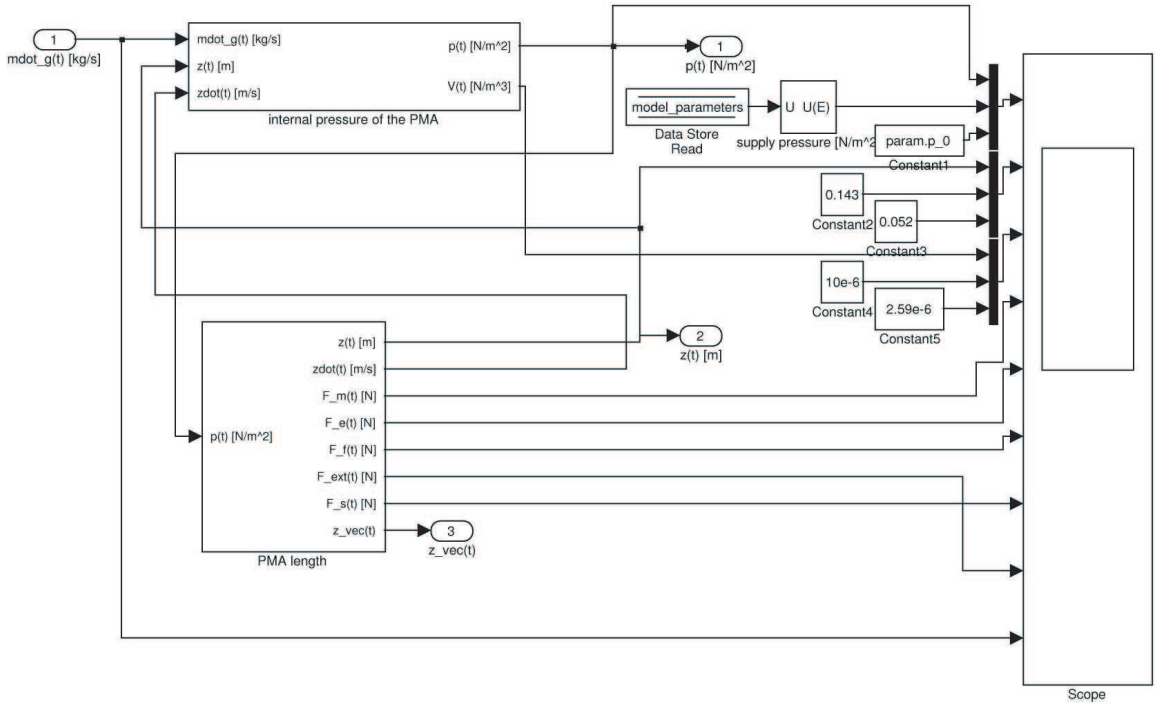

Figure B.39: Intrinsic PMA model in the control of a driven joint with Karnopp friction model

```
dVdz = (a8 - a10*z*z);
F_m = (p - p_0) * dVdz;
```

In the subsystem 'Other forces' (Figure B.44) the other affecting forces are calculated. The elastic force and the slipping friction force are calculated like before. The status is calculated in the Embedded function:

```
% Embedded matlab function
% detects whether the PMA is in slipping or in sticking mode
function status = stickslip(zdot,zdot_thr,F_s,F_thr)
if (abs(zdot) < zdot_thr) && (abs(F_s) < F_thr) %sticking
    status = 0;
else
    status = 1;                                  %slipping
end
```

The sticking friction force is calculated in the Embedded function:

```
% Embedded Matlab function: stick
% Calculates the sticking friction force
function F_s = stick(status,F_m,F_e,F_ext)
if status == 1 %sticking mode
    F_s = 0;
else
    F_s = F_ext - F_e - F_m;
end
```

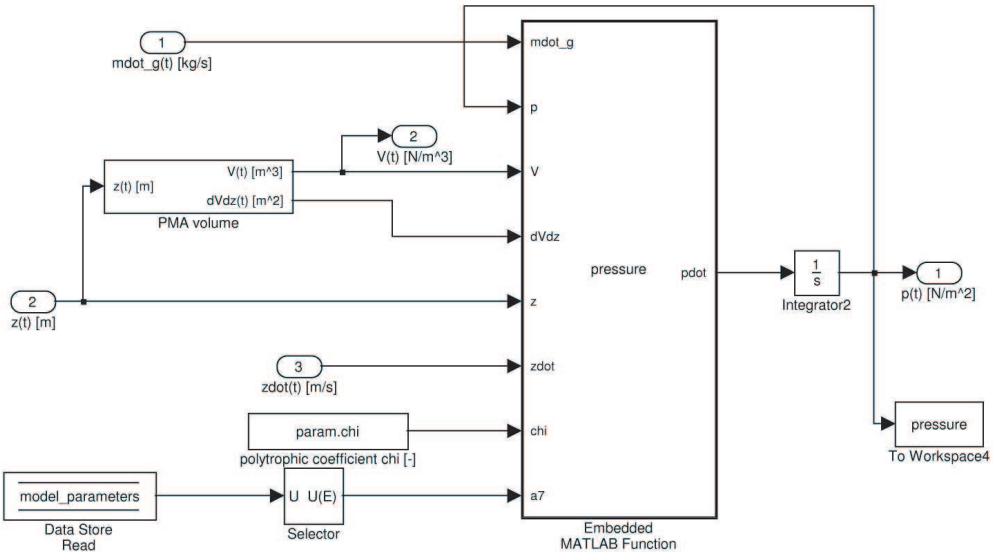

Figure B.40: Internal pressure in the control of a driven joint with Karnopp friction model

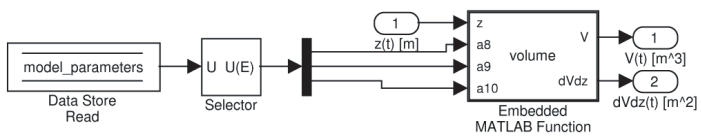

Figure B.41: Volume in the control of a driven joint with Karnopp friction model

The gravitational force is exchanged by the external force. This force is calculated by

```
% Embedded Matlab function: ext
% Calculates the external force
function F_ext = ext(alpha,F_g)
F_ext = F_g*cos(alpha)/sin(alpha/2);
```

Therefore, the length has to be converted to the angle:

```
% Embedded Matlab function: length2ang
% converts the PMA length to the joint angle
function alpha = length2ang(z,L,z0)
alpha = 2*acos(1+(z-z0)/L);
```

In the subsystem 'valve' (Figure B.45) the valve is modeled. The Embedded function is:

```
% Embedded Matlab function: valve
% models the valve
function mdot_g = valve(p,U,a1,a2,a3,a4,a5)
abb = a2*p^a4 - a3*p^a5;
if abb < 0
    mdot_g = - a1 * U * sqrt(-abb);
else
    mdot_g = a1 * U * sqrt(abb);
end
```

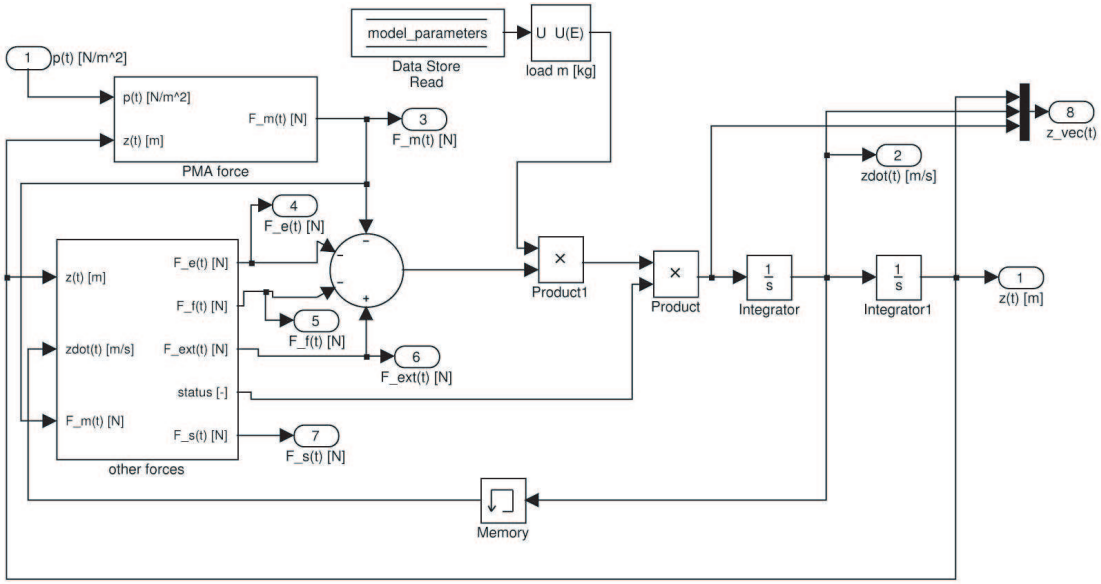

Figure B.42: PMA length in the control of a driven joint with Karnopp friction model

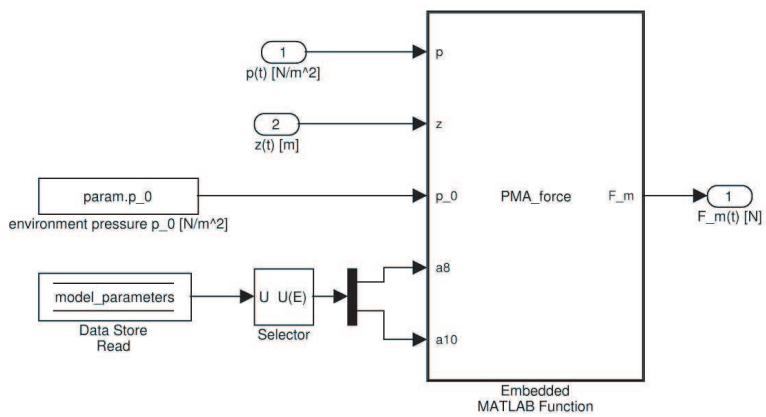

Figure B.43: PMA force in the control of a driven joint with Karnopp friction model

Next the controller implementation is presented. In the subsystem 'PMA_Controller' (Figure B.46) the controller with trajectory computation, tracking control and the inverse system is given.

In the subsystem 'Trajectory computation' (Figure B.47) the desired trajectory and its derivatives are computed. For the constant desired trajectory the constants zero and for the sinusoidal desired trajectory the sinus generators have to be chosen as derivatives.

The desired trajectory is given as angle, so it has to be converted to the length with the subsystem 'angle2length' (Figure B.48) and the Embedded function

```
% Embedded Matlab function: ang2length
```

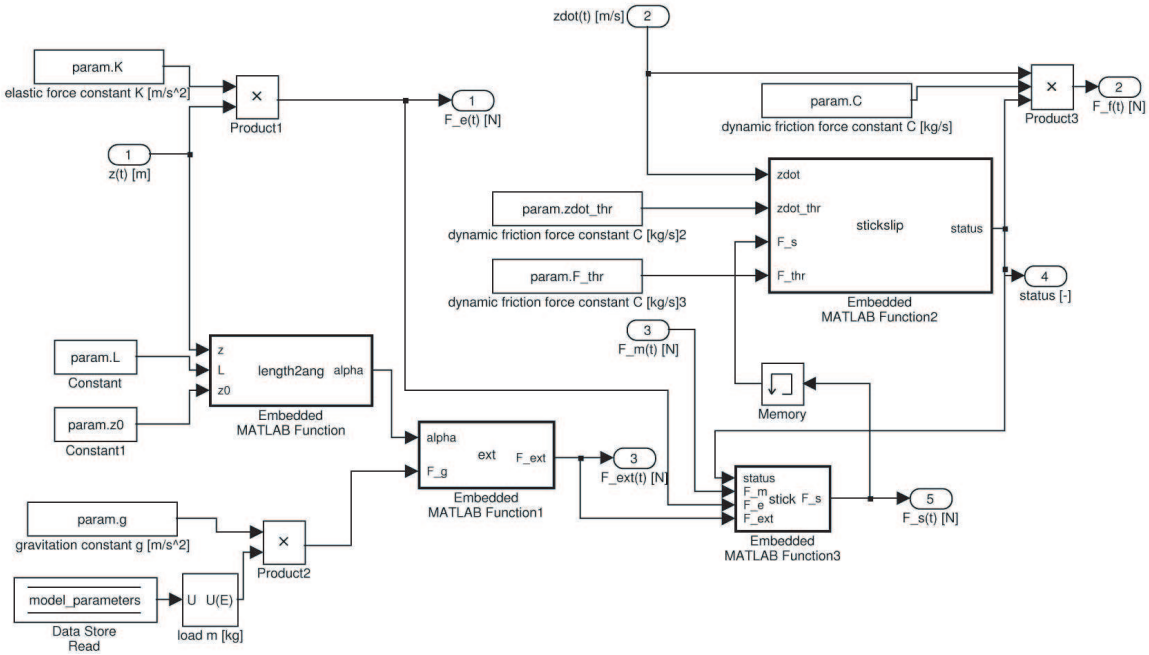

Figure B.44: Other forces in the control of a driven joint with Karnopp friction model

```
% converts the joint angle to the PMA length
   function z = ang2length(alpha,L,z0)
z = L*(cos(alpha/2)-1) + z0;
```

In the subsystem 'Tracking control' (Figure B.49) the linear tracking control takes place with the PMA length. The Embedded function is:

```
% Embedded Matlab function: tracking
% linear tracking control
function ny = tracking(e,e_dot,e_2dot,yd_3dot,K2,K1,K0)
ny = (yd_3dot + K2*e_2dot + K1*e_dot + K0*e);
```

In the subsystem 'Inverse system' (Figure B.50) the intrinsic control signal is computed. The Embedded function is

```
% Embedded Matlab function: inv_sys
% Inverse system, generates input u(t) which cancels the nonlinearities of the system
function u= inv_sys(y,y_dot,y_2dot,x1,ny,a1,a2,a3,a4,a5,a6,a7,a8,a9,a10,g,m_s,p_0,K,C,chi,L,z0)

% External force
psi_0     = 1+(y-z0)/L;
alpha     = 2*acos(psi_0);
alpha_dot = -2*y_dot/(L*sqrt(1-psi_0*psi_0));
F_ext     = m_s*g*cos(alpha)/sin(alpha/2);
F_ext_dot = m_s*g*(-alpha_dot*sin(alpha)*sin(alpha/2)-0.5*alpha_dot*cos(alpha/2)*cos(alpha))/(sin(alpha/2)*sin(al

% Abbrevations
V         = a8*y - a9*y*y*y;
```

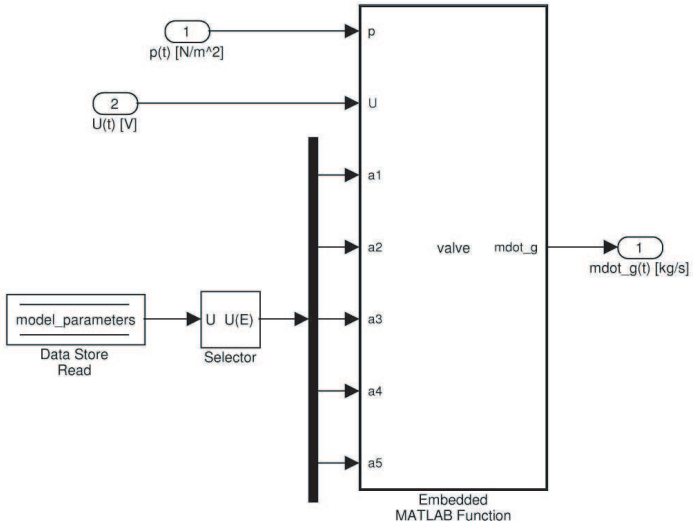

Figure B.45: Valve in the control of a driven joint with Karnopp friction model

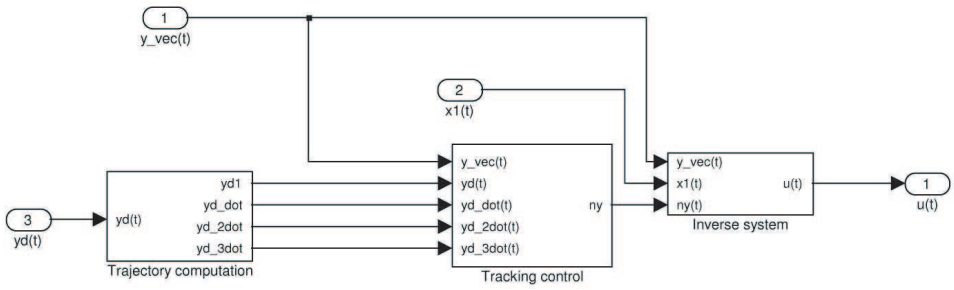

Figure B.46: Controller of a driven joint with Karnopp friction model

```
psi_1    = a1*sqrt(a2*x1^a4 - a3*x1^a5);
psi_2    = a7/V*psi_1;
    psi_3    = chi/V*x1*(a8-a10*y*y)*y_dot;
psi_4    = 2/m_s*a10*(x1-p_0)*y*y_dot - K/m_s*y_dot - C/m_s*y_2dot + F_ext_dot/m_s;
psi_5    = -1/m_s*(a8-a10*y*y)*psi_2;
psi_6    = 1/m_s*(a8-a10*y*y)*psi_3 + psi_4;

% Generation of the input
u=(ny-psi_6)/psi_5;
```

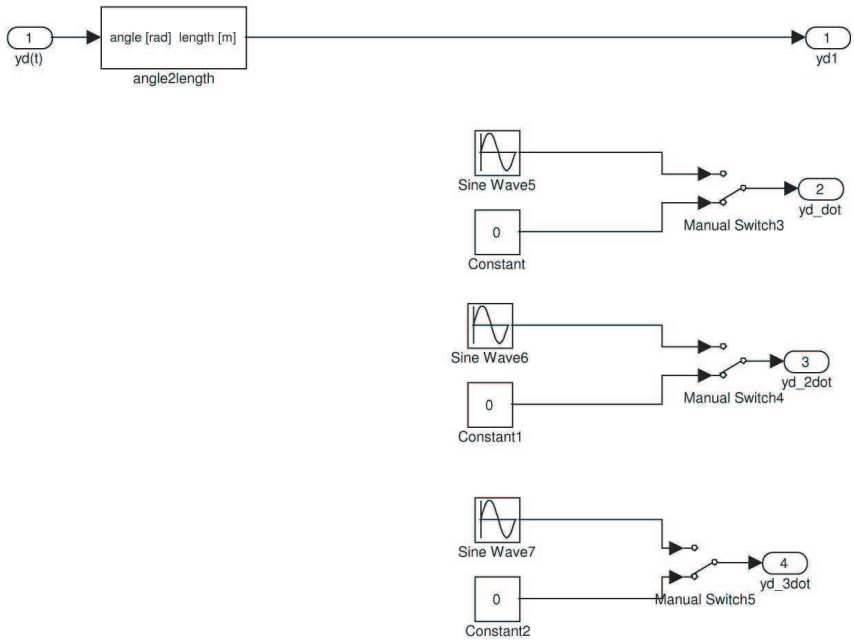

Figure B.47: Trajectory computation for the control of a driven joint with Karnopp friction model

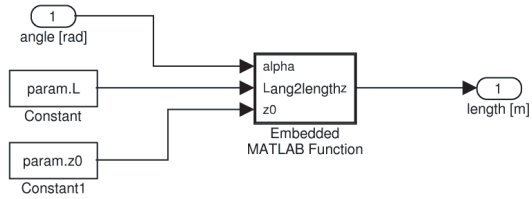

Figure B.48: Conversion of the angle to the length in the control of a driven joint with Karnopp friction model

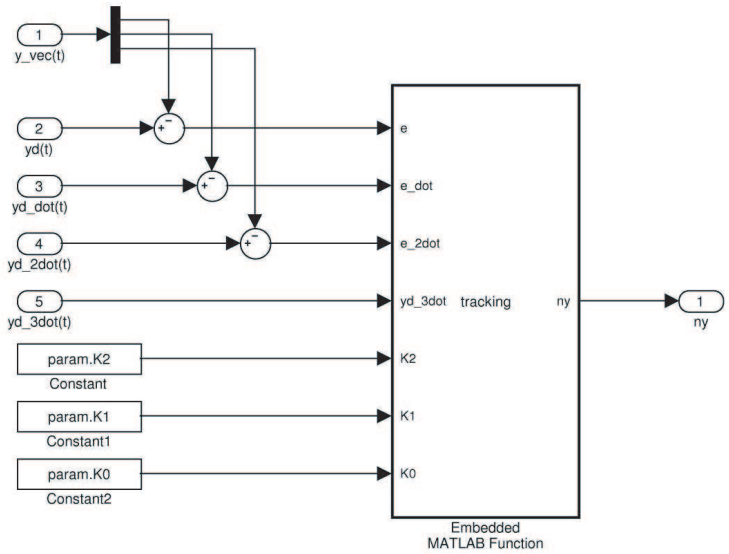

Figure B.49: Tracking control for a driven joint with Karnopp friction model

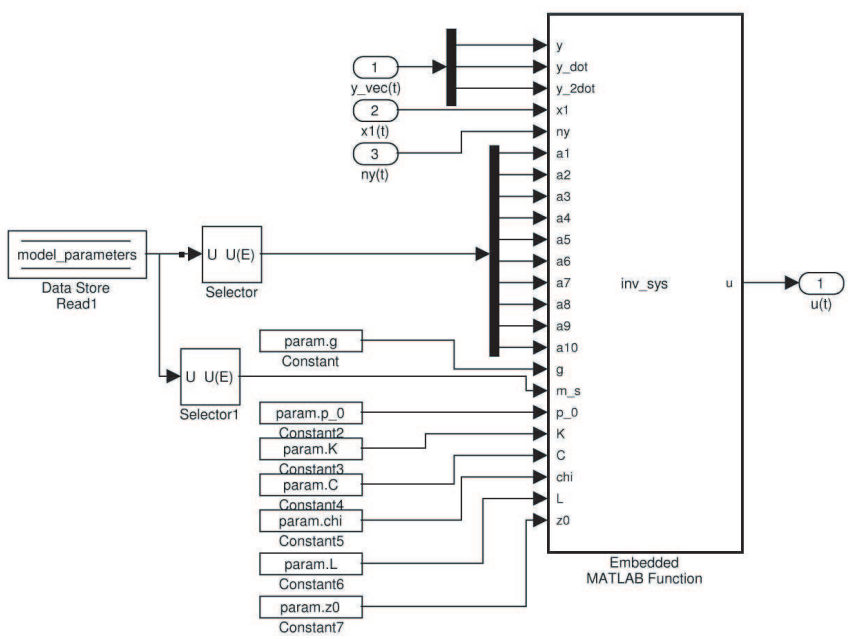

Figure B.50: Inverse system for the control of a driven joint with Karnopp friction model